





| | | |
|--|--------------------|---|
|   | S5L2PP ATBD-NO2 | Reference : KNMI-ESA-S5L2PP-ATBD-001 Version : 5.0 Date : 01 September 2023 |
| | | Page 1/89 |

Sentinel-5 L2 Prototype Processors

Algorithm Theoretical Basis Document for NO2



| | |
|-------------------------------------|--|
| Prepared by : Jos van Geffen (KNMI) | |
| Checked by : Frank Vonk (S&T) | |
| Approved by : Ping Wang (KNMI) | |

The copyright in this document is vested in KNMI. This document may only be reproduced in whole or in part, or stored in a retrieval system, or transmitted in any form, or by any means electronic, mechanical, photocopying or otherwise, either with the prior permission of KNMI or in accordance with the terms of ESA Contract No. 4000118463/16/NL/AI.

| | | |
|--|--------------------|---|
|   | S5L2PP ATBD-NO2 | Reference : KNMI-ESA-S5L2PP-ATBD-001 Version : 5.0 Date : 01 September 2023 |
| | | Page 2/89 |



Additional Authors/Checkers

| | |
|--|--|
| Co-authored by : Henk Eskes (KNMI) | |
| Co-authored by : Folkert Boersma (KNMI) | |
| Co-authored by : Pepijn Veeffkind (KNMI) | |
| Checked by : | |
| Checked by : | |
| Checked by : | |

| | | |
|--|--------------------|---|
|   | S5L2PP ATBD-NO2 | Reference : KNMI-ESA-S5L2PP-ATBD-001 Version : 5.0 Date : 01 September 2023 |
| | | Page 3/89 |

Change Log

| Issue | Date | Item | Comments |
|-------|------------|---|---|
| 0.1 | 2017-02-01 | All | Document creation |
| 0.2 | 2017-02-20 | 4, 6 9, A | First version of sections Sections added |
| 0.3 | 2017-02-24 | 4, 6 7, 8 | Improved and expanded Sections added |
| 1.0 | 2017-02-27 | — | Document released to ESA for review |
| 1.1 | 2017-08-30 | 4.5 6 6.1, 6.3.4 6.2 8.2 9.3 4 – 9 | Aligned requirements to S5L2PP System requirements document RD6 (PCR RID #251) Updated section throughout to reflect latest selected baselines for algorithm (PCR RID #260) Updated Figure 4 and text with S5 L2 auxillary product that will contain snow/ice flag and surface elevation data (PCR RID #257) Updated Figure 4 with S5 L2 product names (PCR RID #252) Algorithm testing and verification expanded Added NO ₂ product size (PCR RID #261) Additional updates and textual improvements |
| 1.2 | 2017-09-11 | 6 6.4.1 B, C | Process scheme (Fig. 4) expanded and text adapted accordingly Cloud fraction & cloud radiance fraction description expanded Appendices added |
| 1.3 | 2017-09-21 | 6.4.2 6.5.1 6.6.1 6.7.3 6.8.1 7.2 7.4 9.3 9.5 4, 6, 7, 9 | Surface albedo description expanded Description of de-stripping approach expanded Description of data assimilation / CTM system expanded Some details on including BRDF effects added Some more information on use of the averaging kernel added Text on sphericity correction of AMF improved Description of components of the error expanded Output product overview expanded and improved Overview of open issues updated Further updates and fine-tuning of the text |
| 1.9 | 2017-09-21 | — | Released to S&T for checking |
| 1.9.1 | 2017-09-28 | 5 | Added as requested by S&T; section numbering adapted accordingly |
| 2.0 | 2017-10-02 | — | Document released to ESA for review |
| 2.0.1 | 2018-02-06 | 2 4.4 6.2.6 6.3.3 6.4.1 6.6.1 | Updated list applicable and reference documents (PDR RID #630) Note added on unit conversion of (ir)radiance (PDR RID #927) Added note that we may update reference spectra (PDR RID #1023) Switched to AAI 354/388 nm pair, in line with OMI and S5P/TROPOMI Set option of use of BRDF to non-baseline (PDR RID #929) Expanded data assimilation description and philosophy (PDR RID #1039) |
| 2.0.2 | 2018-03-13 | 6.3.1 | Co-registration description introduced following discussion at PDR; section & equation numbering and Tables 7 & 22 adapted accordingly |
| 2.1 | 2018-03-15 | — | Document released to ESA |
| 2.1.1 | 2018-07-11 | 6.2 | Changes in text when switching DOAS solver highlighted |

| | | |
|--|--------------------|---|
|   | S5L2PP ATBD-NO2 | Reference : KNMI-ESA-S5L2PP-ATBD-001 Version : 5.0 Page Date : 01 September 2023 4/89 |
|--|--------------------|---|



Change Log – continued

| Issue | Date | Item | Comments |
|-------|--------------------------------|--|---|
| 2.1.2 | 2018-11-15 to 2018-11-22 | — 4.2,4.3 6.2 6.3,6.4,6.7 6.8 7.1,7.2,7.4 9.1,9.2 9.3 9.5 D | Figures 1, 2, 5, 6, 9, 12 redone using TROPOMI data Text updated where needed Text updated in view of switch of DOAS solver QDOAS to S5P/TROPOMI Text updated where needed Product overview Table 17 adapted & text on quality flags expanded Text updated and superfluous figure removed Text and tables updated where needed Text and product detailed output Table 23 updated List of open issues updated Appendix on the qa_value definition added |
| 2.2 | 2018-11-23 | — | Released to S&T for checking |
| 2.2.1 | 2018-12-05 | — | Minor updates and textual correction requested by S&T |
| 3.0 | 2018-12-15 | — | Document released to ESA for review |
| 3.0.1 | 2019-02-04 to 2019-03-28 | 6.2.9 6.2.7 6.3.3 6.7.5, 6.7.6 6.8 9.1 9.4 A D E — | Usage of Level-1B quality flags added (CDR RID #1813) Description of a spike removal algorithm added Clarified possible use of AAI in the future (CDR RID #2172) Clearer specification of tropospheric AMFs in data product Product overview Table 17 and product usage Table 18 updated Computational effort using known hardware specs (CDR RID #1795) Section on breakpoint output parameters added (CDR RID #1778) Description on limiting cloud fraction to [0 : 1] added Table entry #5 added and #8 updated, minor corrections Overview of process configuration parameters added (CDR RID #1675) Minor textual corrections and improvements |
| 3.1 | 2019-05-17 | — | Document released |
| 3.2 | 2021-06-10 to 2021-07-06 | 4.1, 4.2, 4.3 6.1, 6.2, 6.3 6.4, 6.7, 6.8 9.2, 9.3, 9.4 | Minor updates after ESA & EUMETSAT reviews of the DPM (AR1 RID #2928: 6.3.4; #2927: 9.4; #3107: 6.2.6, B.2, C, #3111: 6.4.1; #3113: 6.3.1) as well as some textual improvements |
| 4.0 | 2021-07-12 | — | Document released |
| 4.0.1 | 2021-12-15 | B | Minor updates after ESA & EUMETSAT reviews (AR1 RID #3472) |
| 4.1 | 2022-01-17 | — | Document released |
| 4.1.1 | 2023-06-13 | 6.4.1, 6.8 6.7.3 D | Added what NO ₂ ghost column is & to Table 17 (correct in Table 16) Remark added: AMF LUT values scaled with AMFgeo (SPR4063) Table entry #2: sun glint flag only applied over water (SPR4063) |
| 4.1.2 | 2023-07-11 | 6.3.5.3 | Section added on flagging in the S5 AUX product (SPR4063) |
| 4.1.3 | 2023-07-18 | 6.6.1 | Text on CAMS usage updated to reflect CAMS improvements since 2018 |
| 4.1.4 | 2023-08-10 | 6.3.5 | Sections added on flagging in S5 L2 CLD and AUI products (SPR4063) |
| 5.0 | 2023-09-01 | — | Document released |

Table of Contents

| | |
|---|-----------|
| Change Log | 3 |
| List of Tables | 7 |
| List of Figures | 7 |
| 1 Introduction | 9 |
| 1.1 Purpose and objective | 9 |
| 1.2 Document overview | 9 |
| 1.3 Acknowledgements | 9 |
| 2 Applicable and reference documents | 10 |
| 2.1 Applicable documents | 10 |
| 2.2 Reference documents | 10 |
| 2.3 Electronic references | 11 |
| 3 Terms, definitions and abbreviated terms | 12 |
| 3.1 Terms and definitions | 12 |
| 3.2 Acronyms and abbreviations | 12 |
| 4 Introduction to the Sentinel-5 NO₂ algorithm | 14 |
| 4.1 Nitrogen dioxide in troposphere and stratosphere | 14 |
| 4.2 Heritage | 16 |
| 4.3 Separating stratospheric and tropospheric NO ₂ with a data assimilation system | 17 |
| 4.4 NO ₂ column retrieval for Sentinel-5 | 18 |
| 4.5 NO ₂ data product requirements | 18 |
| 5 Instrument Overview | 19 |
| 6 Detailed algorithm description | 20 |
| 6.1 Overview of the NO ₂ retrieval algorithm | 20 |
| 6.2 DOAS NO ₂ slant column fit | 20 |
| 6.2.1 Measured reflectance | 21 |
| 6.2.2 Wavelength calibration & common wavelength grid | 22 |
| 6.2.3 Minimising the chi-squared merit function | 23 |
| 6.2.4 Modelled reflectance | 24 |
| 6.2.5 Optical density DOAS retrieval | 24 |
| 6.2.6 Reference spectra | 25 |
| 6.2.7 Spike removal | 27 |
| 6.2.8 Input & Output | 28 |
| 6.2.9 Flagging in the Sentinel-5 Level-1b product | 28 |
| 6.3 Other data products needed for the NO ₂ retrieval | 30 |
| 6.3.1 Co-registration of NO ₂ and cloud data | 30 |
| 6.3.2 Sentinel-5 cloud (CLD) product | 31 |
| 6.3.3 Sentinel-5 aerosol index (AUI) product | 31 |
| 6.3.4 Sentinel-5 auxiliary (AUX) product | 31 |
| 6.3.5 Flagging in the CLD, AUI and AUX products | 32 |
| 6.4 Cloud fraction & cloud radiance fraction NO ₂ | 34 |
| 6.4.1 Description | 34 |
| 6.4.2 Surface albedo climatology | 36 |
| 6.4.3 Daily snow/ice flag | 37 |
| 6.4.4 Input & Output | 37 |

| | | |
|----------|---|-----------|
| 6.5 | De-stripping the NO ₂ slant columns | 37 |
| 6.5.1 | Description of the de-stripping approach | 37 |
| 6.5.2 | Input & Output | 38 |
| 6.6 | The data assimilation / chemistry modelling system | 39 |
| 6.6.1 | Description | 39 |
| 6.6.2 | Input & Output | 41 |
| 6.7 | Separation of stratosphere and troposphere & vertical column calculation | 41 |
| 6.7.1 | Separation of stratospheric and tropospheric NO ₂ | 41 |
| 6.7.2 | Air-mass factor and vertical column calculations | 43 |
| 6.7.3 | Altitude dependent AMFs | 44 |
| 6.7.4 | Temperature correction | 46 |
| 6.7.5 | Cloud correction | 46 |
| 6.7.6 | Input & Output | 47 |
| 6.8 | The NO ₂ data product | 47 |
| 6.8.1 | Averaging kernels | 50 |
| 6.9 | Near-real time processing vs. off-line / (re-)processing | 50 |
| 7 | Error analysis | 51 |
| 7.1 | Slant column errors | 51 |
| 7.2 | Errors in the stratospheric (slant) columns | 51 |
| 7.3 | Errors in the tropospheric air-mass factors | 53 |
| 7.4 | Total errors in the tropospheric NO ₂ columns | 54 |
| 8 | Validation | 56 |
| 8.1 | Validation requirements | 56 |
| 8.2 | Algorithm testing and verification | 56 |
| 8.3 | Stratospheric NO ₂ validation | 57 |
| 8.4 | Tropospheric NO ₂ validation | 57 |
| 9 | Feasibility | 58 |
| 9.1 | Estimated computational effort | 58 |
| 9.2 | Static and dynamic input | 58 |
| 9.2.1 | Static input | 58 |
| 9.2.2 | Dynamic input | 59 |
| 9.3 | Output product overview | 59 |
| 9.4 | Breakpoint output parameters | 61 |
| 9.5 | Open issues | 61 |
| A | Effective cloud fraction in the NO₂ window | 63 |
| A.1 | Adjusting albedo to respect physical limits to the cloud fraction | 64 |
| B | Wavelength calibration | 65 |
| B.1 | Description of the problem | 65 |
| B.2 | Non-linear model function and Jacobian | 65 |
| B.2.1 | Prior information for the optimal estimation fit | 67 |
| B.3 | Application of the wavelength calibration in NO ₂ | 67 |
| C | High-sampling interpolation | 68 |
| D | Data quality value: the qa_value flags | 70 |
| E | Overview of process configuration parameters of S5P/TROPOMI NO₂ | 71 |
| E.1 | NO ₂ process configuration | 71 |

| | | |
|--|--------------------|---|
|   | S5L2PP ATBD-NO2 | Reference : KNMI-ESA-S5L2PP-ATBD-001 Version : 5.0 Date : 01 September 2023 |
| | | Page 7/89 |



| | | |
|----------|--|-----------|
| E.1.1 | Wavelength calibration configuration | 71 |
| E.1.2 | DOAS retrieval configuration | 72 |
| E.1.3 | Quality value configuration | 73 |
| E.1.4 | General process configuration | 74 |
| E.1.5 | Input specifications | 75 |
| E.1.6 | Output specifications | 75 |
| E.1.7 | Fixed configuration settings in the code | 76 |
| E.2 | Example XML process control file | 78 |
| F | References | 83 |

List of Tables



| | | |
|----|--|----|
| 1 | NO ₂ data product requirements | 19 |
| 2 | Settings of DOAS retrieval of NO ₂ | 26 |
| 3 | Input of the wavelength calibration | 27 |
| 4 | Output of the wavelength calibration | 27 |
| 5 | Input of the DOAS retrieval | 27 |
| 6 | Output of the DOAS retrieval | 28 |
| 7 | Other data products needed | 30 |
| 8 | NISE snow/ice flags | 37 |
| 9 | Input of cloud fraction & cloud radiance fraction NO ₂ | 38 |
| 10 | Output of cloud fraction & cloud radiance fraction NO ₂ | 38 |
| 11 | Input of the de-stripping correction | 38 |
| 12 | Output of the de-stripping correction | 39 |
| 13 | Output of the CAMS / CTM system | 41 |
| 14 | AMF LUT | 45 |
| 15 | Input of the vertical column processing | 47 |
| 16 | Output of the vertical column processing | 47 |
| 17 | Final NO ₂ vertical column data product | 48 |
| 18 | Data product user applications | 49 |
| 19 | Estimate of AMF errors | 53 |
| 20 | Tropospheric column and uncertainty estimates from OMI | 54 |
| 21 | Static input data | 58 |
| 22 | Dynamic input data | 59 |
| 23 | Data product list of data output file | 60 |
| 24 | Diagnostic output parameters | 62 |
| 25 | Look-up tables for reflectance calculations | 64 |
| 26 | A priori values for the wavelength fit | 67 |
| 27 | Data quality value determination | 70 |

List of Figures

| | | |
|----|--|----|
| 1 | Tropospheric NO ₂ for April 2018 | 14 |
| 2 | Stratospheric NO ₂ for 1 April 2018 | 15 |
| 3 | NO ₂ data record UV/Vis satellite instruments | 16 |
| 4 | NO ₂ retrieval process scheme | 21 |
| 5 | Example irradiance and radiance | 22 |
| 6 | Example measured and modelled reflectance | 25 |
| 7 | Cloud fraction method comparison | 35 |
| 8 | Comparison of stratospheric NO ₂ columns | 40 |
| 9 | NO ₂ forecast and analysis differences | 42 |
| 10 | Tropospheric NO ₂ difference from resolution | 43 |
| 11 | Error in slant column versus SNR | 52 |

| | | |
|--|--------------------|---|
|   | S5L2PP ATBD-NO2 | Reference : KNMI-ESA-S5L2PP-ATBD-001 Version : 5.0 Date : 01 September 2023 |
| | | Page 8/89 |

| | | |
|----|--|----|
| 12 | Tropospheric column and error estimates from TROPOMI | 55 |
| 13 | High sampling interpolation on part of a solar observation | 68 |

| | | |
|--|--------------------|---|
|   | S5L2PP ATBD-NO2 | Reference : KNMI-ESA-S5L2PP-ATBD-001 Version : 5.0 Date : 01 September 2023 |
| | | Page 9/89 |

1 Introduction

1.1 Purpose and objective

This document, identified as KNMI-ESA-S5L2PP-ATBD-001, is the Algorithm Theoretical Basis Document (ATBD) for the Sentinel-5 total and tropospheric NO₂ data products. It is part of a series of ATBDs describing the Sentinel-5 Level-2 Prototype Processors (S5L2PP).

An overview of the Sentinel-5 instrument – measurement principles, spectral resolution, coverage, etc. – can be found in the ATBD of the Level-1b Prototype Processor (L1bPP) [RD1].

The purpose of this document is to describe the theoretical basis and the implementation of the NO₂ Level-2 algorithm for Sentinel-5. The document is maintained during the development phase and the lifetime of the data products. Updates and new versions will be issued in case of changes in the algorithms.



This document is derived from the latest version of the S5P/TROPOMI NO₂ ATBD [RD2].

1.2 Document overview

Section 2 lists the applicable and reference documents; references to peer-reviewed papers and other scientific publications are listed in Appendix F. Section 3 lists the terms and abbreviations specific for this document. Section 4 gives an introduction to the NO₂ data products, their background and their heritage. Section 6 presents a detailed description of the retrieval algorithm, the underlying mathematical equations and the structure, with details in input and output of the main components. Section 7 deals with an error analysis of the NO₂ data product. Section 8 gives a brief overview of validation issues and possibilities, such as campaigns and satellite intercomparisons. And Section 9 lists some aspects regarding the feasibility of the NO₂ data products, such as the computational effort and the auxiliary information needed for the processing.

1.3 Acknowledgements

The authors would like to thank the following people for useful discussions, information, reviews of earlier versions of this document and other contributions: Andreas Richter, Gijsbert Tilstra, Joost Smeets, Maarten Sneep, Mark ter Linden, Michel Van Roozendaal, Piet Stammes, Ping Wang, Thomas Danckaert .

| | | |
|--|--------------------|--|
|   | S5L2PP ATBD-NO2 | Reference : KNMI-ESA-S5L2PP-ATBD-001 Version : 5.0 Page Date : 01 September 2023 10/89 |
|--|--------------------|--|



2 Applicable and reference documents

2.1 Applicable documents

- [AD1] S5L2PP Project Management Plan.
source: S&T; **ref:** ST-ESA-S5L2PP-PMP-001; **issue:** 2.4; **date:** 2019-05-17.
- [AD2] Sentinel-5 Level-2 Prototype Processor Development Requirements Specification.
source: ESA/ESTEC; **ref:** S5-RS-ESA-GR-0131; **issue:** 1.7; **date:** 2018-06-29.

2.2 Reference documents



- [RD1] Sentinel-5/UVNS L1bPP algorithm theoretical basis document.
source: Airbus Defence and Space; **ref:** GS5.RP.ASG.UVNS.00044; **issue:** 8.0; **date:** 2017-10-03.
- [RD2] TROPOMI ATBD of the total and tropospheric NO₂ data products.
source: KNMI; **ref:** S5P-KNMI-L2-0005-RP; **issue:** 2.4.0; **date:** 2022-07-11.
- [RD3] S5L2PP Terms, Definitions and Abbreviations.
source: S&T; **ref:** ST-ESA-S5L2PP-LST-001; **issue:** 2.1; **date:** 2018-08-28.
- [RD4] TROPOMI Instrument and Performance Overview.
source: KNMI; **ref:** S5P-KNMI-L2-0010-RP; **issue:** 0.10.0; **date:** 2014-03-15.
- [RD5] GMES Sentinels 4 and 5 Mission Requirements Document.
source: ESA/ESTEC; **ref:** EOP-SMA/1507/JL-dr; **issue:** 3; **date:** 2011-09-21.
- [RD6] QA4ECV - Quality Assurance for Essential Climate Variables.
source: KNMI; **ref:** EU-project 607405, SPA.2013.1.1-03; **date:** November 2012.
- [RD7] GMES Sentinels 4 and 5 Mission Requirements Traceability Document.
source: ESA/ESTEC; **ref:** EOP-SM/2413/BV-bv; **issue:** 2; **date:** 2017-07-07.
- [RD8] Science Requirements Document for TROPOMI. Volume I: Mission and Science Objectives and Observational Requirements.
source: KNMI, SRON; **ref:** RS-TROPOMI-KNMI-017; **issue:** 2.0.0; **date:** 2008-10-30.
- [RD9] CAPACITY: Operational Atmospheric Chemistry Monitoring Missions – Final report and technical notes of the ESA study.
source: KNMI; **ref:** CAPACITY; **date:** Oct. 2005.
- [RD10] CAMELOT: Observation Techniques and Mission Concepts for Atmospheric Chemistry – Final report of the ESA study.
source: KNMI; **ref:** RP-CAM-KNMI-050; **date:** Nov. 2009.
- [RD11] TRAQ: Performance Analysis and Requirements Consolidation – Final report of the ESA study.
source: KNMI; **ref:** RP-ONTRAQ-KNMI-051; **date:** Jan. 2010.
- [RD12] NO2 PGE Detailed Processing Model.
source: Space Systems Finland; **ref:** TN-NO2-0200-SSF-001; **issue:** 1.2; **date:** 2010-04-21.
- [RD13] QA4ECV D4.2 - Recommendations on best practices for retrievals for Land and Atmosphere ECVs..
source: KNMI; **ref:** EU-project 607405, SPA.2013.1.1-03; **date:** April 2016.
- [RD14] S5P/TROPOMI Static input for Level 2 processors.
source: KNMI/SRON/BIRA/DLR; **ref:** S5P-KNMI-L2CO-0004-SD; **issue:** 4.0.0; **date:** 2016-03-21.
- [RD15] EPS-SG Sentinel-5 Level 1B Product Format Specification.
source: EUMETSAT; **ref:** EUM/LEO-EPSSG/SPE/14/772065; **issue:** v3A; **date:** 2018-03-09.
- [RD16] Sentinel 5 L2 Prototype Processors: Co-registration processing description.
source: TriOpSys; **ref:** TOS-ESA-S5L2PP-TN-1501; **issue:** 2.1; **date:** 2019-05-17.
- [RD17] Sentinel-5 L2 Prototype Processor – Algorithm Theoretical Baseline Document for Cloud data product.
source: KNMI; **ref:** KNMI-ESA-S5L2PP-ATBD-005; **issue:** 3.1; **date:** 2019-05-02.

| | | |
|--|--------------------|--|
|   | S5L2PP ATBD-NO2 | Reference : KNMI-ESA-S5L2PP-ATBD-001 Version : 5.0 Page Date : 01 September 2023 11/89 |
|--|--------------------|--|

- [RD18] Sentinel-5 L2 Prototype Processor – Algorithm Theoretical Baseline Document for Absorbing Aerosol Index.
source: KNMI; **ref:** KNMI-ESA-S5L2PP-ATBD-002; **issue:** 3.1; **date:** 2019-05-02.
- [RD19] An improved temperature correction for OMI NO₂ slant column densities from the 405-465 nm fitting window.
source: KNMI; **ref:** TN-OMIE-KNMI-982; **issue:** 1.0; **date:** 2017-01-24.
- [RD20] Dutch OMI NO₂ (DOMINO) data product v2.0 – see URL
<https://www.temis.nl/airpollution/no2.php>.
source: KNMI; **ref:** OMI_NO2_HE5_2.0_2011; **date:** 18 August 2011.
- [RD21] Determine the effective cloud fraction for a specific wavelength.
source: KNMI; **ref:** S5P-KNMI-L2-0115-TN; **issue:** 2.0.0; **date:** 2019-04-10.
- [RD22] Algorithm theoretical basis document for the TROPOMI L01b data processor.
source: KNMI; **ref:** S5P-KNMI-L01B-0009-SD; **issue:** 8.0.0; **date:** 2017-06-01.
- [RD23] Wavelength calibration in the Sentinel-5 precursor Level 2 data processors.
source: KNMI; **ref:** S5P-KNMI-L2-0126-TN; **issue:** 1.0.0; **date:** 2015-09-11.

2.3 Electronic references

- [ER1] TEMIS website: NO₂ data product page. <https://www.temis.nl/airpollution/no2.php>.
- [ER2] QA4ECV website. <http://www.qa4ecv.eu/>.
- [ER3] QA4ECV NO₂ ECV precursor data. <http://www.qa4ecv.eu/ecv/no2-pre>.
- [ER4] GCOS Essential Climate Variables.
<http://www.wmo.int/pages/prog/gcos/index.php?name=EssentialClimateVariables>.
- [ER5] CAMS website. <http://atmosphere.copernicus.eu/>.
- [ER6] Vandaele et al. NO₂ cross sections. <http://spectrolab.aeronomie.be/no2.htm>.
- [ER7] What are outliers in the data?
<https://www.itl.nist.gov/div898/handbook/prc/section1/prc16.htm>.
- [ER8] Q. L. Kleipool, M. R. Dobber, J. F. De Haan et al.; OMI Surface Reflectance Climatology (2010).
<https://disc.gsfc.nasa.gov/datasets?page=1&source=AURA~OMI>.
- [ER9] L. G. Tilstra, O. N. E. Tuinder, P. Wang et al.; Surface reflectivity climatologies from UV to NIR determined from Earth observations by GOME-2 and SCIAMACHY (2017). https://temis.nl/surface/gome2_1er.php.
- [ER10] M. J. Brodzik and J. S. Stewart; Near Real-Time SSM/I EASE-Grid Daily Global Ice Concentration and Snow Extent. Boulder, Colorado USA. NASA National Snow and Ice Data Center (2016); 10.5067/3KB2JPLFPK3R. Updated daily; <http://nsidc.org/data/NISE>.
- [ER11] TM5 website. <http://www.projects.science.uu.nl/tm5/>.

| | | |
|--|--------------------|---|
|   | S5L2PP ATBD-NO2 | Reference : KNMI-ESA-S5L2PP-ATBD-001 Version : 5.0 Date : 01 September 2023 |
| | | Page 12/89 |

3 Terms, definitions and abbreviated terms



General terms, definitions and abbreviated terms that are used in S5L2PP project are described in [RD3]. Terms, definitions and abbreviated terms that are specific for this document can be found below.

3.1 Terms and definitions

The symbols related to the data product described in this document can be found in the data product overview list of Table 23.

3.2 Acronyms and abbreviations

| | |
|-----------|---|
| AAI | Absorbing Aerosol Index |
| ACE | Atmospheric Chemistry Experiment |
| AMF | Air-mass factor |
| ATBD | Algorithm Theoretical Baseline Document |
| BIRA-IASB | Belgian Institute for Space Aeronomy |
| BRDF | Bidirectional Reflectance Distribution Function |
| CAMS | Copernicus Atmosphere Monitoring Service |
| CF | Climate and Forecast metadata conventions |
| CTM | Chemistry Transport Model |
| DA/CTM | Data Assimilation / Chemistry Transport Model |
| DAK | Doubling-Adding KNMI |
| DOAS | Differential Optical Absorption Spectroscopy |
| DOMINO | Dutch OMI NO ₂ data products of KNMI for OMI |
| DPM | Detailed Processor Model |
| ECMWF | European Centre for Medium-Range Weather Forecast |
| ECV | Essential Climate Variables |
| ENVISAT | Environmental Satellite |
| EOS-Aura | Earth Observing System (Chemistry & Climate Mission) |
| ERBS | Earth Radiation Budget Satellite |
| ERS | European Remote Sensing satellite |
| EUMETSAT | European Organisation for the Exploitation of Meteorological Satellites |
| FRESCO | Fast Retrieval Scheme for Clouds from the Oxygen A band |
| GCOS | Global Climate Observing System |
| GOME | Global Ozone Monitoring Experiment |
| HALOE | Halogen Occultation Experiment |
| IFS | ECMWF Integrated Forecast System |
| IPA | Independent pixel approximation |
| IPCC | Intergovernmental Panel on Climate Change |
| ISRF | Instrument Spectral Response Function (<i>aka</i> slit funtion) |
| LER | Lambertian-Equivalent Reflectivity |
| LUT | Look-up table |
| KNMI | Royal Netherlands Meteorological Institute |
| MACC | Monitoring Atmospheric Composition and Climate |
| MAX-DOAS | Multi-axis DOAS |
| MERIS | Medium Resolution Imaging Spectrometer |
| MetOp | Meteorological Operational Satellite |
| MODIS | Moderate Resolution Imaging Spectroradiometer |

| | | |
|--|--------------------|--|
|   | S5L2PP ATBD-NO2 | Reference : KNMI-ESA-S5L2PP-ATBD-001 Version : 5.0 Page Date : 01 September 2023 13/89 |
|--|--------------------|--|

| | |
|-----------|--|
| NISE | Near-real-time Ice and Snow Extent |
| NRT | near-real time (i.e. processing within 3 hours of measurement) |
| OMI | Ozone Monitoring Instrument |
| OMNO2A | OMI NO2 slant column data product (at NASA) |
| OSIRIS | Optical Spectrograph and Infrared Imager System |
| OSISAF | Ocean & Sea Ice Satellite Application Facility |
| PDGS | Sentinel-5Precursor Payload Data Ground Segment (at DLR) |
| POAM | Polar Ozone and Aerosol Measurements |
| QA4ECV | Quality Assurance for Essential Climate Variables |
| S&T | Science & Technology B.V. |
| S5 | Sentinel-5 instrument |
| S5P | Sentinel-5Precursor mission (with TROPOMI) |
| SAGE | Stratospheric Gas and Aerosol Experiment |
| SCIAMACHY | Scanning Imaging Absorption Spectrometer for Atmospheric Cartography |
| SDC | Satellite Data Centre (at KNMI) |
| SME | Solar Mesosphere Explorer |
| SNR | Signal-to-Noise Ratio |
| SPOT | Système Pour l'Observation la Terre |
| TM4, TM5 | Data assimilation / chemistry transport model (version 4 or 5) |
| TM4NO2A | NO ₂ data products of KNMI for GOME, SCIAMACHY and GOME-2 |
| TOA | Top-of-atmosphere |
| TROPOMI | Tropospheric Monitoring Instrument |
| UARS | Upper Atmosphere Research Satellite |
| UNFCCC | United Nations Framework Convention on Climate Change |

4 Introduction to the Sentinel-5 NO₂ algorithm

4.1 Nitrogen dioxide in troposphere and stratosphere

Nitrogen dioxide (NO₂) and nitrogen oxide (NO) – together usually referred to as nitrogen oxides (NO_x = NO + NO₂) – are important trace gases in the Earth's atmosphere, present in both the troposphere and the stratosphere. They enter the atmosphere as a result of anthropogenic activities (notably fossil fuel combustion and biomass burning) and natural processes (such as microbiological processes in soils, wildfires and lightning). Approximately 95% of the NO_x emissions is in the form of NO. During daytime, i.e. in the presence of sunlight, a photochemical cycle involving ozone (O₃) converts NO into NO₂ (and vice versa) on a timescale of minutes, so that NO₂ is a robust measure for concentrations of nitrogen oxides (Solomon [1999], Jacob [1999]).

In the troposphere NO₂ plays a key role in air quality issues, as it directly affects human health [World Health Organisation, 2003]. In addition nitrogen oxides are essential precursors for the formation of ozone in the troposphere (e.g. Sillman et al. [1990]) and they influence concentrations of OH and thereby (shorten) the lifetime of methane (CH₄) (e.g. Fuglestad et al. [1999]). Although NO₂ is a minor greenhouse gas in itself, the indirect effects of NO₂ on global climate change are probably larger, with a presumed net cooling effect mostly driven by a growth in aerosol concentrations through nitrate formation from nitrogen oxides and enhanced levels of oxidants (e.g. Shindell et al. [2009]). Deposition of nitrogen is of great importance for eutrophication [Dentener et al., 2006], the response of the ecosystem to the addition of substances such as nitrates and phosphates – negative environmental effects include the depletion of oxygen in the water, which induces reductions in fish and other animal populations.

For typical levels of OH the lifetime of NO_x in the lower troposphere is less than a day. For Riyadh, for example, Beirle et al. [2011] find a lifetime of about 4.0 ± 0.4 hours, while at higher latitudes (e.g. Moscow) the lifetime can be considerably longer, up to 8 hour in winter, because of a slower photochemistry in that season. For Switzerland Schaub et al. [2007] report lifetimes of 3.6 ± 0.8 hours in summer and $13.1 \pm (3.8)$ hours in winter. With lifetimes in the troposphere of only a few hours, the NO₂ will remain relatively close to its source, making the NO_x sources well detectable from space. As an example, Fig. 1 shows distinct hotspots of NO₂ pollution over the highly industrialised and urbanised regions of London, Rotterdam and the Ruhr area in the monthly average tropospheric NO₂ for April 2018 over Europe derived from TROPOMI data.

In the stratosphere NO₂ is involved in some photochemical reactions with ozone and thus affects the ozone layer

TROPOMI NO₂ tropospheric column, April 2018

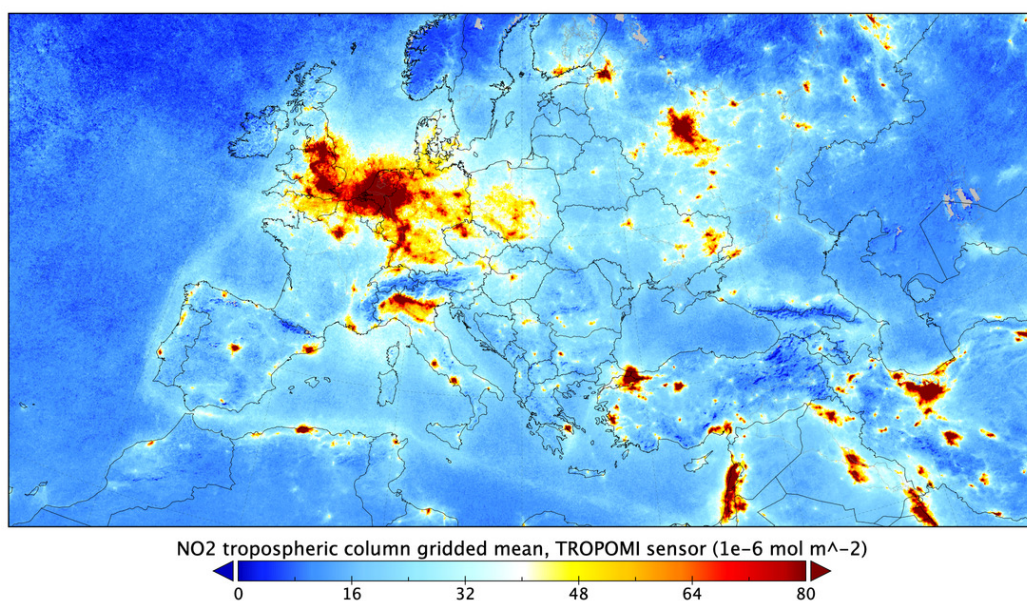


Figure 1: Monthly average distribution of tropospheric NO₂ columns for April 2018 over Europe based on TROPOMI data, derived with processor version 1.2.0.

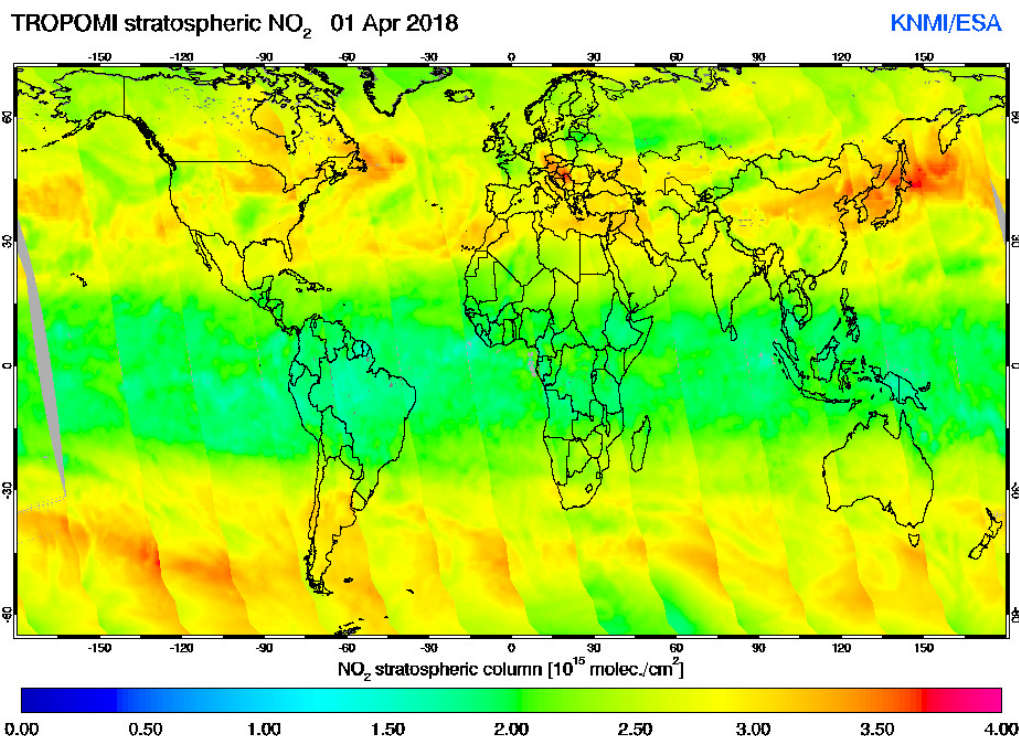


Figure 2: Distribution of stratospheric NO₂ on 1 April 2018 along the individual TROPOMI orbits, derived with processor version 1.2.0. The image shows that atmospheric dynamics creates variability in the stratospheric columns, mainly at mid-latitudes. Furthermore we can see the effect of the increase of NO₂ in the stratosphere during daytime leading to jumps from one orbit to the next. Note that the colour scale range is different from range in Fig. 1.

(Crutzen et al. [1970]; Seinfeld and Pandis [2006]). The origin of NO₂ in the stratosphere is mainly from oxidation of N₂O in the middle stratosphere, which leads to NO_x, which in turn acts as a catalyst for ozone destruction (Crutzen et al. [1970]; Hendrick et al. [2012]). But NO_x can also suppress ozone depletion by converting reactive chlorine and hydrogen compounds into unreactive reservoir species (such as ClONO₂ and HNO₃; Murphy et al. [1993]).

Fig. 2 shows, as an example, the stratospheric NO₂ distribution derived from TROPOMI measurements on 1 April 2018 at the 13:30 overpass local time. The image shows variability related to atmospheric transport and diurnal variability in the stratosphere. In a study into the record ozone loss, triggered by enhanced NO_x levels, in the exceptionally strong Arctic polar vortex in Spring 2011, Adams et al. [2013] showed the usefulness of such data when investigating the anomalous dynamics and chemistry in the stratosphere. With their higher spatial resolution and signal-to-noise ratio, S5P/TROPOMI and Sentinel-5 will clearly be well-suited to help understand the stratospheric NO₂ content and its implications for the ozone distribution.

From observed trends in N₂O emissions one would expect a trend in stratospheric NO₂ with potential implications for persistent ozone depletion well into the 21st century [Ravishankara et al., 2009]. There have been some reports of such trends in stratospheric NO₂, for instance from New Zealand [Liley et al., 2000] and northern Russia [Gruzdev and Elokhov, 2009]. On the other hand, Hendrick et al. [2012] report that changes in the NO_x partitioning in favour of NO may well conceal the effect of trends in N₂O. S5P/TROPOMI and Sentinel-5 will continue the important record of stratospheric NO₂ observations that started with GOME in 1995, and improve the detectability of trends.

Over unpolluted regions most NO₂ is located in the stratosphere (typically more than 90%). For polluted regions 50–90% of the NO₂ is located in the troposphere, depending on the degree of pollution. Over polluted regions, most of the tropospheric NO₂ is found in the planetary boundary layer, as has been shown among others in campaigns using measurements made from aeroplanes, such as INTEX (e.g. Hains et al. [2010]). In areas with strong convection, enhanced NO₂ concentrations are observed at higher altitudes due to production of NO_x by lightning (e.g. Ott et al. [2010]).

The important role of NO₂ in both troposphere and stratosphere implies that it is not only important to know the total

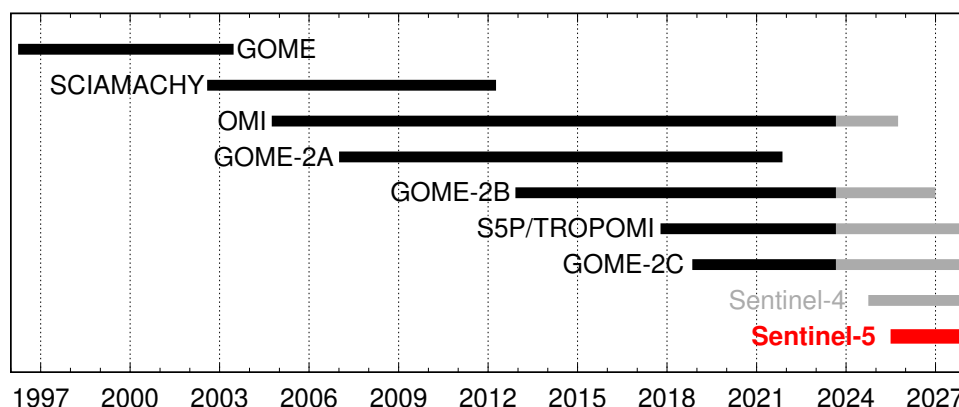


Figure 3: Overview of the European UV/Vis polar orbiting and geostationary backscatter satellite instruments capable of retrieving tropospheric and stratospheric NO₂ column data since the launch of GOME aboard ERS-2.

column density of NO₂, but rather the tropospheric NO₂ and stratospheric NO₂ concentrations separately. A proper separation between the two is therefore important, in particular for areas with low pollution, where the stratospheric concentration forms a significant part of the total column.

4.2 Heritage



Tropospheric concentrations of NO₂ are monitored all over the world by a variety of remote sensing instruments – ground-based, in-situ (balloon, aircraft) or satellite-based – each with its own specific advantages, and to some extent still under development.

Stratospheric NO₂ has been measured by a number of satellite instruments since the 1980s, such as the spectrometer aboard SME (1981–1989; Mount et al. [1984]), SAGE-II/III (ERBS/Meteor-3M, 1984–2005; Chu and McCornick [1986]), HALOE (UARS, 1991–2005; Gordley et al. [1996]), POAM (SPOT-3, 1993–1996; Randall et al. [1998]), SCIAMACHY (ENVISAT, 2002–2012; Bovensmann et al. [1999], Sierk et al. [2006]), OSIRIS (Odin, 2001–present; Llewellyn et al. [2004], Adams et al. [2016]), and ACE (SCISAT-1, 2003–present; Bernath et al. [2005]).

Over the past 22 years tropospheric NO₂ has been measured from UV/Vis backscatter satellite instruments such as GOME (ERS-2, 1995–2011; Burrows et al. [1999]), SCIAMACHY (ENVISAT, 2002–2012; Bovensmann et al. [1999]), OMI (EOS-Aura, 2004–present; Levelt et al. [2006]) and the GOME-2 instruments [Munro et al., 2006] aboard MetOp-A (2007–2021), MetOp-B (2012–present) and MetOp-C (2019–present), and the OMPS instrument [Yang et al., 2014] on the Suomi NPP platform (2011–present) and the NOAA-20 satellite (2017–present). S5P/TROPOMI (see [RD4]; Veeckind et al. [2012]) and Sentinel-5 (see [RD1]) will extend the records of these observations, as will the forthcoming geostationary platforms GEMS [Bak et al., 2013], Kim [2020]; launched in 2020), TEMPO [Zoogman et al., 2017] and Sentinel 4 [Ingmann et al., 2012], [RD5]. Figure 3 shows the timelines of the NO₂ data records of these instruments. Note that S5P/TROPOMI, OMI, the GOME-2 instruments and Sentinel-5 provide (near-)global coverage in one day, and that Sentinel-4 is a geostationary instrument.

For the UV/Vis backscatter instruments that observe NO₂ down into the troposphere, KNMI operates – in close collaboration with BIRA-IASB, NASA and DLR – a continuous data processing system, the results of which are freely available via the TEMIS website [ER1]. The approach is called DOMINO (for OMI, Boersma et al. [2011]) and TM4NO2A (for GOME, SCIAMACHY and GOME-2), and is based on a DOAS retrieval, a pre-calculated air-mass factor (AMF) look-up table and a data assimilation / chemistry transport model for the separation of the stratospheric and tropospheric contributions to the NO₂ column and for a-priori profile shapes of NO₂ in the troposphere. The data has been used for a variety of studies in areas like validation (see e.g. Boersma et al. [2009], Hains et al. [2010], Lamsal et al. [2010]), trends (see e.g. Van der A et al. [2008], Stavrou et al. [2008], Dirksen et al. [2011], Castellanos and Boersma [2012], DeRuyter et al. [2012]), and NO_x emission and lifetime estimates (see e.g. Lin et al. [2010], Beirle et al. [2011], Mijling and Van der A [2012], Wang et al. [2012]).

The European Quality Assurance for Essential Climate Variables (QA4ECV) project ([RD6], [ER2], Boersma et al. [2018]) has led to a homogeneous reprocessing dataset of NO₂ for the sensors GOME, SCIAMACHY, OMI and

| | | |
|--|--------------------|---|
|   | S5L2PP ATBD-NO2 | Reference : KNMI-ESA-S5L2PP-ATBD-001 Version : 5.0 Date : 01 September 2023 |
| | | Page 17/89 |



GOME-2A. This project has investigated and improved all the individual steps/modules in the NO₂ retrieval. The new NO₂ datasets are available via the QA4ECV project website at [ER3]. Essential Climate Variables (ECVs) are defined by GCOS (see [ER4]) to support the work of the UNFCCC and the IPCC, and they include NO₂. Recent studies (e.g. Hakkarainen et al. [2016]) have shown that NO₂ may serve as a marker for identifying anthropogenic sources of CO₂. Currently the QA4ECV v1.1 data records end with 2017 for OMI and 2016 for GOME-2A, though the OMI QA4ECV v1.1 record is continued in an off-line processing stream at KNMI (accessible via [ER1]), also for the benefit of comparisons against S5P/TROPOMI results. Due to IT equipment issues the OMI/QA4ECV dataset ends on 29 March 2021; a follow-up dataset, based on new collection-4 OMI data, with reprocessing of the full mission, is currently being set up.

4.3 Separating stratospheric and tropospheric NO₂ with a data assimilation system

The NO₂ data processing system starts with a retrieval step that determines the NO₂ slant column density, which represents the total amount of NO₂ along the line of sight, i.e. from the Sun via the Earth's atmosphere and surface to the satellite. To determine the tropospheric NO₂ slant column density, the stratospheric NO₂ slant column density is subtracted from the total slant column provided by a DOAS retrieval performed on a spectrum of backscattered light measured by a satellite instrument, after which the tropospheric sub-column is converted to the tropospheric vertical NO₂ column.

Several approaches to estimate the stratospheric NO₂ amount have been used. The approach we follow (see Sect. 6 for details) uses NO₂ analyses from the Copernicus Atmosphere Monitoring Service (CAMS; [ER5]) system. As fall-back option, the DOMINO approach is proposed, where the fields of a chemistry transport model are adjusted by way of data assimilation to estimate the stratospheric NO₂ column consistent with the satellite observations [Boersma et al., 2011]. Other methods applied elsewhere include the following.

- a) The wave analysis method uses subsets of satellite measurements over unpolluted areas to remove known areas of pollution, i.e. areas with potentially large amounts of tropospheric NO₂, from a 24-hour composite of the satellite measured NO₂ and expands the remainder with a planetary wave analysis across the whole stratosphere, followed where necessary by a second step to mask pollution events (e.g. Bucsela et al. [2006]). This approach has been used between 2004 and 2012 for the OMI NO₂ Standard Product (SP) of NASA/KNMI.
- b) The reference sector method method uses a north-to-south region over the Pacific Ocean that is assumed to be free of tropospheric NO₂, as there are no (surface) sources of NO₂, so that all NO₂ measured is assumed to be in the stratosphere (e.g. Richter and Burrows [2002], Martin et al. [2002]). This stratospheric NO₂ is then assumed to be valid in latitudinal bands for all longitudes. In some implementations this method is extended with a spatial filtering to include other relatively clean areas across the world (e.g. Bucsela et al. [2006], Valks et al. [2011]).
- c) Image processing techniques assume that the stratospheric NO₂ shows only smooth and low-amplitude latitudinal and longitudinal variations (e.g. Leue et al. [2001], Wenig et al. [2003]). This approach will probably miss the finer details in the stratospheric NO₂ distribution (as is the case for methods *a* and *b* above). The next version of the OMI NO₂ SP will use a similar approach [Bucsela et al., 2013].
- d) Independent stratospheric NO₂ data, such as collocated limb measurements (e.g. Beirle et al. [2010], Hilboll et al. [2013b]) or data taken from a chemistry transport model (e.g. Hilboll et al. [2013a]), can be subtracted from the total (slant) column measurements to find the tropospheric NO₂ concentrations. Unfortunately limb collocated stratospheric measurements are not available for satellite retrievals from the GOME(-2), OMI, S5P/TROPOMI and Sentinel-5 sensors. Nevertheless this approach is potentially very useful for comparison and validation studies. Possible cross-calibration problems between the stratospheric and the total measurements would complicate the approach.
- e) STRatospheric Estimation Algorithm from Mainz (STREAM), [Beirle et al., 2016]. The STREAM approach is based on the total column measurements over clean, remote regions as well as over clouded scenes where the tropospheric column is effectively shielded. STREAM is a flexible and robust interpolation algorithm and does not require input from chemical transport models. It was developed as a verification algorithm for the upcoming satellite instrument TROPOMI, as a complement to the operational stratospheric correction based on data assimilation. STREAM was successfully applied to the UV/vis satellite instruments GOME 1/2, SCIAMACHY, and OMI. It overcomes some of the artifacts of previous algorithms, as it is capable of reproducing some of the gradients of stratospheric NO₂, e.g., related to the polar vortex, and reduces interpolation errors over continents.
- f) The Standard Product 2 (SP2) includes a new stratosphere-troposphere separation approach (Bucsela et al. [2013]). This approach has aspects in common with STREAM. It is based on the measurements only and

| | | |
|--|--------------------|---|
|   | S5L2PP ATBD-NO2 | Reference : KNMI-ESA-S5L2PP-ATBD-001 Version : 5.0 Date : 01 September 2023 |
| | | Page 18/89 |

uses tropospheric pollution masking and subsequent interpolation over the masked areas.

These ways of treating the stratospheric NO₂ field may not be accurate enough to capture the variability of the stratospheric NO₂ in latitudinal and longitudinal direction, as well as in time. At the same time it is not certain whether these methods do actually separate stratospheric NO₂: some of the NO₂ interpreted as "stratospheric" may be in the (higher) troposphere.

Also the assimilation approach suffers from these uncertainties, but in a different way since actual meteorological fields are used to model the dynamical and chemical variability of NO_x in the stratosphere and free troposphere. The assimilation analyses the retrieved total slant column with a strong forcing to the observations over clean regions (regions with small tropospheric column amounts). The data assimilation ensures that the model simulations of the stratospheric NO₂ column agrees closely with the satellite measurements. The modelled stratospheric NO₂ (slant column) amount is subtracted from the full column observation to derive the tropospheric column.

The use of a data assimilation system to provide stratospheric NO₂ concentrations has been shown to provide realistic results, as indicated by validation studies. For example, Hendrick et al. [2012] found a good agreement between satellite retrievals using data assimilation to estimate the stratospheric NO₂ column (GOME, SCIAMACHY and GOME-2) and ground-based measurements at the station of Jungfraujoch.

In the DOMINO data assimilation approach, meteorological fields are used to drive a chemistry transport model (CTM), while NO₂ slant column data are assimilated to regularly update the three-dimensional NO₂ distribution of the CTM. The data assimilation ensures that the model simulations of the stratospheric NO₂ column agrees closely with the satellite measurements. The advantages of the use of data assimilation are manifold:

- The system models the chemistry (diurnal cycle) and dynamics of the stratosphere based on meteorological analyses.
- Data assimilation provides a realistic error estimate of the stratospheric NO₂ column [Dirksen et al., 2011].
- The height of the tropopause, obtained from the meteorological data, provides an accurate point of separation of the stratospheric from the tropospheric NO₂ column.
- The result of the data assimilation is a comprehensive understanding of 3-D NO₂ distributions that covers the whole world, taking into account the temporal variability of the NO₂ profiles and the natural variability of the stratospheric NO₂ column amount as described by the weather analysis that drives the CTM.

4.4 NO₂ column retrieval for Sentinel-5

The Sentinel-5 data processing of total and tropospheric NO₂ (described in Sect. 6.1) will be based on the retrieval set up for the QA4ECV project, the S5P/TROPOMI mission, which in turn was based on the DOMINO system (see Sect. 4.2 on the heritage). Sentinel-5 will thus extend the long-term record of NO₂ data, produced using a reliable, well-established and well-described processing system (see Boersma et al. [2004], Boersma et al. [2007] and Boersma et al. [2011]). The Sentinel-5 data processing system will thus benefit from a number of improvements developed for and to be implemented in the DOMINO, S5P/TROPOMI and QA4ECV systems.

The Sentinel-5 NO₂ processing will take place in two locations, (cf. Sect. 6.1): the per orbit processing (DOAS, AMF, etc.) will take place at the EUMETSAT processing centre, while the data assimilation system will run externally (CAMS) and provide daily input to the EUMETSAT processing centre.

For the output format, it is the aim to be consistent with the S5P/TROPOMI developed file format. In order to comply with the SI unit definitions, the S5P/TROPOMI and Sentinel-5 NO₂ data product files give the trace gas columns in mol/m², rather than in the commonly used unit molec/cm². For convenience sake, the text and figures of this document will remain in the latter unit; only the tables listing the input (Sect. 9.2) and output (Sect. 9.3) dataset use the SI based units. The multiplication factor to convert mol/m² to molec/cm² is $N_A/10^{-4} = 6.02214 \times 10^{19}$, with N_A Avogadro's number (the multiplication factor to convert mol/m² to DU is 2241.15). Note that the (ir)radiance data is given in terms of mol/m²/... rather than photons/cm²/... since the latter is not an SI unit; the conversion factor for these is also $N_A/10^{-4}$.

4.5 NO₂ data product requirements

The GMES Sentinels-4, -5 and -5 Precursor Mission Requirements Document [RD7], the Science Requirements Document for S5P/TROPOMI [RD8] and Sentinel-5 [AD2] provide the requirements for the S5P/TROPOMI and

Table 1: NO₂ baseline data product requirements for Sentinel-5 as given in [AD2] (see also [RD7]). Depending on the scenario the least stringent of the absolute and the relative requirement applies. Note that the horizontal resolution for Sentinel-5 is $7.5 \times 7.3 \text{ km}^2$ at nadir [RD1].

| | |
|-------------------------------|--|
| Total column | $1.3 \times 10^{15} \text{ molec/cm}^2$ or 20% |
| Tropospheric column | $1.3 \times 10^{15} \text{ molec/cm}^2$ or 20% |
| Total column stability | $2.6 \times 10^{14} \text{ molec/cm}^2$ or 4% per decade |
| Tropospheric column stability | $2.6 \times 10^{14} \text{ molec/cm}^2$ or 4% per decade |


Sentinel-5 missions. These requirements are based on the findings of the CAPACITY [RD9], CAMELOT [RD10] and TRAQ [RD11] studies. The requirements for the Sentinel-5 NO₂ column data products are given in Table 1 and can be summarised as follows: The uncertainty in the NO₂ total column density shall be smaller than $1.3 \times 10^{15} \text{ molec/cm}^2$ or 20%; depending on the scenario the least stringent of the absolute and the relative requirement applies. The Level-2 product quality requirements shall be applicable for SZA (sun zenith angles) up to 80° and OZA (observation zenith angles) up to 66°. Note that these requirements refer to a set of representative test scenarios. It is not possible to meet the requirements for all pixels. In particular, when the surface albedo is very small and SZA is close to 80°, or when the scene is nearly fully cloud covered the retrieval errors will be higher.

The uncertainties stated in Table 1 include retrieval errors as well as instrument errors. Over polluted areas, air-mass factor related errors will dominate the uncertainties; these relate to uncertainties in the characterisation of clouds and aerosols and to the surface albedo. Over rural areas, with low NO₂ concentrations, errors in tropospheric NO₂ are mostly driven by random noise related to the instrument's Signal-to-Noise Ratio (SNR), uncertainties in the estimate of the stratospheric NO₂ column, and uncertainties in the NO₂ profile.

For a discussion on the error analysis of the slant and vertical NO₂ column data, see Sect. 7.

5 Instrument Overview

A description of the Sentinel 5 instrument and performance can be found in [RD1].

| | | |
|---|--------------------|---|
|  | S5L2PP ATBD-NO2 | Reference : KNMI-ESA-S5L2PP-ATBD-001 Version : 5.0 Date : 01 September 2023 |
| | | Page 20/89 |

6 Detailed algorithm description

6.1 Overview of the NO₂ retrieval algorithm

The Sentinel-5 data processing of total and tropospheric NO₂ will be based on the system set up for S5P/TROPOMI (see [RD2]), which incorporates developments made during the QA4ECV project and builds on the DOMINO processing system set up for OMI data. In this way it will extend the long-term record of NO₂ data, produced using a well-described processing system (see Boersma et al. [2004], Boersma et al. [2007] and Boersma et al. [2011]), with improvements related to Sentinel-5 and state-of-the-art scientific insights. A new aspect compared to Sentinel-5P is the direct use of Copernicus Atmosphere Monitoring Service (CAMS; [ER5]) NO₂ analyses and forecasts.

In physical terms the retrieval process consists of a three-step procedure, performed on each measured Level-1b radiance spectrum:

1. the retrieval of a total NO₂ slant column density (N_s) from the Level-1b radiance and irradiance spectra measured by Sentinel-5 using a DOAS (Differential Optical Absorption Spectroscopy) method,
2. the separation of the N_s into a stratospheric ($N_s^{\text{strat}} = N_v^{\text{strat}} * M^{\text{strat}}$) and a tropospheric (N_s^{trop}) part on the basis of information coming from a data assimilation system, and
3. the conversion of the tropospheric slant column density into a tropospheric vertical column density ($N_v^{\text{trop}} = N_s^{\text{trop}} / M^{\text{trop}}$),

where M^{trop} and M^{strat} are the tropospheric and stratospheric air-mass factor (AMFs), which are derived from a look-up table of altitude-dependent AMFs and actual, daily information on the vertical distribution of NO₂ from the TM5-MP model on a $1^\circ \times 1^\circ$ grid; the altitude-dependent AMF depends on the satellite geometry, terrain height, cloud fraction and height and surface albedo.

Figure 4 shows a schematic of the processing chain for individual Sentinel-5 Level-1b orbit data that will run at the EUMETSAT processing facility. In the figure rectangular shapes indicate processes with input and output, and parallelogram shapes are static and dynamic data files or data structures (depending on the implementation); these elements are discussed in more detail in subsequent sections. The processing starts from the Level-1b data (top-left) and also needs input from the Sentinel-5 cloud, absorbing aerosol index (AAI; note that the official trigram for the product is 'AUI') and support data products. Process configuration files are not shown in Fig. 4 for clarity; an overview of the configuration parameters is given in Appendix E.

The CAMS/CTM system, shown by the dashed block on the right in the figure, will run on an external system. It is currently foreseen that this will be the CAMS [ER5] system running at ECMWF. As fallback option this could be the TM5/DOMINO system running at KNMI, assimilating S5 real-time observations. In NRT processing the output of the CAMS/CTM system is a forecast of the NO₂ profile shapes and the pressure and temperature profiles for today based on the assimilation of NO₂ slant column data from yesterday's S5 orbits. An off-line reprocessing could be based on several products, including archived daily analyses or reanalyses from CAMS. For more information on the CAMS/CTM system, see Sect. 6.6.

6.2 DOAS NO₂ slant column fit

The baseline method to determine NO₂ total slant columns is DOAS (see Platt [1994], Platt and Stutz [2008]), but there are different ways to implement a DOAS retrieval. The official OMI processor, called OMNO2A, which provides the slant column data for the DOMINO system, uses a non-linear intensity fit approach (Boersma et al. [2011], Van Geffen et al. [2015], Van Geffen et al. [2020], [RD12]). This approach is used also for the S5P/TROPOMI processing, but in the latter the DOAS equation solver is an optimal estimation (OE) routine based on Rodgers [2000], which is also used for the wavelength calibration.

In the initial stage of the NO₂ processing of S5 using QDOAS as DOAS solver was considered, also used in the DOAS retrieval of other S5 trace gases (SO₂, HCHO, ...). But with the change to the flexible and reliable OE routine in the S5P/TROPOMI NO₂ processing (beginning of 2018), it was decided to use that processing in full for S5 NO₂. This has a number of advantages over switching to QDOAS:

- the S5P/TROPOMI NO₂ processing chain is running operationally, i.e. the full chain is known to work well

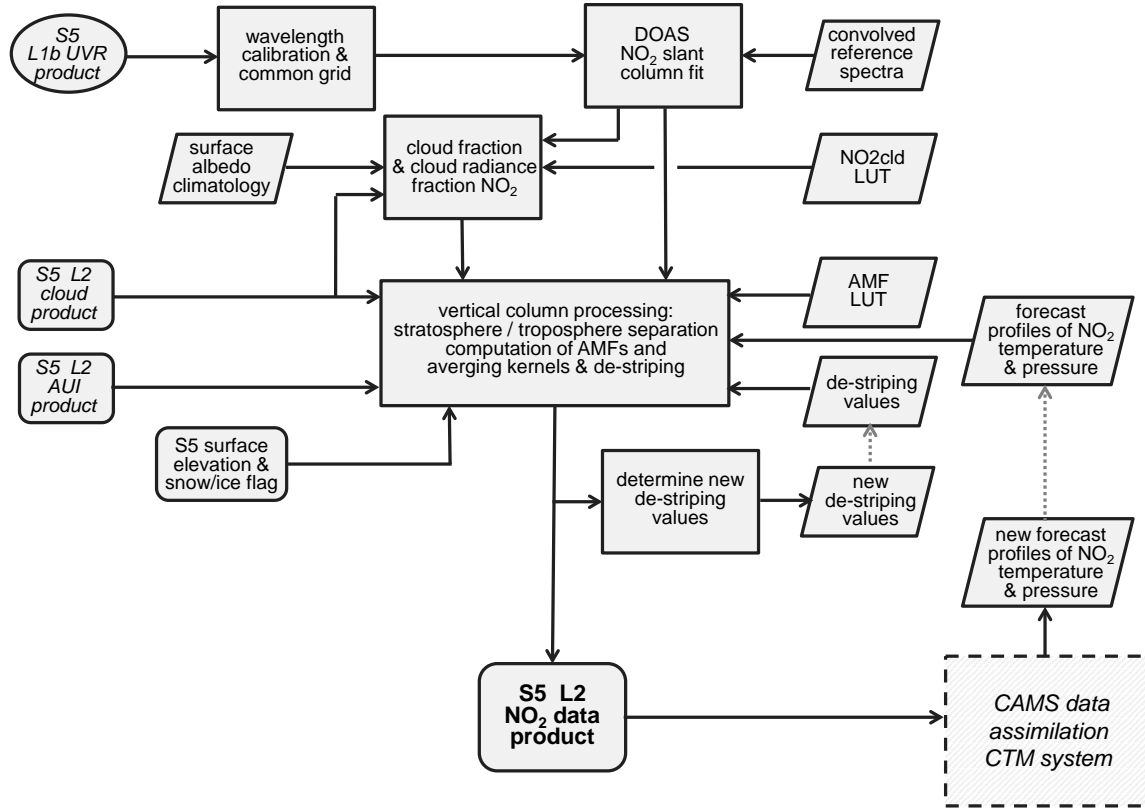


Figure 4: Per orbit process in the NO₂ retrieval system for Sentinel-5 to be run at EUMATSAT. Some elements of the Sentinel-5 Level-2 cloud data products serve as input to the NO₂ retrieval, while the AAI is passed on to the NO₂ data product as flag for the user of the data. The surface elevation and an up-to-date snow/ice flag are provided to the NO₂ processing via an auxiliary Sentinel-5 data product. The atmospheric chemistry data assimilation system on the right runs elsewhere and provides input to the EUMETSAT processing system. Process configuration files (detailed in App. E) are not shown for clarity. See Sect. 6.1 for a general description and subsequent sections for further details.

- consistency between the NO₂ processing of S5P and S5
- no adaptations of QDOAS for the NO₂ processing are needed
- calculation of the reflectance for the cloud (radiance) fraction (Sect. 6.4.1) is proven
- the S5P/TROPOMI solver includes a non-linear implementation of the correction of the Ring effect (Sect. 6.2.4), which we believe to be physically better than the way it is done in QDOAS

The following subsections describe the elements of the DOAS retrieval in detail.

6.2.1 Measured reflectance

The reflectance spectrum $R_{\text{meas}}(\lambda)$ observed by the satellite instrument is the ratio of the radiance at the top of the atmosphere, $I(\lambda)$, and the extraterrestrial solar irradiance, $E_0(\lambda)$, where I also depends on the viewing geometry, but those arguments are left out for brevity:

$$R_{\text{meas}}(\lambda) = \frac{\pi I(\lambda)}{\mu_0 E_0(\lambda)} \quad (1)$$

where E_0 and I are recorded at the same wavelength pixel on the detector and given on the same wavelength grid (see Sect. 6.2.2), and $\mu_0 = \cos(\theta_0)$ is the cosine of the solar zenith angle. The E_0 is measured once a day, when Sentinel-5 crosses the terminator along a given orbit, and this daily irradiance spectrum is used for the radiance measurements of subsequent orbits until a new E_0 is available. Since in Eq. (1) the factor π/μ_0 becomes very large at high solar zenith

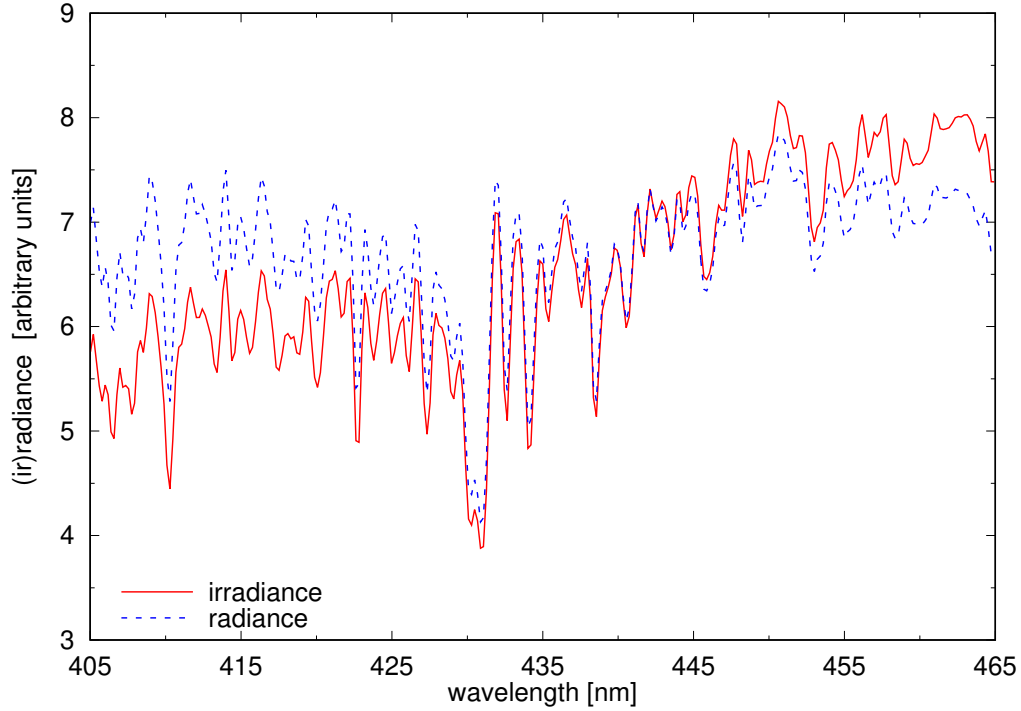


Figure 5: Example of the irradiance (red solid line) and radiance (blue dashed line) measured by S5P/TROPOMI on 4 July 2018 during orbit 03747 in the NO₂ fit window. The spectra have been scaled to fit on the same y-axis.

angle, the algorithm internally actually uses the sun-normalised radiance $I(\lambda)/E_0(\lambda)$; note that this ratio is sometimes also called reflectance. Figure 5 shows an example of E_0 and I measured by S5P/TROPOMI.

The measured reflectance will be evaluated in a specific wavelength window. For OMI and S5P/TROPOMI this is 405 – 465 nm and it is the baseline for Sentinel-5 retrievals; when real data becomes available the possible need to adapt the wavelength window will be investigated.

In order to be able to form the ratio in Eq. (1) two steps are required: $I(\lambda)$ and $E_0(\lambda)$ are wavelength calibrated and subsequently brought to a common wavelength grid; see Sect. 6.2.2.



6.2.2 Wavelength calibration & common wavelength grid

The first processing block shown in the scheme of Figure 4 depicts the wavelength calibration of the radiance and irradiance spectrum. Using the subscripts 'nom' and 'cal' to denote nominal (i.e. from the Level-1b data product) and calibrated wavelengths, respectively, the calibrated (ir)radiance to be used in Eq. (1) is given by:

$$\begin{aligned} E_0(\lambda_{\text{cal}}^{E0}) &= E_0(\lambda_{\text{nom}}^{E0} + w_s^{E0} + w_q^{E0}(\lambda_{\text{nom}}^{E0} - \lambda_0)) \\ I(\lambda_{\text{cal}}) &= I(\lambda_{\text{nom}} + w_s + w_q(\lambda_{\text{nom}} - \lambda_0)) \end{aligned} \quad (2)$$

where w_s represents a wavelength shift and w_q a wavelength stretch ($w_q > 0$) or squeeze ($w_q < 0$), with w_q defined w.r.t. the central wavelength of the fit window λ_0 . In view of numerical stability, the wavelengths are scaled to the range $[-1 : +1]$ over the fit window 405 – 465 nm, so that computationally $\lambda_0 = 0$. Each wavelength calibration of Eq. (2) comes with its own χ_w^2 as a goodness-of-fit. Once S5 Level-1b spectra are available the need to include w_q will be investigated; initially $w_q = w_q^{E0} = 0$ will be set.

The wavelength calibration uses the same wavelength calibration approach (which is described in Appendix B) for the irradiance and for the radiance, except that the radiance calibration includes a term to take the Ring effect into account. (The Ring fit coefficient, say: W_{ring} , of the radiance calibration is not a physically relevant output parameter: it is not needed in the standard output product, but it may serve as a diagnostic parameter.) This wavelength calibration is dedicated to the NO₂ fit window. For the irradiance spectra it is performed at the start of the processing of a given granule, while for the radiance spectra it is performed prior to forming the measured reflectance of Eq. (1).

| | | |
|--|--------------------|--|
|   | S5L2PP ATBD-NO2 | Reference : KNMI-ESA-S5L2PP-ATBD-001 Version : 5.0 Page Date : 01 September 2023 23/89 |
|--|--------------------|--|

In order to form the measured reflectance $R_{\text{meas}}(\lambda_{\text{cal}})$, the radiance $I(\lambda)$ and irradiance $E_0(\lambda)$ need to be brought onto a common wavelength grid, i.e. one has to be interpolated to the other; this step is assumed to be included in the wavelength calibration block in Figure 4. For S5 the same approach will be used to form the common wavelength grid as used in the OMNO2A and S5P/TROPOMI processing, where a high-sampling interpolation method (described in Appendix C) is used to interpolate $E_0(\lambda)$ to the $I(\lambda)$ wavelength grid, taking advantage of the fact that a reference solar spectrum $E_{\text{ref}}(\lambda)$ – convolved with the instrument slit function – is available at high spectral resolution. In order to avoid possible extrapolations, both these steps are performed on a wavelength range that is 1 nm wider than the fit window, i.e. the measured reflectance is formed on the common wavelength grid and then cut to the fit window.

6.2.3 Minimising the chi-squared merit function

In space-borne DOAS, $R_{\text{meas}}(\lambda)$ results from the scattering and absorption of light along the possible photon paths between Sun and satellite instrument, where λ is the common wavelength grid mentioned above, i.e. the calibrated radiance wavelength λ_{cal} ; for brevity the subscript 'cal' is omitted in the following. The effective, integrated absorption due to NO₂ along the average photon path is represented by the total NO₂ slant column density (N_s). The DOAS spectral fitting attempts to find the optimal modelled reflectance spectrum $R_{\text{mod}}(\lambda)$ by minimising the chi-squared merit function, i.e. the smallest possible differences between the observed and modelled reflectance spectrum.

In the non-linear intensity fit approach used for OMI, S5P/TROPOMI and S5, the precision of the (ir)radiance spectra is taken into account, and the merit function looks like this:

$$\chi^2 = \sum_{i=1}^{n_\lambda} \left(\frac{R_{\text{meas}}(\lambda_i) - R_{\text{mod}}(\lambda_i)}{\Delta R_{\text{meas}}(\lambda_i)} \right)^2 \quad (3)$$

with n_λ the number of wavelengths in the fit window and $\Delta R_{\text{meas}}(\lambda_i)$ the precision of the measurements, which depends on the precision of the radiance and irradiance measurements as given in the Level-1b product:

$$\Delta R_{\text{meas}}(\lambda_i) = \frac{1}{E_0(\lambda_i)} \sqrt{(\Delta I(\lambda_i))^2 + (\Delta E_0(\lambda_i))^2 \cdot (R_{\text{meas}}(\lambda_i))^2} \quad (4)$$

i.e. on the signal-to-noise (SNR) of the measurements. Radiance spectral pixels flagged in the Level-1b data as bad or as suffering from saturation are filtered out before doing any further processing step. Note that in case the precision of the (ir)radiance would not be considered, $\Delta R_{\text{meas}}(\lambda_i) = 1$ in Eq. (4).



Solving the merit function is essentially a non-linear problem due to the presence of non-linear terms (the Ring effect and, possibly, an intensity offset term) in the modelled reflectance (see Sect. 6.2.4). The S5P/TROPOMI processor, to be used for S5, contains an optimal estimation (OE) routine to perform the minimisation of the merit function. For the χ^2 minimisation suitable a-priori values of the fit parameters were selected and the a-priori errors are set very large, so as not to limit the solution of the fit, while for numerical stability reasons a pre-whitening of the data is performed. (Whitening transforms a vector of random variables with a known covariance matrix into a set of new variables whose covariance is the identity matrix, meaning that they are uncorrelated and each have variance 1; cf. Rodgers [2000], Ch. 2.)

A number of fitting diagnostics is provided by the fitting procedure. Estimated slant column and fitting coefficient uncertainties are obtained from the covariance matrix of the standard errors, which is given as a standard output of the OE procedure. The SCD error estimates are scaled with the square-root of normalised χ^2 , where χ^2 is normalised by $(n_\lambda - D)$, with n_λ the number of wavelengths in the fit window and D the degrees of freedom of the fit, which is almost equal to the number of fit parameters. All fitting coefficients are provided in the NO₂ output data file as diagnostic data.

The magnitude of χ^2 is a measure for how good the fit is. Another measure for the goodness of the fit is the so-called root-mean-square (RMS) error, which is defined as follows:

$$R_{\text{RMS}} = \sqrt{\frac{1}{n_\lambda} \sum_{i=1}^{n_\lambda} (R_{\text{meas}}(\lambda_i) - R_{\text{mod}}(\lambda_i))^2} \quad (5)$$

where the difference $R_{\text{meas}}(\lambda) - R_{\text{mod}}(\lambda)$ is usually referred to as the residual of the fit.

| | | |
|--|--------------------|--|
|   | S5L2PP ATBD-NO2 | Reference : KNMI-ESA-S5L2PP-ATBD-001 Version : 5.0 Page Date : 01 September 2023 24/89 |
|--|--------------------|--|

6.2.4 Modelled reflectance

In the intensity fit approach the modelled reflectance in Eqs. (3–5) is written as follows:

$$R_{\text{mod}}(\lambda) = P(\lambda) \cdot \exp \left[- \sum_{k=1}^{n_k} \sigma_k(\lambda) \cdot N_{s,k} \right] \cdot \left(1 + C_{\text{ring}} \frac{I_{\text{ring}}(\lambda)}{E_0(\lambda)} \right) \quad (6)$$

In this equation $\sigma_k(\lambda)$ are the cross section (i.e. reference spectrum) and $N_{s,k}$ the slant column amount of molecule $k = 1, \dots, n_k$ taken into account in the fit (NO_2 , O_3 , etc.), C_{ring} the Ring fitting coefficient and $I_{\text{ring}}(\lambda)$ the synthetic Ring spectrum (generated from an $E_{\text{ref}}(\lambda)$ reference irradiance) and $E_0(\lambda)$ the measured irradiance. The Ring spectrum describes the differential spectral signature arising from inelastic Raman scattering of incoming sunlight by N_2 and O_2 molecules. The last term in Eq. (6) describes both the contribution of elastic scattering to the differential absorption signatures (i.e. the 1), and the modification of these differential structures by inelastic scattering (the $+C_{\text{ring}} \cdot I_{\text{ring}}(\lambda)/E_0(\lambda)$ term) to the reflectance spectrum due to the Ring effect, with $E_0(\lambda)$ the measured solar spectrum, used in Eq. (1). The sources of the reference spectra used are discussed in Sect. 6.2.6.

The polynomial:

$$P(\lambda) = \sum_{m=0}^{n_p} a_m \lambda^m \quad (7)$$

is introduced to account for spectrally smooth structures resulting from molecular (single and multiple) scattering and absorption, aerosol scattering and absorption, and surface albedo effects. Because of the polynomial term, only the highly structured differential absorption features contribute to the fit of the slant column densities. As mentioned in Sect. 6.2.2 the wavelengths are scaled to the range $[-1 : +1]$ over the fit window in view of numerical stability, hence the polynomial coefficients are defined on that wavelength range.

Figure 6 shows the measured reflectance spectrum of the spectra shown in Fig. 5 and the modelled reflectance determined by the S5P/TROPOMI processor, as well as the residual spectrum of the fit. Table 2 provides an overview of the DOAS settings of the QA4ECV and S5P/TROPOMI NO_2 retrievals; the latter are the basis for the Sentinel-5 NO_2 retrievals.

Several DOAS applications include an intensity offset correction, constant or linear in wavelength, to improve the retrievals in some spectral ranges. The precise physical origin of such an intensity offset is not known, but it is thought to be related to instrumental issues (e.g. incomplete removal of straylight or dark current in Level-1b spectra) and/or atmospheric issues (e.g. incomplete removal of Ring spectrum structures, vibrational Raman scattering (VRS) in clear ocean waters); see, for example, Platt and Stutz [2008], [Richter et al., 2011], [RD13], [Lampel et al., 2015].

In Eq. (6) such an intensity offset correction would be represented by an additional term on the right hand side:

$$\dots + \frac{S_{\text{off}}}{E_0(\lambda)} \cdot \sum_{m=0}^{n_{\text{off}}} c_m \lambda^m \quad (8)$$

with S_{off} a scaling factor (configuration option) and fit parameters c_m ; in most applications $n_{\text{off}} = 0$ or 1 if an intensity offset is included. The possibility of an intensity offset correction has been implemented in the S5P/TROPOMI and S5 NO_2 slant column processors, but this option is initially turned off as (i) it has not been tested yet, (ii) we would first like to understand the physical meaning and implications of such a correction term, and (iii) we need to investigate whether it might be relevant for S5P/TROPOMI NO_2 retrievals. Therefore we do not know yet whether the intensity offset correction will be used for the Sentinel-5 NO_2 retrievals.

6.2.5 Optical density DOAS retrieval

Many implementations of DOAS deploy a linearised version of Eq. (6), including the Ring effect as a pseudo-absorber, giving the equation in terms of optical depth rather than in terms of reflectances. This so-called optical density fit approach is, for example, used in QDOAS and the QA4ECV NO_2 retrievals.

In this approach the modelled spectrum is created on the basis of the natural logarithm of the reflectance. The intensity offset, if included, is added to measured radiance, so that Eq. (1) is re-written as:

$$\ln [R_{\text{meas}}(\lambda)] = \ln \left[\frac{I(\lambda) + P_{\text{off}}(\lambda) S_{\text{off}}}{E_0(\lambda)} \right] \quad (9)$$

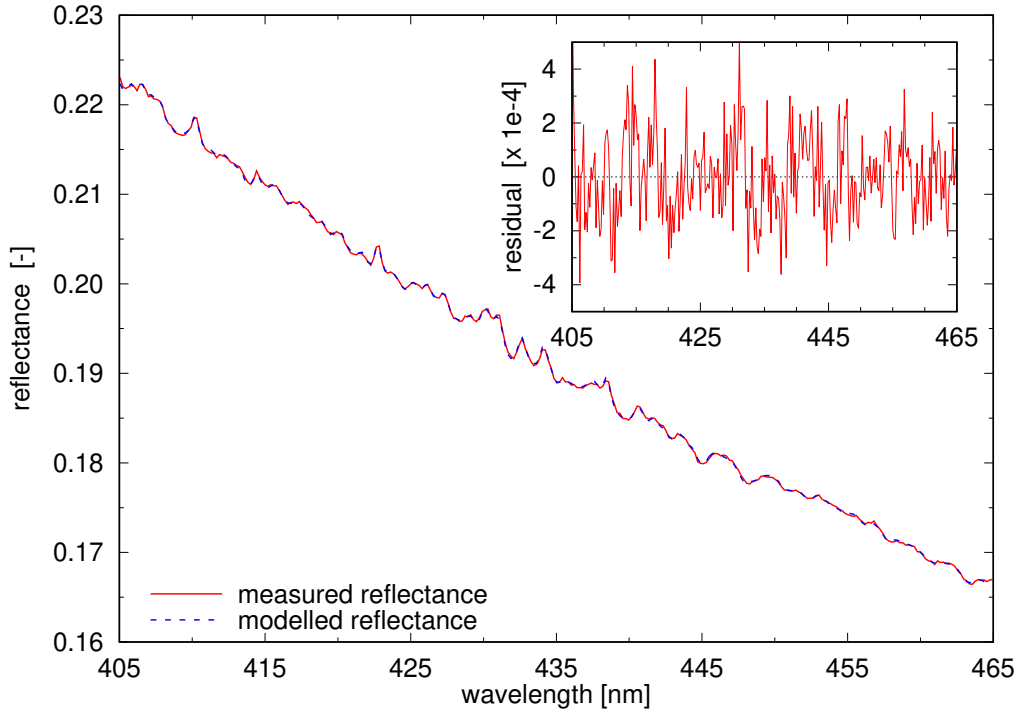


Figure 6: Example of the measured reflectance (red solid line) derived from the spectra shown in Fig. 5 and the modelled reflectance (blue dashed line) derived by the S5P/TROPOMI processor. The inset shows the residual of the fit, i.e. the measured minus the modelled reflectance spectrum; note that the vertical scale is different from the main panel. The RMS of this fit is 1.6×10^{-4} .

where the intensity offset polynomial is given by $P_{\text{off}}(\lambda) = \sum_{m=0}^{n_{\text{off}}} c_m \lambda^m$ and S_{off} is some suitable scaling factor (QDOAS computes this dynamically from some average of the measured solar spectrum $E_0(\lambda)$ in the DOAS fit window). The intercomparisons carried out within the QA4ECV project [ER2] have shown that the using a function propotional to $1/E_0(\lambda)$ gives more stable results than using $1/I(\lambda)$, as is done in several DOAS applications.

The modelled reflectance is re-written as:

$$\ln[R_{\text{mod}}(\lambda)] = P^*(\lambda) - \sum_{k=1}^{n_k} \sigma_k(\lambda) \cdot N_{s,k} - \sigma_{\text{ring}}(\lambda) \cdot C_{\text{ring}}^* \quad (10)$$

where the DOAS polynomial $P^*(\lambda)$ and the Ring parameter C_{ring}^* are similar to those in Eq. (6), but the coefficients have a somewhat different meaning. The relation between C_{ring} and C_{ring}^* is discussed briefly by Van Geffen et al. [2020].

The merit function Eq. (3) then becomes:

$$\chi^2 = \sum_{i=1}^{n_\lambda} \left(\frac{\ln[R_{\text{meas}}(\lambda_i)] - \ln[R_{\text{mod}}(\lambda_i)]}{\Delta R_{\text{meas}}(\lambda_i)} \right)^2 \quad (11)$$

where in most application QDOAS is set not to perform a weighting with the (ir)radiance precision of the (ir)radiance, in which case $\Delta R_{\text{meas}}(\lambda_i) = 1$. And the RMS of Eq. (5) becomes:

$$R_{\text{RMS}} = \sqrt{\frac{1}{n_\lambda} \sum_{i=1}^{n_\lambda} \left(\ln[R_{\text{meas}}(\lambda_i)] - \ln[R_{\text{mod}}(\lambda_i)] \right)^2} \quad (12)$$

6.2.6 Reference spectra

The selection of the reference spectra for the trace gas cross sections in the DOAS fit is driven by whether a species shows substantial absorption in the wavelength range relevant for NO_2 retrieval, and will exploit the best available









| | | |
|--|--------------------|---|
|         | S5L2PP ATBD-NO2 | Reference : KNMI-ESA-S5L2PP-ATBD-001 Version : 5.0 Date : 01 September 2023 |
| | | Page 26/89 |

Table 2: Settings for the NO₂ DOAS retrieval. The baseline settings for Sentinel-5 retrieval are the settings used in the S5P/TROPOMI NO₂ retrieval. For comparison, the settings used for the NO₂ retrieval in the QA4ECV project are given as well. Related items are grouped together through horizontal lines. The last column points to the section that discusses the setting.

| QDOAS retrieval setting | Settings for S5P/TROPOMI | Settings for OMI QA4ECV v1.1 | See Sect. |
|---|---|---|-----------|
| wavelength range | 405 – 465 nm | 405 – 465 nm | 6.2.1 |
| irradiance calibration type | prior to DOAS fit | prior to DOAS fit | 6.2.2 |
| irradiance calibration coefficients | w_s^{E0} | w_s^{E0}, w_q^{E0} | |
| radiance calibration type | prior to DOAS fit | part of DOAS fit | |
| radiance calibration coefficients | w_s | w_s, w_q | |
| common wavelength grid | $E_0(\lambda) \rightarrow I(\lambda)$ | $I(\lambda) \rightarrow E_0(\lambda)$ | 6.2.2 |
| interpolation method | high-sampling | spline | |
| least-square fit weighing | yes | no | 6.2.3 |
| type of fit | intensity | optical density | |
| max. number of iterations | 20 | 3 | |
| primary trace gas | NO ₂ | NO ₂ | 6.2.4 |
| secondary trace gases | O ₃ , O ₂ -O ₂ , | O ₃ , O ₂ -O ₂ , | & 6.2.5 |
| | H ₂ O _{vap} , H ₂ O _{liq} | H ₂ O _{vap} , H ₂ O _{liq} | |
| pseudo-absorbers | Ring | Ring | & 6.2.6 |
| DOAS polynomial n_p | 5 (6 coeff.) | 4 (5 coeff.) | |
| intensity offset polynomial n_{off} | [not used] | 0 (1 coeff.) | |
| intensity offset scale factor S_{off} | [config option] | dynamic, average of E_0 | |
| spike removal | $Q_f = 3.0$ | tolerance factor 5 | 6.2.7 |

sources. Experience with NO₂ retrievals for OMI in OMNO2A and the retrievals of multiple instruments in QA4ECV has shown that alongside NO₂ we need to account for absorption by ozone (O₃), the O₂-O₂ collision complex, water vapour (H₂O_{vap}) and liquid water (H₂O_{liq}). In addition to that Rotational Raman Scattering (RRS), i.e. the inelastic part of the Rayleigh scattering (the Ring effect), has to be accounted for. And for the wavelength calibration and the high-sampling interpolation (cf. Sect. 6.2.2), as well as for forming the pseudo cross section σ_{ring} (cf. Sect. 6.2.4) a high resolution solar reference spectrum is needed.

High-resolution laboratory measured absorption cross sections will be pre-convolved with the Sentinel-5 instrument slit function (or: instrument spectral response function, ISRF) and sampled at a resolution of 0.01 nm to create the necessary cross sections. Given the relative smoothness of these convolved cross sections, interpolation to the radiance wavelength grid (cf. Sect. 6.2.2) is performed by way of a 4th degree spline interpolation. The final set of convolved reference spectra is¹:

- trace gas cross sections $\sigma_k(\lambda)$:
 - NO₂ from Vandaele et al. [1998] at 220 K; see [ER6]
 - O₃ from Gorshchev et al. [2014] and Serdyuchenko et al. [2014] at 243 K
 - Water vapour (H₂O_{vap}) based on HITRAN 2012 data (see Van Geffen et al. [2015] and Sect. 4.1 of [RD14])
 - O₂-O₂ from Thalman and Volkamer [2013] at 293 K
 - Liquid water (H₂O_{liq}) from Pope and Frey [1997], resampled at 0.01 nm with a cubic spline interpolation
- a differential Ring cross section σ_{ring} , determined from the effective Ring spectrum $I_{ring}(\lambda)$ from Chance and Spurr [1997] and a reference solar spectrum $E_{ref}(\lambda)$ (see also Van Geffen et al. [2015] and Sect. 4.2 of [RD14])
- a high-resolution solar reference spectrum $E_{ref}(\lambda)$ from Chance and Kurucz [2010]

The temperature for the O₃, H₂O_{vap} and O₂-O₂ cross section spectra is fixed. Variation of these cross section

¹ This list is currently in line with those in use for S5P/TROPOMI; before Sentinel-5 is launched more recent reference spectra may be selected.



| | | |
|--|--------------------|--|
|   | S5L2PP ATBD-NO2 | Reference : KNMI-ESA-S5L2PP-ATBD-001 Version : 5.0 Page Date : 01 September 2023 27/89 |
|--|--------------------|--|

Table 3: Input of the wavelength calibration & common wavelength grid process.

| Parameter | Symbol | Physical Unit | Range / Remark | Source (Sect.) |
|--------------------------|-----------------------------|-----------------------------|--------------------------|------------------------|
| radiance | $I(\lambda_{nom})$ | mol/s/m ² /nm/sr | — | S5 L1b UVR product † |
| radiance error | $\Delta I(\lambda_{nom})$ | mol/s/m ² /nm/sr | — | S5 L1b UVR product † |
| irradiance | $E_0(\lambda_{nom})$ | mol/s/m ² /nm | — | S5 L1b UVR product † |
| irradiance error | $\Delta E_0(\lambda_{nom})$ | mol/s/m ² /nm | — | S5 L1b UVR product † |
| solar zenith angle | θ_0 | ° | $\theta_0 \leq 88^\circ$ | S5 L1b UVR product |
| high-res. solar spectrum | $E_{ref}(\lambda)$ | mol/s/m ² /nm | pre-convolved | auxiliary data (6.2.6) |
| effective Ring spectrum | $I_{ring}(\lambda)$ | mol/s/m ² /nm | pre-convolved | auxiliary data (6.2.6) |

†) Wavelength pixels for which the radiance and/or irradiance are flagged as bad pixel should be skipped automatically by the retrieval software.

Table 4: Output of the wavelength calibration & common wavelength grid process.

| Parameter | Symbol | Physical Unit | Range / Remark | Destination |
|-----------------------------|----------------------------------|---------------|----------------|-----------------------------------|
| measured reflectance | $R_{meas}(\lambda_{cal})$ | 1 | — | DOAS process: Table 5 |
| measured reflectance error | $\Delta R_{meas}(\lambda_{cal})$ | 1 | — | DOAS process: Table 5 |
| irradiance calib. shift * | w_s^{E0} | nm | — | NO ₂ product: Table 17 |
| irradiance calib. stretch * | w_q^{E0} | 1 | — | NO ₂ product: Table 17 |
| irradiance calib. χ^2 | $(\chi_w^{E0})^2$ | 1 | — | NO ₂ product: Table 17 |
| radiance calib. shift * | w_s | nm | — | NO ₂ product: Table 17 |
| radiance calib. stretch * | w_q | 1 | — | NO ₂ product: Table 17 |
| radiance calib. χ^2 | χ_w^2 | 1 | — | NO ₂ product: Table 17 |

Table 5: Input of the DOAS retrieval process.

| Parameter | Symbol | Physical Unit | Range / Remark | Source (Sect.) |
|--|----------------------------------|----------------------------------|--------------------------|------------------------|
| measured reflectance | $R_{meas}(\lambda_{cal})$ | 1 | — | Sect. 6.2.2, Table 4 |
| measured reflectance error | $\Delta R_{meas}(\lambda_{cal})$ | 1 | — | Sect. 6.2.2, Table 4 |
| solar zenith angle | θ_0 | ° | $\theta_0 \leq 88^\circ$ | S5 L1b UVR product |
| NO ₂ reference spectrum | $\sigma_{NO_2}(\lambda)$ | m ² /mol | pre-convolved | auxiliary data (6.2.6) |
| O ₃ reference spectrum | $\sigma_{O_3}(\lambda)$ | m ² /mol | pre-convolved | auxiliary data (6.2.6) |
| O ₂ -O ₂ reference spectrum | $\sigma_{O_2-O_2}(\lambda)$ | m ⁵ /mol ² | pre-convolved | auxiliary data (6.2.6) |
| H ₂ O _{vap} reference spectrum | $\sigma_{H_2O_{vap}}(\lambda)$ | m ² /mol | pre-convolved | auxiliary data (6.2.6) |
| H ₂ O _{liq} reference spectrum | $\sigma_{H_2O_{liq}}(\lambda)$ | 1/m | pre-convolved | auxiliary data (6.2.6) |
| effective Ring spectrum | $I_{ring}(\lambda)$ | mol/s/m ² /nm | pre-convolved | auxiliary data (6.2.6) |

†) Wavelength pixels for which the radiance and/or irradiance are flagged as bad pixel should be skipped automatically by the retrieval software.

temperatures has little effect on the fit residual in the retrieval of NO₂ slant columns, since the shape of the differential NO₂ cross section is in good approximation invariant of temperature. In the case of S5, the baseline is to use an NO₂ cross section that has been measured for 220 K.

Note that the amplitude of the differential cross section features has a significant temperature dependence which is important to account for. The resulting NO₂ slant column are corrected for deviations from 220 K at later retrieval steps, as described in Sect. 6.7.4.

6.2.7 Spike removal

In order to remove strong outliers in the DOAS fit residual (caused by, e.g., high-energy particles hitting the CCD detector, variations in the dark current, or bad pixels not correctly flagged in the Level-1b data), a "spike removal" algorithm is implemented in the DOAS process block; after removal of such an outlier from the measured reflectance, the NO₂ DOAS fit is redone to provide the final fit parameters.



| | | |
|--|--------------------|--|
|   | S5L2PP ATBD-NO2 | Reference : KNMI-ESA-S5L2PP-ATBD-001 Version : 5.0 Page Date : 01 September 2023 28/89 |
|--|--------------------|--|

Table 6: Output of the DOAS retrieval process; parameters marked with * have a corresponding error estimate $\Delta(\text{parameter})$.

| Parameter | Symbol | Physical Unit | Range / Remark | Destination |
|--|-----------------------------|----------------------------------|----------------------------|--|
| NO ₂ slant column * | N_{s,NO_2} | mol/m ² | — | NO ₂ product: Table 17 & Sect. 6.5.2 |
| O ₃ slant column * | N_{s,O_3} | mol/m ² | — | NO ₂ product: Table 17 |
| O ₂ -O ₂ slant column * | N_{s,O_2-O_2} | mol ² /m ⁵ | — | NO ₂ product: Table 17 |
| H ₂ O _{vap} slant column * | $N_{s,H_2O_{vap}}$ | mol/m ² | — | NO ₂ product: Table 17 |
| H ₂ O _{liq} slant column * | $N_{s,H_2O_{liq}}$ | m | — | NO ₂ product: Table 17 |
| Ring effect coefficient * | C_{ring} | 1 | — | NO ₂ product: Table 17 |
| polynomial coefficients * | a_m | 1 | $m = 0, 1, \dots, n_p$ | NO ₂ product: Table 17 |
| intensity offset coefficients * | c_m | 1 | $m = 0, 1, \dots, n_{off}$ | NO ₂ product: Table 17 |
| chi-squared | χ^2 | 1 | — | NO ₂ product: Table 17 |
| RMS error | R_{RMS} | 1 | — | NO ₂ product: Table 17 |
| no. of spectral points | n_λ | 1 | — | NO ₂ product: Table 17 |
| no. of iterations | n_i | 1 | — | NO ₂ product: Table 17 |
| degrees of freedom | D | 1 | — | NO ₂ product: Table 17 |
| reflectance at λ_{c,NO_2} † | $R_{mod}(\lambda_{c,NO_2})$ | 1 | — | Sect. 6.4 (Table 9) NO ₂ product: Table 17 |

†) The value of λ_{c,NO_2} is a configuration parameter; default: $\lambda_{c,NO_2} = 440$ nm.

The "spike removal" algorithm implemented for S5P/TROPOMI uses the so-called box-plot method [ER7], which determines lower and upper values based on the first and third quartiles, Q_1 and Q_3 , i.e. the 25th and 75th percentile of a distribution (the second quartile, Q_2 , is the median). If a certain value is larger than $Q_3 + Q_f \cdot Q_{3-1}$ or lower than $Q_1 - Q_f \cdot Q_{3-1}$, with $Q_{3-1} = Q_3 - Q_1$ the inter-quartile range and Q_f a suitable multiplication factor, it is termed an outlier. The so-called inner and outer fences have $Q_f = 1.5$ and $Q_f = 3.0$, respectively. As the description in the S5P/TROPOMI NO₂ ATBD ([RD2], App. F) shows, the latter fences are the better choice. Usage and threshold of the spike removal are configuration parameters (App. E.1.2).

6.2.8 Input & Output

Table 3 lists the input and Table 4 the output of the wavelength calibration & common wavelength grid step described in Sect. 6.2.2.

Table 5 lists the input and Table 6 the output of the DOAS retrieval process. Note that the input of the DOAS fit also consists of a number of configuration options – these are discussed above and summarised in Table 2; see also the list of configuration parameters in App. E.1.2.


6.2.9 Flagging in the Sentinel-5 Level-1b product

The S5L2PP will use the flag information in the Level-1b product as follows:

1. For processing-critical flags that apply to a ground pixel, an error flag for the ground pixel will be set in the Level-2 output product, and processing for the ground pixel is skipped.
2. For flags that apply to a ground pixel that potentially impact processing in a non-critical way, a warning flag for the ground pixel is set in the Level-2 output product, and processing for the ground pixel is performed.
3. For processing-critical flags that apply to a spectral pixel, the processing will assume a missing value for the spectral pixel and apply an algorithm specific evaluation of the missing values for each ground pixel
4. Flags that do not impact processing are ignored.

Summary of the Level-1b flag usage [RD15]:

- Per product:

| | | |
|---|--------------------|--|
|  | S5L2PP ATBD-NO2 | Reference : KNMI-ESA-S5L2PP-ATBD-001 Version : 5.0 Page Date : 01 September 2023 29/89 |
|---|--------------------|--|

- overall_quality_flag
Not used in processing
- Per scanline:
 - measurement_quality
Flags are applied to each ground pixel within the scanline
Error: proc_skipped, irr_out_range
Warning: south_atlantic_anomaly, spacecraft_manoeuvre
- Per ground pixel:
 - ground_pixel_quality
Error: geolocation_error
Warning: solar_eclipse, sun_glint_possible
 - spectral_calibration_quality
Error: –
Warning: any set flag (and nominal wavelength assignment will be propagated to the algorithm instead of calibrated assignment)
 - detector_column_qualification
Error: flags skipped, uvn_prepost and uvn_overscan
- Per row:
 - detector_row_qualification
Flags apply for each spectral pixel in the row, and hence impact each ground pixel in the corresponding scanline: Any set flag except for uvn_higain imply "invalid/missing" spectral pixel, and will be handled as described below.
- Per spectral pixel:
 - spectral_channel_quality
A pixel with any set flag will be treated as "invalid/missing" pixel, and be handled in an algorithm-specific way, as impact of one or more invalid spectral pixels is algorithm-specific
 - quality_level
A quality_level that is below a configurable threshold will be treated as "invalid/missing" pixel, and be handled in an algorithm-specific way, as impact of one or more invalid spectral pixels is algorithm-specific

The usage of these flags in the NO₂ processor beyond the overall usage can be summarised as follows:

- ground_pixel_quality | solar_eclipse
→ Use pixel, adjust qa_value (see App. D; factor is a configuration parameter App. E.1.3)
- ground_pixel_quality | sun_glint_possible →
Use pixel, adjust qa_value (see App. D; factor is a configuration parameter App. E.1.3)
- measurement_quality | south_atlantic_anomaly →
Use pixel, adjust qa_value (see App. D; factor is a configuration parameter App. E.1.3)
- spectral_channel_quality | all flags put together →
Do not use the spectral pixel, i.e. exclude it from the fitting process; in the S5P/TROPOMI NO₂ processor this is done by setting the error on the measurement to 10⁴ times the measurement, thus effectively removing the spectral pixel from the fit without removing it from the wavelength grid.
Depending on the number of missing spectral pixels within the NO₂ fit window, ground pixel flags may be raised:
 - If more than processing.radianceFractionMinWarning spectral pixels are missing, raise warning flag.
 - If more than processing.radianceFractionMinError spectral pixels are missing, raise error flag.
where the two fractions are configuration parameters, with in addition separate configuration parameters for saturation flagging (see App. E.1.4),
- detector_row_qualification →
Expected to be treated via the spectral_channel_quality flags, as mentioned in the summary usage list.



| | | |
|--|--------------------|--|
|   | S5L2PP ATBD-NO2 | Reference : KNMI-ESA-S5L2PP-ATBD-001 Version : 5.0 Page Date : 01 September 2023 30/89 |
|--|--------------------|--|

Table 7: Other Sentinel-5 data products needed for the NO₂ retrieval; parameters marked with * have a corresponding error estimate $\Delta(\text{parameter})$.

| Parameter | Symbol | Physical Unit | Range / Remark | Destination |
|--|------------------|---------------|----------------|---|
| <i>Sentinel-5 co-registered cloud product; Sect. 6.3.1 & 6.3.2</i> | | | | |
| surface albedo | A_s | 1 | — | NO ₂ product: Table 17 |
| cloud albedo * | A_c | 1 | — | NO ₂ product: Table 17 & Sect. 6.4.4 |
| cloud fraction * | f_{eff} | 1 | — | NO ₂ product: Table 17 |
| cloud pressure * | p_c | Pa | — | NO ₂ product: Table 17 & Sect. 6.4.4 |
| scene pressure * | p_{sc} | Pa | — | NO ₂ product: Table 17 |
| scene albedo * | A_{sc} | 1 | — | NO ₂ product: Table 17 |
| FRESCO's snow/ice flag † | — | — | — | NO ₂ product: Table 17 |

Sentinel-5 co-registered AUI product; Sect. 6.3.1 & 6.3.3

| | | | | |
|-------------------------|---|---|----------------------------|-----------------------------------|
| absorbing aerosol index | — | 1 | 354/388 nm wavelength pair | NO ₂ product: Table 17 |
|-------------------------|---|---|----------------------------|-----------------------------------|

Sentinel-5 auxiliary product; Sect. 6.3.4

| | | | | |
|-----------------------|-------------------|----|---------------|---|
| surface pressure | p_s | Pa | — | NO ₂ product: Table 17 & Sect. 6.4.4 |
| surface elevation | z_s | m | pixel-average | NO ₂ product: Table 17 & Sect. 6.4.4 |
| daily snow/ice flag † | f_{NISE} | 1 | — | NO ₂ product: Table 17 & Sect. 6.4.4 |

†) FRESCO's snow/ice flag is needed only if it differs from the snow/ice flag of the S5 auxiliary product.

6.3 Other data products needed for the NO₂ retrieval

This section discusses the Sentinel-5 data other than the Level-1b measurements needed by the NO₂ processing system, shown by the boxes on the left in Figure 4. Table 7 lists the datasets of these external data sources.

6.3.1 Co-registration of NO₂ and cloud data



A small misalignment between ground pixel field-of-view of the VIS, NIR and UV bands, used for the NO₂ retrieval (Sect. 6.2), for the cloud retrieval (Sect. 6.3.2), and for the AAI retrieval (Sect. 6.3.3), respectively, is expected for the Sentinel-5 measurements. To account for this, the S5 Level-2 cloud and AAI data are co-registered to the NO₂ data using a co-registration algorithm that is generic for all S5L2PP processors and detailed in [RD16].

The cloud pressure from the general S5 co-registration products only uses the geometric pixel area overlap for the co-registration, which may lead to the use of cloud pressures with high uncertainties in the weighted average, and therefore to high uncertainties in the final cloud pressure. For this reason the NO₂ processing uses a different approach for the cloud pressure co-registration.

From experience it is known that the cloud pressure precision is commonly underestimated and may provide insufficient protection against the inclusion of uncertainties in the co-registered cloud pressures. Using just the cloud fraction for a weighted average could be a valid solution to this issue, but to be on the safe side, both cloud fraction (f_c) and cloud pressure precision (Δp_c) are used in the weighting.

For each of the pixel overlap areas A_i , the cloud pressure weighting factor $p_{f,i}$, the factored cloud pressure $p_{c,i}^*$, the weight of the averaging w_i , and the final cloud pressure p_c^* are given by:

$$p_{f,i} = \frac{f_{c,i}}{\Delta p_{c,i}}, \quad p_{c,i}^* = p_{c,i} \cdot A_i \cdot p_{f,i}, \quad w_i = A_i \cdot p_{f,i}, \quad p_c^* = \frac{\sum_i p_{c,i}^*}{\sum_i w_i} \quad (13)$$

| | | |
|--|--------------------|---|
|   | S5L2PP ATBD-NO2 | Reference : KNMI-ESA-S5L2PP-ATBD-001 Version : 5.0 Date : 01 September 2023 |
| | | Page 31/89 |

This procedure is applied to the cloud pressure weighting only; the other cloud parameters are co-registered following the general S5 approach, i.e. just using the overlap areas. An overlap area that is < 0.001 of the total pixel area is neglected in the co-registration.

6.3.2 Sentinel-5 cloud (CLD) product

For the NO₂ data product we will include a number of datasets from the Sentinel-5 cloud product [RD17], which is similar to the FRESCO-S cloud algorithm used in, e.g., the NO₂ retrieval for S5P/TROPOMI. Some of these are used in the data assimilation system (either directly or indirectly), others are included in the NO₂ data product to serve the user. To account for a small misalignment between ground pixel field-of-view of the VIS and NIR and bands, the S5 cloud product is co-registered to the NO₂ data before usage (Sect. 6.3.1). For the NO₂ retrieval the co-registration is in particular relevant for the cloud pressure, scene pressure and scene albedo; the cloud fraction is determined for the NO₂ fit window itself (see Sect. 6.4).

The Sentinel-5 cloud product does not provide the geometric cloud fraction but rather a radiometric equivalent cloud fraction: an effective cloud fraction, f_{eff} , that results in the same top-of-atmosphere radiance as the real cloud, based on an optically thick Lambertian cloud with a fixed albedo of $A_c = 0.8$ (which may be adapted in case of very bright scenes) at the cloud pressure level, p_c . This approach has proven to be useful for trace gas retrieval, and the errors introduced to the trace gas retrievals are usually small (and minimal for a fixed cloud albedo of $A_c = 0.8$; see Wang et al. [2008], who evaluated this for ozone and NO₂) when compared to scattering cloud models (Koelemeijer et al. [2001]; Stammes et al. [2008]).

As for S5P/TROPOMI, we assume that the surface elevation dataset (Sect. 6.3.4), available in the Sentinel-5 auxiliary product and used for the Sentinel-5 cloud product, is a pixel-average representative (interpolated) terrain height from a high-resolution digital elevation map.

We note that in the OMI or QA4ECV processor use is made of the surface pressure and orography as provided by the assimilation model (TM5 in this case, based on ECMWF weather analyses). This model surface pressure is time dependent, reflecting low and high pressure weather patterns, but is provided at the model resolution, which is expected to be coarse compared to the S5 footprint.

The model surface pressure will be corrected based on the method described in Zhou et al. [2009] and Boersma et al. [2011]. This correction computes a new surface pressure based on the difference between the corresponding spatially coarse terrain height and the actual, pixel-averaged terrain height based on a high resolution digital elevation map [Maasakkers et al., 2013].

6.3.3 Sentinel-5 aerosol index (AUI) product

For the NO₂ data product we will include the Absorbing Aerosol Index (AAI) at the wavelength pair 354/388 nm from the Sentinel-5 AUI product [RD18]; this pair is chosen to be in line with the AAI pair used in OMI and S5P/TROPOMI processing. To account for a small misalignment between ground pixel field-of-view of the UV and NIR and bands, the S5 AUI product is co-registered to the NO₂ data before usage (Sect. 6.3.1).


The NO₂ retrieval itself does not use the AAI for pixel selection: it is additional information that could be of use for the NO₂ data user. In a future update, the AAI value may, however, be included in the determination of the `qa_value` (Sect. 6.8 and App. D). Configuration parameters to be able to do this are already available in the S5P/TROPOMI code (App. E.1.3); for the moment the threshold is set so large that the flag will not be raised.

6.3.4 Sentinel-5 auxiliary (AUX) product

Two datasets needed for the NO₂ data product will be delivered to the processor by way of an Sentinel-5 auxiliary product:

- the surface pressure, given at the NO₂ ground pixel
- the surface elevation, averaged over the Sentinel-5 footprint
- a daily snow/ice flag, which is discussed further in Sect. 6.4.3

Both are used in the calculation of the cloud fraction & cloud radiance fraction in the NO₂ window (Sect. 6.4) and are transferred to the NO₂ data product.

| | | |
|---|--------------------|---|
|  | S5L2PP ATBD-NO2 | Reference : KNMI-ESA-S5L2PP-ATBD-001 Version : 5.0 Date : 01 September 2023 |
| | | Page 32/89 |

6.3.5 Flagging in the CLD, AUI and AUX products



The usage of quality information from the S5 L2 external products by the NO₂ algorithm, omitting flags that originate from the Level-1b product which are listed in Sect. 6.2.9, is discussed below. This quality information is checked *after* the DOAS retrieval step (Sect. 6.2) is fully performed, so as to ensure that DOAS retrieval results are available for as many ground pixels as possible, even if further processing of the ground pixel is not possible.

6.3.5.1 Flagging in the CLD product

- General usage remark (cf. Sect. 6.3.2):
The NO₂ algorithm copies a number of data variables of the CLD product to the output file for information to the user; the cloud pressure (p_c), scene pressure (p_{sc}) and scene albedo (A_{sc}) are potentially used by the NO₂ algorithm.
This means that if an error occurred in the CLD algorithm, the cloud information cannot be used by the NO₂ algorithm, which in turn means that the vertical column calculation cannot be performed for the ground pixel in question.
- CLD product quality variable `qa_value`:
 - CLD product `qa_value` ≤ 0.5
Meaning: Pixel quality is degraded
Action: Set all cloud variables in the NO₂ product to FillValue
→ NO₂ `qa_value` = 0
 - `qa_value` > 0.5
Meaning: Pixel quality is sufficient
Action: Pixel can be used
- Error flags from the CLD algorithm are assumed to have assured that the CLD `qa_value` < 0.5 , with the above mentioned effect, and hence the NO₂ algorithm ignores these error flags without propagation:
 - `convergence_error`
 - `retrieval_error`
 - `mandatory_aux_data_missing_error`
 - `measurement_quality_error`
 - `insufficient_radiance_pixels_error`
 - `l2_wavelength_calibration_error`
 - `l2_irradiance_wavelength_calibration_error`
- Warning flags from the CLD algorithm may have had an impact on the CLD `qa_value`, with the above mentioned effect, and hence the NO₂ algorithm ignores these error flags without propagation:
 - `cloud_warning`
 - `data_range_warning`
- Filter flags from the CLD product are not used by the NO₂ algorithm and as far as known not relevant, hence the NO₂ algorithm ignores these filter flags without propagation:
 - `sza_filter`
 - `vza_filter`
 - `detector_row_qualification_error`
 - `fill_value`

6.3.5.2 Flagging in the AUI product



- General usage remark (cf. Sect. 6.3.3):
The NO₂ algorithm copies the absorbing aerosol index of the 354/388 nm pair to the output product as additional information for the user, without further use by the NO₂ algorithm (the NO₂ `qa_value` is currently not adjusted by it; cf. App. D).
- AUI product quality variable `qa_value`:

| | | |
|--|--------------------|--|
|   | S5L2PP ATBD-NO2 | Reference : KNMI-ESA-S5L2PP-ATBD-001 Version : 5.0 Page Date : 01 September 2023 33/89 |
|--|--------------------|--|

- qa_value ≤ 0.5
Meaning: Pixel quality is degraded
Action: Set absorbing aerosol index variable in the NO₂ product to FillValue
→ no effect on NO₂ qa_value
- qa_value > 0.5
Meaning: Pixel quality is sufficient
Action: Pixel can be used
- Error flags from the AUI algorithm are assumed to have assured that the AUI qa_value < 0.5 , with the above mentioned effect, and hence the NO₂ algorithm ignores these error flags without propagation:
 - mandatory_aux_data_missing_error
 - geolocation_error
 - measurement_quality_error
 - l2_wavelength_calibration_error
 - l2_irradiance_wavelength_calibration_error
- Warning flags from the AUI algorithm may have had an impact on the AUI qa_value, with the above mentioned effect, and hence the NO₂ algorithm ignores these error flags without propagation:
 - irradiance_wavelength_calibration_warning
 - radiance_wavelength_calibration_warning
 - sza_warning
 - vza_warning
 - data_range_warning
 - aui_warning
 - data_range_warning
- Filter flags from the CLD product are not used by the NO₂ algorithm and as far as known not relevant, hence the NO₂ algorithm ignores these filter flags without propagation:
 - detector_row_qualification_error

6.3.5.3 Flagging in the AUX product

- Quality variable processing_quality_flag:
 - meteo_static_fallback_warning
Meaning: Meteo data (from ECMWF) missing → Using static fallback data
Action: Ignore flag → data not relevant for the NO₂ algorithm
 - meteo_outside_validity_range_warning
Meaning: Meteo data (from ECMWF) outside validity range → Using latest available data from ECMWF
Action: Ignore flag → data not relevant for the NO₂ algorithm
 - chemistry_static_fallback_warning
Meaning: Chemistry data (from CAMS) missing → Using static fallback data
Action: Ignore flag → data not relevant for the NO₂ algorithm
 - marine_outside_validity_range_warning
Meaning: Marine data (from CMEMS) outside validity range → Using latest available data from CMEMS
Action: Ignore flag → data not relevant for the NO₂ algorithm
 - marine_static_fallback_warning
Meaning: Marine data (from CMEMS) missing → Using static fallback data
Action: Ignore flag → data not relevant for the NO₂ algorithm
 - snow_ice_meteo_fallback_warning
Meaning: Snow/ice data (from NISE) missing → Using meteo data (from ECMWF)
Action: Propagate flag → no change in qa_value of the NO₂ algorithm

| | | |
|--|--------------------|--|
|   | S5L2PP ATBD-NO2 | Reference : KNMI-ESA-S5L2PP-ATBD-001 Version : 5.0 Page Date : 01 September 2023 34/89 |
|--|--------------------|--|

- snow_ice_static_fallback_warning
Meaning: Snow/ice data (from NISE) missing and Meteo data (from ECMWF) not available → Using static fallback data
Action: Propagate flag → no change in qa_value of the NO₂ algorithm
- dem_fallback_warning
Meaning: Surface altitude is from fallback DEMB
Action: Propagate flag → no change in qa_value of the NO₂ algorithm
- tropopause_computation_fallback_warning
Meaning: Using thermal tropopause pressure according to WMO definition, because it was not possible to calculate dynamic tropopause pressure based on Potential Vorticity (PV)
Action: Ignore flag → data not relevant for the NO₂ algorithm
- default_tropopause_warning
Meaning: Using default tropopause pressure, WMO conditions not met in configured pressure interval
Action: Ignore flag → data not relevant for the NO₂ algorithm
- chemistry_reactive_gas_outside_validity_range_warning
Meaning: Chemistry data (from CAMS) outside validity range → Using latest available data from CAMS
Action: Ignore flag → data not relevant for the NO₂ algorithm
- chemistry_greenhouse_gas_outside_validity_range_warning
Meaning: Chemistry data (from CAMS) outside validity range → Using latest available data from CAMS
Action: Ignore flag → data not relevant for the NO₂ algorithm
- Quality variable qa_value:
 - qa_value ≤ 0.5
Meaning: Pixel quality is degraded
Action: Pixel can be used → warning flags relevant for the NO₂ product are present
 - qa_value > 0.5
Meaning: Pixel quality is sufficient
Action: Pixel can be used

6.4 Cloud fraction & cloud radiance fraction NO₂

6.4.1 Description

The FRESKO-S Sentinel-5 cloud product (Sect. 6.3.2) – which is based on the FRESKO+ algorithm [Wang et al., 2008] – provides, among others, an effective cloud fraction, f_{eff} , at the wavelength of the O₂ A-band around 758 nm.

Because of the large difference in wavelength between the O₂ A-band and the NO₂ retrieval window, the effective cloud fraction retrieved by FRESKO in the O₂ A-band may not be exactly representative for the cloud fraction in the NO₂ window, although Van Diedenhoven et al. [2007] found that cloud parameters retrieved from UV and O₂ A-band measurements showed good consistency for cloud fractions > 0.2; for mostly clear skies, FRESKO provides somewhat higher cloud fractions than UV-based retrievals. In addition, a (small) misalignment between ground pixel field-of-view of the VIS and NIR bands, containing the NO₂ retrieval window and the O₂ A-band, respectively, is expected for the Sentinel-5 measurements; this misalignment is accounted for in the co-registration processing step mentioned in Sect. 6.3.1.

For these reasons, the baseline option for the Sentinel-5 NO₂ retrieval is to (i) use the cloud pressure p_c from FRESKO-S and (ii) retrieve the cloud fraction ($f_{\text{eff},\text{NO}_2}$) and cloud radiance fraction (w_{NO_2}) from the NO₂ spectral window itself. The latter can be done by fitting the observed continuum top-of-atmosphere reflectance R_{TOA} to a simulated reflectance constructed with the independent pixel approximation and radiative transfer calculations for the clear-sky and cloudy-sky part of the pixel, using the appropriate surface albedo in that spectral window, A_{s,NO_2} , as forward model parameter. Here A_{s,NO_2} is taken from the albedo climatology discussed in Sect. 6.4.2) at 440 nm, interpolated linearly in time, and using nearest neighbour sampling in latitude and longitude.

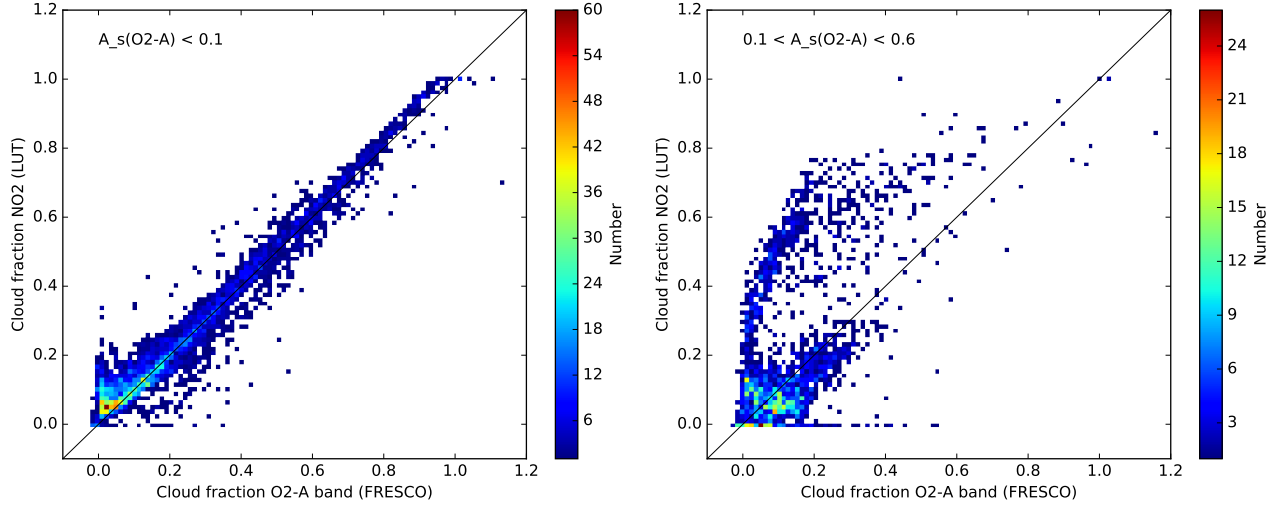


Figure 7: Comparison between the cloud fraction retrieved in the O₂ A-band by the FRESCO-S algorithm (f_{eff} ; x-axis) and in the NO₂ fit window using the new LUT approach ($f_{\text{eff,NO}_2}$; y-axis) from one GOME-2A orbit, excluding snow/ice ground pixels. The comparison is shown for ground pixels with small surface albedo in the O₂ A-band ($A_s < 0.1$; *left panel*), with an average difference between the two of 0.013 ± 0.001 , and intermediate surface albedo levels ($0.1 < A_s < 0.6$; *right panel*), typical for vegetation scenes.

The approach is very similar to FRESCO-S and explicitly accounts for Rayleigh scattering and detailed in Appendix A. The LUT assumes that the reflectance at TOA is defined as:

$$R_{\text{TOA}}(\lambda_{\text{c,NO}_2}) = \frac{\pi I(\lambda_{\text{c,NO}_2})}{\mu_0 E_0(\lambda_{\text{c,NO}_2})} \rightarrow R_{\text{mod}}(\lambda_{\text{c,NO}_2}) \quad (14)$$

which could be determined from the observed spectrum, averaged over a small wavelength interval, but that may lead to unexpected values, e.g. in case of spikes in the measurement or missing wavelength pixels. Instead, the modelled reflectance of Eq. (6) is evaluated at $\lambda_{\text{c,NO}_2} = 440$ nm, without taking the absorbing trace gases into account: $R_{\text{TOA}}(\lambda) = P(\lambda) \cdot (1 + C_{\text{ring}})$, where the C_{ring} term is included because Rayleigh scattering is a combination of elastic Cabannes scattering and inelastic Raman scattering without the spectral structures of the latter. The trace gas absorption is not taken into account here because the reflectance LUT used for the determination of the cloud fraction does not include trace gas absorption either. The cloud fraction $f_{\text{eff,NO}_2}$ is then given by:


$$f_{\text{eff,NO}_2} = \frac{R_{\text{TOA}} - R_s}{R_c - R_s} \quad (15)$$

and from these follows the cloud radiance fraction (i.e. the radiance weighted cloud fraction) in the NO₂ window:

$$w_{\text{NO}_2} = \frac{f_{\text{eff,NO}_2} R_c}{R_{\text{TOA}}} = \frac{f_{\text{eff,NO}_2} R_c}{f_{\text{eff,NO}_2} R_c + (1 - f_{\text{eff,NO}_2}) R_s} \quad (16)$$

which is used in the computation of the air-mass factor (AMF; see Sect. 6.7.5). Here R_c and R_s are the reflectances from the cloudy part and the clear-sky part of the pixel, respectively, which follow from the LUT and determine the $f_{\text{eff,NO}_2}$; see Appendix A. The NO₂ column below the clouds, i.e. the TM5-MP NO₂ profile integrated from the surface to the cloud pressure level, is called the ghost column (N_V^{ghost}). Both R_c and R_s depend on the viewing geometry, the assumed (cloud) albedo, the surface pressure and the cloud pressure. In the DOMINO v2 and TM4NO2A processing of data from OMI, GOME-2 and their predecessors, these radiances were calculated following the analytical approach of Vermote and Tanré [1992], using f_{eff} from the cloud retrieval process for the same instrument. For S5P/TROPOMI and Sentinel-5, the cloud radiance fraction will be determined using LUTs and $f_{\text{eff,NO}_2}$, the cloud fraction in the NO₂ fit window as described above.

Figure 7 shows a comparison of the effective cloud fractions from the O₂ A-band and in the NO₂ fit window for small surface albedo in the O₂ A-band ($A_s < 0.1$) and for intermediate surface albedo levels ($0.1 < A_s < 0.6$). The latter albedos are typical for vegetation scenes, for which the surface albedo is strongly wavelength dependent, which clearly

| | | |
|---|--------------------|---|
|  | S5L2PP ATBD-NO2 | Reference : KNMI-ESA-S5L2PP-ATBD-001 Version : 5.0 Date : 01 September 2023 |
| | | Page 36/89 |

leads to different cloud fractions. Given that the cloud fractions depends strongly on the underlying surface albedo and that for the two retrievals different surface albedo climatologies are used (GOME-2 for the O₂ A-band and OMI for the NO₂ window), even for low surface albedo ($A_s < 0.1$) small differences in the cloud fraction can be expected.

The nodes of the LUT limit the calculation of the $f_{\text{eff},\text{NO}_2}$ to solar zenith angles $\theta_0 \lesssim 89.93^\circ$. For solar zenith angles larger than that, we set $f_{\text{eff},\text{NO}_2}$ equal to the cloud fraction from the Sentinel-5 cloud product (f_{eff} ; see Table 7), and use that in Eq. (16).

The non-baseline option for S5 will be an explicit treatment of the angle-dependence of the surface albedo, based on the Bidirectional Reflectance Distribution Function (BRDF; see Sect. 6.4.2). This modification of the description of the albedo has direct implications for the cloud algorithm as well. In the coming years a BRDF approach for albedo, clouds and air-mass factors will be developed. The details of the approach will be given in future updates of this NO₂ ATBD.

Baseline – Cloud fractions will be determined in the NO₂ fit window, and
Cloud pressure, scene pressure and scene albedo will be retrieved from the O₂ A-band

Baseline – The cloud retrieval will be based on the Lambertian reflector approximation

Non-baseline – The cloud retrieval will account for the BRDF effects in the surface albedo

6.4.2 Surface albedo climatology

The surface albedo climatology used in recent OMI NO₂ retrieval reprocessings is the OMI Lambertian-equivalent reflectivity (LER; note that the official trigram for the product is 'RFL') product, aggregated to a grid of $0.5^\circ \times 0.5^\circ$; see Kleipool et al. [2008], which describes a climatology made from 5 years of OMI data [ER8] at 440 nm. This climatology (version 3) is also chosen as the baseline for the S5P/TROPOMI NO₂ retrievals. The climatological value of the surface albedo will be adapted in case the snow/ice flag (cf. Sect 6.4.3) indicates there may be substantial differences in albedo.

The OMI albedo climatology is considered to be the best currently available source of information for the surface albedo, because of its spectral coverage in the NO₂ fit region, its relatively high spatial resolution, and the seamless transition between land and sea. An additional advantage is that the Kleipool-climatology [Kleipool et al., 2008] has been derived from observations taken at similar local times and under similar viewing conditions as the S5P/TROPOMI observations will be taken.

Because of the different overpass time, the approach is less suitable for Sentinel-5. Besides that the Kleipool surface albedo climatology does not cover the near-infrared wavelengths in use by the FRESCO-S algorithm of the Sentinel-5 cloud product. FRESCO-S of Sentinel-5 will make use of the albedo climatology derived from GOME-2 observations from Tilstra et al. [2017] [ER9] available at $0.25^\circ \times 0.25^\circ$ resolution. GOME-2 has an overpass time similar to Sentinel-5. Because of it's availability, and because of the similar overpass time the GOME-2 climatology seems therefore the best input for the S5 NO₂ processing.

However, accounting for the anisotropic properties of surface reflectance is foreseen as a baseline for the Sentinel-5 NO₂ retrieval algorithm. At this moment work is on-going to develop an NO₂ retrieval (e.g. for OMI) using improved surface albedo data, and accounting for the BRDF effects, for instance in the QA4ECV [RD6] project. This is based on BRDF products provided by sensors like MODIS or possibly Sentinel-3. An alternative is the refinement of the GOME-2 product with a viewing angle dependency, which partly accounts for BRDF. Another very important aspect is the resolution of the albedo dataset. The GOME-2 ground pixels are very coarse compared to Sentinel-5, and the use of higher-resolution sounder data should be investigated, e.g. from Sentinel-3. This has the potential to substantially reduce the overall tropospheric NO₂ retrieval uncertainty. LER data products are foreseen based on Sentinel-5P data, which will largely improve the horizontal resolution. However, the overpass time is different which may introduce systematic biases. The availability and quality of existing albedo products will be further investigated in the coming years, and will be reported in updates of this ATBD.

Baseline – Use of GOME-2 Tilstra et al. [2017] climatology *or* the OMI Kleipool et al. [2008] climatology

Non-baseline – Use of surface albedo products (BRDF) from other satellite sources (MODIS, Sentinel-3, S5P/TROPOMI), or a refinement of the GOME-2 climatology with viewing angle dependency

Table 8: Overview of the NISE snow/ice flags $f_{\text{NISE-}}$.

| f_{NISE} | meaning |
|-------------------|---------------------------------|
| 000 | snow-free land |
| 001-100 | sea ice concentration (percent) |
| 101 | permanent ice |
| 103 | dry & wet snow |
| 252 | mixed pixels at coastlines |
| 253 | suspect ice value |
| 254 | error value |
| 255 | ocean |

6.4.3 Daily snow/ice flag

A daily snow/ice flag (at pixel centre, defined above land and ocean), e.g. based on the snow/ice cover information from NASA, the NISE product [ER10] (the NISE flag values are listed in Table 8), will be available to the NO₂ processing system via a Sentinel-5 auxiliary data product. As a fallback for missing NISE data, ECMWF snow/ice information could perhaps be used. An alternative might be the use of a snow/ice flag provided by the Sentinel-3 mission, as the origin of that data product may be of higher spatial resolution than the NISE data.

With this snow/ice flag the NO₂ processing will select which cloud parameters will be used for the determination of the AMFs and subsequent vertical NO₂ columns. When the NISE snow/ice flag, f_{NISE} , indicates that there is more than a 1% snow/ice coverage, the retrieval will move to scene mode by setting the cloud radiance fraction Eq. (16) equal to 1.0. The A_{sc} and p_{sc} from FRESKO-S are then used to determine the effective albedo and pressure of this (fictitious) cloud. Which mode is used can be found via the selection criteria of the `qa_value` definition, listed in Appendix D.

Note that the FRESCO-S algorithm used for the S5 cloud product (Sect. 6.3.2) also contains a snow/ice flag; if that flag differs from the snow/ice flag of the S5 auxiliary product the FRESCO snow/ice flag should be in the output data product file as well.

6.4.4 Input & Output

Table 9 lists the input and Table 10 the output of the cloud fraction & cloud radiance fraction NO_2 .

6.5 De-stripping the NO₂ slant columns

6.5.1 Description of the de-stripping approach

The OMI measurements show across-track biases (stripes) in NO₂ resulting from viewing zenith angle dependent calibration errors in the OMI backscatter reflectances. Given that S5 will be measuring with a CCD detector similar to the one used by OMI, the possibility of stripes occurring in the S5 NO₂ data cannot be ruled out. For this reason an option will be included in the Level-2 processor that allows for a de-striping correction on the NO₂ slant column data. A similar option has been developed for S5P/TROPOMI. Once S5 Level-1b spectra are available we will investigate whether the de-striping correction option needs to be turned on.

The de-stripping is performed on orbits over the Pacific (longitude between $150^{\circ}\text{W} - 180^{\circ}\text{W}$), and in the tropical zonal belt, in order to avoid as much as possible tropospheric pollution hotspots which may cause cross track variability. A slant column correction is determined for each viewing angle. In order to reduce noise, these correction factors are averaged over a certain time period (for OMI this is 7 days, or about 7 Pacific orbits). The corrections are stored in a stripe correction file which contains the corrections determined on the previous day. This file needs to be read during the processing of each orbit in order to apply the correction. The slant column stripe amplitudes, $N_{\text{s},\text{NO}_2}^{\text{corr}}$, will also be written to the NO_2 data product file for each orbit.

The $N_{\text{s,NO}_2}^{\text{corr}}$ amplitudes are determined and updated by comparing measured slant columns $(N)_{\text{s,NO}_2}$ with slant columns derived from the model profiles $(N_{\text{s,NO}_2}^{\text{mod}})$, using the averaging kernels (**A**) and air-mass factors (*M*) resulting from the retrieval. The correction is computed after the completion of the retrieval step of the Pacific orbits.

Table 9: Input of cloud fraction & cloud radiance fraction NO₂ process.

| Parameter | Symbol | Physical Unit | Range / Remark | Source (Sect.) |
|---------------------------------------|-----------------------------|---------------|-------------------------------|--|
| reflectance at λ_{c,NO_2} † | $R_{mod}(\lambda_{c,NO_2})$ | 1 | — | DOAS process: Table 6 as defined in Eq. (14) |
| solar zenith angle | θ_0 | ° | $\theta_0 \leq 89.93^\circ$ ‡ | S5 L1b UVR product |
| viewing zenith angle | θ | ° | $\theta \leq 89.93^\circ$ ‡ | S5 L1b UVR product |
| solar azimuth angle | ϕ_0 | ° | — | S5 L1b UVR product |
| viewing azimuth angle | ϕ | ° | — | S5 L1b UVR product |
| pixel centre longitude | ϑ_{geo} | ° | — | S5 L1b UVR product |
| pixel centre latitude | δ_{geo} | ° | — | S5 L1b UVR product |
| measurement time | t | s | — | S5 L1b UVR product |
| daily snow/ice flag | f_{NISE} | 1 | see Sect. 6.4.3 | S5 auxiliary product |
| surface elevation | z_s | m | [−500 : 16250] | S5 auxiliary product |
| surface pressure | p_s | Pa | [1076 : 95] | S5 cloud product |
| cloud albedo | A_c | 1 | — | S5 cloud product |
| cloud pressure | p_c | Pa | [1076 : 95] | S5 cloud product |
| surface albedo NO ₂ window | $A_{s,NO_{two}}$ | 1 | at 440 nm | auxiliary data (6.4.2) |
| look-up table | — | — | — | auxiliary data (6.4.1) |

†) The value of λ_{c,NO_2} is a configuration parameter; default: $\lambda_{c,NO_2} = 440$ nm.

‡) For $\theta_0 > 89.93^\circ$: f_{eff,NO_2} is set equal to the f_{eff} from the cloud product when computing w_{NO_2} ; cf. Eq. (16).

Table 10: Output of cloud fraction & cloud radiance fraction NO₂ process.

| Parameter | Symbol | Physical Unit | Range / Remark | Destination |
|---|----------------|---------------|----------------|-----------------------------------|
| cloud fraction NO ₂ | f_{eff,NO_2} | 1 | see Eq. (15) | NO ₂ product: Table 17 |
| cloud radiance fraction NO ₂ | w_{NO_2} | 1 | see Eq. (16) | NO ₂ product: Table 17 |

†) The value of λ_{c,NO_2} is an attribute to this dataset in the output.

Table 11: Input of the de-stripping correction step.

| Parameter | Symbol | Physical Unit | Range / Remark | Source (Sect.) |
|---|---------------------|--------------------|--------------------|----------------------------------|
| NO ₂ slant column | N_{s,NO_2} | mol/m ² | — | DOAS process: Table 5 |
| NO ₂ slant column computed from model a-priori | N_{s,NO_2}^{mod} | mol/m ² | — | VCD processing block (Sect. 6.7) |
| previous de-stripping amplitudes | N_{s,NO_2}^{corr} | mol/m ² | — | de-stripping data file |
| averaging kernel | A | — | — | Air-mass factor module |
| total AMF | M | — | — | Air-mass factor module |
| ground pixel index | — | — | across-track index | S5 L1b UVR product |
| scanline index | — | — | along-track index | S5 L1b UVR product |

For use in the Sentinel-5 processing chain within the S5L2PP project and later at EUMETSAT the algorithm to determine the correction factors will be removed from the air mass factor module and will be implemented as a separate processor. The application of the correction factors is part of the AMF module.

Baseline — De-stripping is available as option, but is turned off

Non-baseline — De-stripping turned on

6.5.2 Input & Output

Table 11 lists the input and Table 12 the output of the de-stripping correction process.



| | | |
|--|--------------------|---|
|   | S5L2PP ATBD-NO2 | Reference : KNMI-ESA-S5L2PP-ATBD-001 Version : 5.0 Date : 01 September 2023 |
|--|--------------------|---|

Table 12: Output of the de-stripping correction step.

| Parameter | Symbol | Physical Unit | Range / Remark | Destination |
|-----------------------------|---------------------|--------------------|----------------|--|
| new de-stripping amplitudes | N_{s,NO_2}^{corr} | mol/m ² | — | NO ₂ product: Table 17 & de-stripping data file |

6.6 The data assimilation / chemistry modelling system

6.6.1 Description

The retrieval of NO₂ is based on two main a-priori pieces of information, namely the NO₂ profile shape in the troposphere, and the column amount of NO₂ in the stratosphere. The goal is to retrieve the best possible S5 NO₂ satellite estimates on the global scale for both the NRT and Offline products, based on fully operational time-varying high-quality NO₂ profile estimates. The Copernicus Atmosphere Monitoring Service (CAMS) global NO₂ forecast product will be used as baseline to achieve this goal.

On 27 June 2023 the CAMS system received an upgrade to Cy48R1. This major upgrade introduced, among many other changes, a full stratospheric chemistry with the addition of 63 trace gas species [Huijnen et al., 2016]. A preliminary evaluation of this upgrade with TROPOMI observations shows that this upgrade of the CAMS system simulates realistic distributions and seasonal changes of the stratospheric NO₂ column [Eskes et al., 2023]. The assimilation of S5P/TROPOMI NO₂ in the CAMS real-time analysis system was activated on 13 October 2021 (with the upgrade to Cy47R3). At the time of writing the CAMS system is assimilating the tropospheric NO₂ column (TROPOMI, GOME-2). With the inclusion of stratospheric chemistry in Cy48R1 the assimilating of the total NO₂ column would be an attractive option to improve in particular the estimate of the stratospheric column and make this consistent with the satellite columns.

The operational retrievals of S5P/TROPOMI, are based on the TM5-MP chemistry-transport model, operated at KNMI. An offline reprocessing of NO₂ data for GOME, SCIAMACHY, OMI, and GOME-2 was recently completed in the European QA4ECV project based on the same system [Boersma et al., 2018]. The TM5-MP chemistry-transport model is used in these products to assimilate the NO₂ data and to produce stratospheric NO₂ column forecasts at 1 degree resolution, consistent with the satellite observations, as well as to produce space-time collocated tropospheric profiles of NO₂ used as a-priori for the tropospheric column.

The CAMS system offers several advantages over TM5-MP:

- The system is operational and the delivery of forecasts is guaranteed
- The horizontal and vertical resolution of the CAMS system is higher
- The modelling of chemistry in the troposphere and stratosphere is more advanced, and the CAMS system is an integrated self-consistent approach for both meteorology and chemistry
- The data assimilation scheme is more advanced

An advantage of the TM5-MP system is that the assimilation system has been optimised to produce a bias-free stratospheric column estimate consistent with the satellite observations. In case a total column assimilation is implemented in CAMS in the coming years, both the stratospheric NO₂ as well as the tropospheric NO₂ concentrations will be adjusted. The stratospheric column analysis is then expected to be of high quality and hopefully can be used directly to separate troposphere and stratosphere in the S5 retrieval.

However, the retrieval of tropospheric NO₂ is very sensitive to biases in the stratosphere, which will cause offsets in the tropospheric background columns. Therefore the quality of the CAMS NO₂ forecast product should be checked carefully. Estimates of uncertainties in the stratospheric column can independently be obtained by comparing the model column (kernel convoluted) with the observations over areas with a clean troposphere. When needed, bias corrections (e.g. global mean, or zonal mean) should be applied to the CAMS model forecasts to remove offsets. Figure 8 provides a simple example how this can be done.

Additional remarks:

- The S5 NO₂ retrieval will use forecasts of CAMS (not the analyses) which are typically reflecting the observations of the day before. In this way we avoid fine-scale local influences of the analysis on the observation itself over emission hotspots (which could lead to nasty systematic biases).

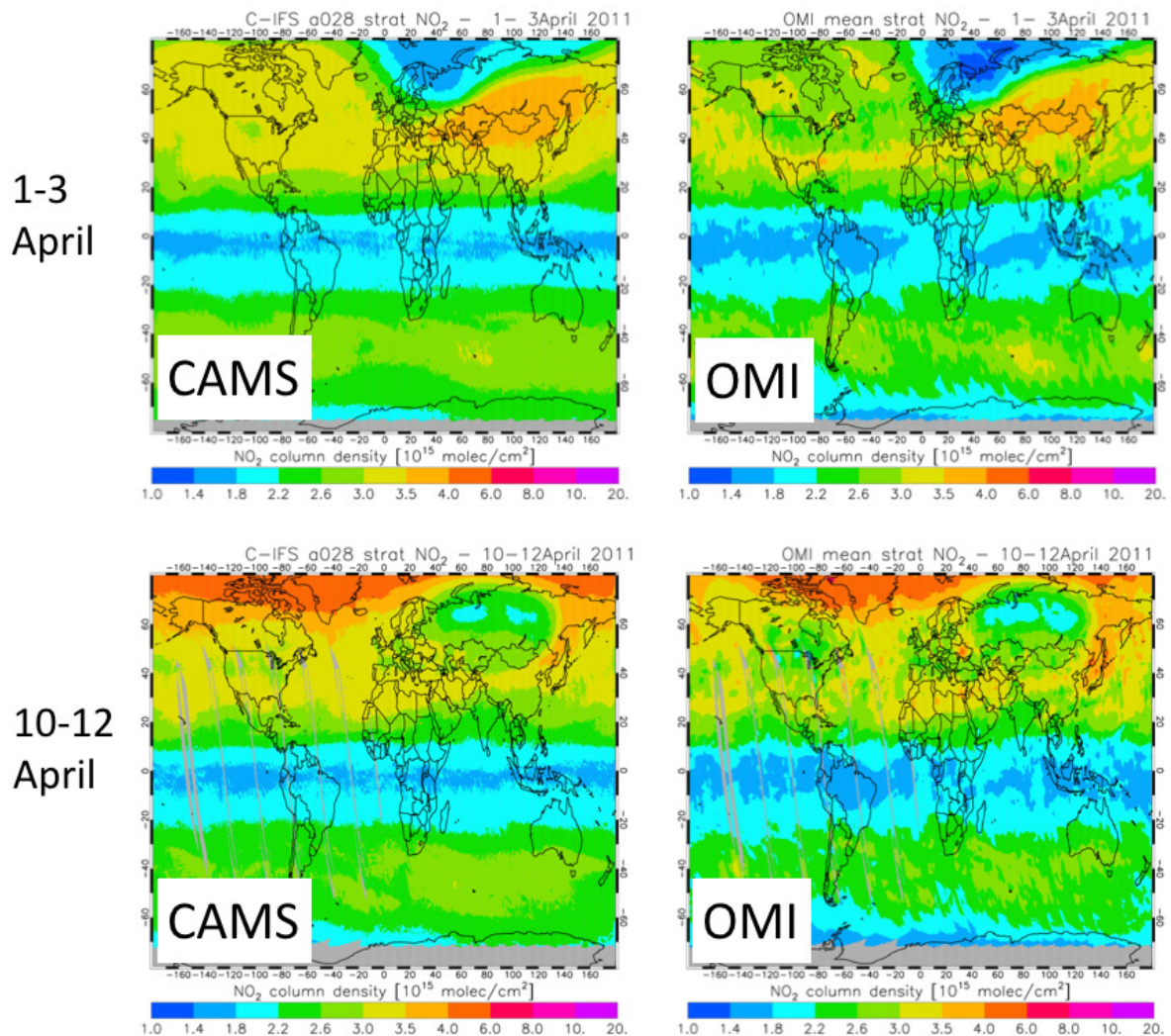


Figure 8: Comparison of the stratospheric NO₂ column from a (preliminary) free model run with the CAMS modelling system and from the QA4ECV OMI NO₂ product. The CAMS model configuration used here includes a full description of stratospheric chemistry using the chemical mechanism from the BASCOE stratospheric assimilation system included in the ECMWF Integrated Forecast System (IFS). Note that for this example the CAMS result has been bias corrected by adding 5×10^{14} molec/cm² to the modelled stratospheric column. After this correction a good match is found between the CAMS model and the OMI data product, with very similar dynamical variability and zonal dependency. This preliminary result gives confidence that CAMS results, complemented with simple bias corrections, may be efficient to provide an accurate separation of stratosphere and troposphere. (Image source: Vincent Huijnen, KNMI.)

- The CAMS analysis will make use of the averaging kernels. This implies that the analysis is NOT depending on the a-priori (which are the CAMS profiles) and there is no bootstrap issue in this respect to assimilate S5 data in the CAMS system.
- The (errors in the) diurnal variation of the model in the stratosphere could possibly result in East-West biases in the tropospheric column. Such across-track errors may be reduced with an extension of the "destriping" code discussed in Sect 6.5.
- In the coming years the CAMS analysis system is expected to adjust NO_x sources during the assimilation of the S5 (S5P) NO₂ data, in addition to adjusting concentrations as is currently done. This approach is anticipated to result in a stronger impact of the satellite data, resulting in more accurate tropospheric profiles and especially also improved forecasts.

CAMS typically provides output every 3 hours. This will cause problems especially for retrievals close to the day-night



| | | |
|---|--------------------|--|
|   | S5L2PP ATBD-NO2 | Reference : KNMI-ESA-S5L2PP-ATBD-001 Version : 5.0 Page Date : 01 September 2023 41/89 |
|---|--------------------|--|

Table 13: Output of the CAMS / CTM system.

| Parameter | Symbol | Physical Unit | Range / Remark | Destination |
|--|--------------|---------------|---|-----------------------------------|
| NO ₂ profile | n_{l,NO_2} | 1 | $l = 1, 2, \dots, n_l$ | NO ₂ product: Table 17 |
| temperature profile | T_l | K | $l = 1, 2, \dots, n_l$ | NO ₂ product: Table 17 |
| pressure level coefficients | A_l, B_l | 1 | $l = 0, 1, \dots, n_l$ | NO ₂ product: Table 17 |
| index of the tropopause pressure level | l_{tp} | — | using the WMO-1985 temperature gradient criterion | NO ₂ product: Table 17 |
| surface elevation | z_s^{mod} | m | model resolution | NO ₂ product: Table 17 |
| surface pressure | p_s^{mod} | Pa | model resolution | NO ₂ product: Table 17 |

transition (especially for higher latitudes) where NO₂ concentrations change rapidly. Two options are currently discussed with ECMWF (also for Sentinel 4), namely either CAMS provides hourly or 30 minutes output, or an efficient time interpolation method needs to be included in the processor.

The CAMS developments will be closely followed and will be described in more detail in future updates of this ATBD. As fall-back option the approach developed for S5P/TROPOMI using the TM5 model may be applied to S5 as well, either for the stratospheric column alone, or for the tropospheric profile as well.

Baseline – Use CAMS NO₂ stratospheric and tropospheric profile forecasts and analyses

Non-baseline – The TM5 modelling and assimilation system developed for S5P will be used for S5 as well

6.6.2 Input & Output

Table 13 lists the information is obtained from the CAMS/CTM system, necessary for the subsequent processing in the calculation of the AMF (see Sect. 6.7.2) needed for the conversion of the tropospheric slant column to the tropospheric vertical column and the final NO₂ data product (see Sect. 6.8).

Note that the tropopause layer is not provided directly by the CAMS system, but is computed from the CAMS temperature fields.

Note that the model divides the atmosphere in n_l layers. The pressure level coefficients determine the pressure at the $n_l + 1$ levels separating the layers: $p_l = A_l + B_l \cdot p_s$, for $l = 0, 1, \dots, n_l$, with p_s the surface pressure for the given S5 ground pixel. The pressure for the layer l , for which the concentration (volume mixing ratio) n_{l,NO_2} and the temperature T_l are given, is then midway between the level pressures p_{l-1} and p_l . And the layer with index l_{tp} contains the tropopause.

6.7 Separation of stratosphere and troposphere & vertical column calculation

The central element of the NO₂ processing chain performs a number of tasks based on the information gathered together in the above mentioned steps:

- separation of the stratospheric and tropospheric NO₂ slant columns
- application of the de-stripping correction coefficients (if turned on)
- determination of the AMFs
- calculation of the stratospheric and tropospheric NO₂ vertical columns
- calculation of the averaging kernels
- determination of new de-stripping correction coefficients (if needed)

6.7.1 Separation of stratospheric and tropospheric NO₂

Below we provide an overview of the non-baseline option of using the TM5 model (Williams et al. [2017]; Boersma et al. [2011]; Dirksen et al. [2011]; Maasakkers et al. [2013]). Details of the CAMS baseline option will be provided later.

The S5P/TROPOMI processing is based on the TM5 CTM (Huijnen et al. [2010a]; Huijnen et al. [2010b]; Williams et al. [2017]; [ER11]). This is a major improvement over the previous generation data assimilation system operated at

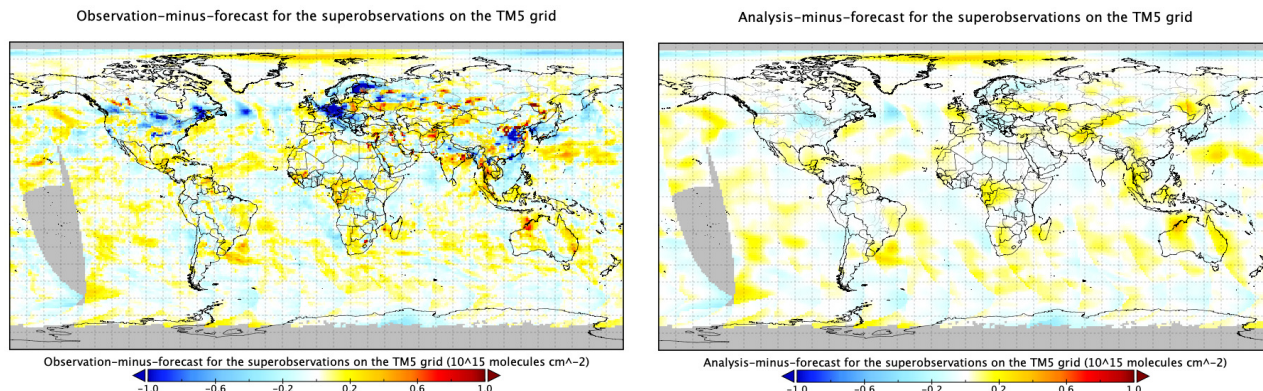


Figure 9: Observation-minus-forecast (OmF, *left panel*) and analysis-minus-forecast (AmF, *right panel*) differences in NO₂ slant columns divided by the geometric AMF, for 1 April 2018. The observations are averaged to "superobservations" on the 1° × 1° grid of the TM5-MP model. The model forecast is simulating the observations using the kernels and air-mass factors. The OmF demonstrates clear differences (dark-blue and bright-red spots) between the model forecast and TROPOMI concerning the fine-scale distribution of tropospheric pollution. The AmF plot shows that the assimilation hardly changes the tropospheric distribution, but efficiently updates the stratospheric fields over the more unpolluted regions like the oceans.

KNMI for GOME, SCIAMACHY, OMI, and GOME-2, which uses an older version of the TM CTM (TM4; e.g. Dentener et al. [2003]). The main advantage of the transition to TM5 is the better spatial resolution (1° × 1°), updated information on (NO_x) emissions, and improved description of relevant physical (photolysis rate constants) and chemical (reaction rate constants) processes in that model.

The TM5 CTM assimilates the NO₂ columns. The main purpose of this is the adjustment of the stratospheric column amount to be consistent (approximately bias-free) with the satellite observations. Because total reactive nitrogen (NO_y) is a well-conserved quantity in the stratosphere, with relatively small source and sink contributions, the information from the observations can be stored in the model over long time periods. The stratospheric wind will transport the stratospheric analysis results from the oceans and remote regions to the polluted areas.

The retrieval averaging kernels are used [Eskes and Boersma, 2003], which includes the (stratospheric and tropospheric) temperature corrections described above. The assimilation is based on the Kalman filter technique, with a prescribed parameterisation of the horizontal correlations between forecast errors, and using the concept of superobservations [Boersma et al., 2016]. A simplified modelling of the observation error is introduced [Dirksen et al., 2011] which optimises the stratospheric analysis. Effectively this approach causes only small adjustments over polluted regions, and a strong forcing to the observed NO₂ columns over clean regions (oceans and remote land areas).

Fig. 9 provides an example of the "observation minus forecast" (O–F) and the model forcing ("analysis minus forecast", A–F) for TROPOMI data of 1 April 2018. The difference between the two panels of Fig. 9 illustrates the effect of the assimilation: considerable O–F differences, resulting mostly from (anthropogenic) tropospheric NO₂ sources, have only a minor influence on the analysis. On the other hand, synoptic-scale structures in O–F persist in the A–F differences. That the A–F differences are much smaller (generally less than $\pm 0.15 \times 10^{15}$ molec/cm²) than the O–F differences (up to $\pm 1.0 \times 10^{15}$ molec/cm²) demonstrates that most tropospheric contributions are effectively discounted by the assimilation procedure.

Once the slant columns have been assimilated, the integral from the layer above the tropopause to the upper TM5 layer provides the stratospheric slant column that can be isolated from the total slant column, giving the tropospheric slant column (cf. Sect. 6.7.2):

$$N_s^{\text{trop}} = N_s - N_s^{\text{strat}} \quad (17)$$

A CTM is considered to be the best source of information for a priori NO₂ vertical profiles. For the S5 retrievals we need high spatial resolution operational model fields, and CAMS is the logical candidate. At the moment the resolution of the global forecasts is about 40 km.

The effect of the improved spatial resolution is illustrated by Figure 10, which shows the difference between averaged tropospheric NO₂ columns from the OMI sensor from 20–30 October 2004 retrieved with TM5 at 3° × 2° and at 1° × 1°.

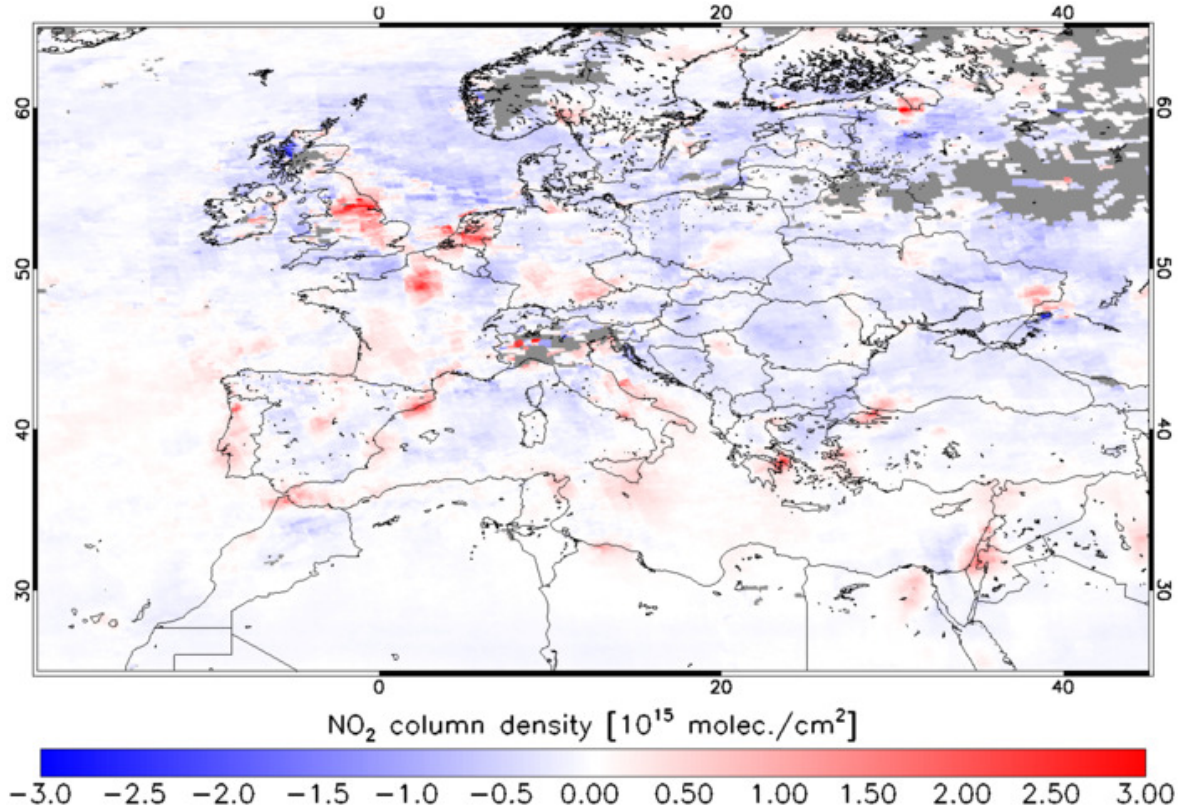


Figure 10: Tropospheric NO₂ from OMI retrieved with TM5 at a resolution of 1° × 1° minus retrieved with TM5 at a resolution of 3° × 2° for 20–30 October 2004 over Europe.

The retrieval with the higher resolution profile shapes clearly captures the pollution hotspots in Europe (e.g. Madrid, Paris) much better, leading to more pronounced contrasts between the high concentrations near the sources of pollution and lower background (ventilated) pollution levels. To better capture the sources of air pollution is an important target of the S5 mission.

6.7.2 Air-mass factor and vertical column calculations

The S5 NO₂ algorithm will use as default pre-calculated air-mass factor look-up tables to convert the tropospheric and stratospheric slant columns into meaningful vertical columns. The AMF, denoted by the symbol M , is the ratio of the slant column density of the absorbing trace gas along the (slant) optical path from sun to satellite, and the vertical column density above the point at the surface area the satellite is viewing. The total vertical column density then follows from the retrieved total slant column density:



$$N_v = N_s / M \quad (18)$$

The AMF depends on the vertical profile of the trace gas and can be written as (Palmer et al. [2001]; Eskes and Boersma [2003]):

$$M = \frac{\sum_l m_l v_l c_l}{\sum_l v_l}, \quad m_l \equiv \delta N_s / \delta v_l \quad (19)$$

with m_l the altitude dependent AMFs (see Sect. 6.7.3) that describe the vertically resolved sensitivity to NO₂, v_l the column density, and c_l the temperature correction term discussed below (see Sect. 6.7.4) for layer $l = 1, 2, \dots, n_l$ [Boersma et al., 2004]. The altitude-dependent AMFs depend on retrieval (forward model) parameters, including the satellite viewing geometry, as well as surface albedo and surface pressure, cloud fraction, and cloud pressure.

The data assimilation system provides an estimate for the stratospheric vertical profile with a stratospheric column amount (N_v^{strat}) in close agreement to the satellite observations (cf. Fig. 9). Summation over the layers above the

| | | |
|--|--------------------|--|
|   | S5L2PP ATBD-NO2 | Reference : KNMI-ESA-S5L2PP-ATBD-001 Version : 5.0 Page Date : 01 September 2023 44/89 |
|--|--------------------|--|

tropopause level ($l > l_{tp}$) to top-of-atmosphere ($l = n_l$) and multiplication with the box AMF provides the stratospheric AMF, from which the stratospheric slant column can then be calculated:

$$N_s^{\text{strat}} = N_v^{\text{strat}} \cdot M^{\text{strat}} = \sum_{l=l_{tp}+1}^{n_l} m_l v_l c_l \quad (20)$$

Note that there is a fundamental difference between N_v and N_v^{strat} . The total column N_v is a satellite-observed quantity, related to the true profiles through the averaging kernel. In contrast, the stratospheric column N_v^{strat} is a model quantity, the direct sum of the model layer subcolumns from the tropopause to the top of the atmosphere. A comparisons of N_v^{strat} with an other model or a profile measurement should therefore *not* make use of the averaging kernels!

Subtracting N_s^{strat} from the total slant column and using the tropospheric AMF, determined by adding up the layers from the surface ($l = 1$) up to and including the tropopause level ($l = l_{tp}$) in Eq. (19), then gives the tropospheric vertical column:

$$N_s^{\text{trop}} = N_s - N_s^{\text{strat}} \quad \Rightarrow \quad N_v^{\text{trop}} = N_s^{\text{trop}} / M^{\text{trop}} \quad (21)$$

Note that the total vertical column N_v in Eq. (18) is *not* the same as sum of the partial vertical columns:

$$N_v^{\text{sum}} \equiv N_v^{\text{trop}} + N_v^{\text{strat}} \neq N_v \quad (22)$$

Our best physical estimate of the NO_2 vertical column at any given place is the sum N_v^{sum} . Users who, for example, wish to assimilate NO_2 total columns should, however, use the total column N_v for this. The total column N_v depends strongly on the modelled ratio of the stratospheric and tropospheric sub-columns, a dependency which is partly removed in the summed product. For data assimilation use is made of the averaging kernels, and in this way the resulting analyses are not dependent on the a-priori (including the ratio of the model tropospheric and stratospheric column).

In the absence of atmospheric scattering and in a plane-parallel atmosphere, a so-called geometric AMF, denoted by M^{geo} , can be defined by way of a simple function of the solar zenith angle θ_0 and of the viewing zenith angle θ :

$$M^{\text{geo}} = \frac{1}{\cos \theta_0} + \frac{1}{\cos \theta} \quad (23)$$

This quantity is used in the criteria for the `qa_value` (see Appendix D) but not written to the output data product. The ratio $N_v^{\text{geo}} = N_s / M^{\text{geo}}$ could be called the geometric column density, to distinguish it from the vertical column densities computed using AMFs that contain model information [Van Geffen et al., 2020].

6.7.3 Altitude dependent AMFs

The altitude-dependent AMFs, or vertical sensitivities, are calculated with a radiative transfer model by adding a small, optically thin amount of NO_2 to the model atmosphere layer l for an atmosphere that is otherwise devoid of NO_2 , and subsequently ratioing the excess NO_2 slant column (simulated with a radiative transfer model) to the vertical column added to that layer ($m_l = \delta N_s / \delta v_l$) [Lorente et al., 2017]. The model atmosphere does not include aerosols and describes the Earth's surface as a Lambertian reflector.

As radiative transfer model we will use the Doubling-Adding KNMI (DAK) radiative transfer model (De Haan et al. [1987]; Stammes et al. [2001]), version 3.2, which has the possibility to include a pseudo-sphericity correction. The radiative transfer calculations will take the sphericity of the atmosphere into account, with Rayleigh scattering (including multiple scattering effects) and polarisation correction included (see Boersma et al. [2011] and references therein). The DAK model atmosphere consists of a Lambertian surface albedo, and an adjustable number of atmospheric layers. Atmospheric data are from the standard AFGL midlatitude summer profile. We calculate the AMF at 437.5 nm, near the middle of the spectral fitting window, for the corresponding TROPOMI NO_2 slant column retrievals; this is a suitable choice for both the small (425 – 450 nm) and wide (405 – 465 nm) fit windows, as demonstrated in the QA4ECV-project ([RD6], [ER2], see document [RD13]).

The altitude-dependent AMFs are stored in a look-up table (LUT) as a function of solar zenith angle (θ_0), viewing zenith angle (θ), relative azimuth angle (ϕ_{rel}), Lambertian surface albedo (A_s), surface pressure (p_s), and (midlevel) atmospheric pressure (p_l). This 6-dimensional LUT is to be extended with more reference points compared to earlier versions in order to respect the anticipated increase in variability of Sentinel-5 retrieval parameters (coarser OMI pixels have less variability in spatially smeared surface albedo and surface pressure values than anticipated for Sentinel-5).





| | | |
|--|--------------------|--|
|   | S5L2PP ATBD-NO2 | Reference : KNMI-ESA-S5L2PP-ATBD-001 Version : 5.0 Page Date : 01 September 2023 45/89 |
|--|--------------------|--|

Table 14: Quantities and their reference points in the AMF look-up table to be used in the Sentinel-5 NO₂ data processing to convert the tropospheric slant column into the tropospheric vertical column. The lower limit of $\cos(\theta)$ in the list is related to the maximum value of θ for Sentinel-5, which is 72° (as for OMI). Note that if BRDF effects are taken into account, the number of dimensions of this LUT will be increased.

| Quantity | Number of reference points | Values at reference points |
|---|----------------------------|---|
| Solar zenith angle $\cos(\theta_0)$ | 17 | 1.00, 0.95, 0.90, 0.80, 0.70, 0.60, 0.50, 0.45, 0.40, 0.35, 0.30, 0.25, 0.20, 0.15, 0.10, 0.05, 0.03 |
| Viewing zenith angle $\cos(\theta)$ | 11 | 1.00, 0.95, 0.90, 0.80, 0.70, 0.60, 0.50, 0.45, 0.40, 0.35, 0.30 |
| Relative azimuth angle $180^\circ - \phi - \phi_0 $ | 10 | 0°, 20°, 40°, 60°, 80°, 100°, 120°, 140°, 160°, 180° |
| Surface albedo A_s | 26 | 0.00, 0.01, 0.02, 0.03, 0.04, 0.05, 0.06, 0.07, 0.08, 0.09, 0.10, 0.12, 0.14, 0.16, 0.18, 0.20, 0.25, 0.30, 0.35, 0.40, 0.50, 0.60, 0.70, 0.80, 0.90, 1.00 |
| Surface pressure p_s [hPa] | 14 | 1048, 1036, 1024, 1013, 978, 923, 840, 754, 667, 554, 455, 372, 281, 130 |
| Atmospheric pressure p_l [hPa] | 174 | 1054.995, 1042.82, 1030.78, 1018.89, 1007.13, 995.51, 984.0309, 972.67, 961.45, 950.35, 939.39, 928.55, 917.84, 907.24, 896.71, 886.24, 875.88, 865.65, 855.54, 845.54, 835.67, 825.90, 816.26, 806.72, 797.12, 787.47, 777.93, 768.51, 759.21, 750.01, 740.93, 731.96, 723.09, 714.33, 705.65, 697.04, 688.54, 680.14, 671.85, 663.65, 655.56, 647.56, 639.66, 631.86, 624.07, 616.30, 608.62, 601.03, 593.54, 586.15, 578.85, 571.63, 564.51, 557.48, 550.44, 543.39, 536.43, 529.56, 522.77, 516.08, 509.47, 502.9492, 496.50, 490.14, 483.75, 477.32, 470.97, 464.71, 458.53, 452.44, 446.42, 440.49, 434.63, 428.86, 423.12, 417.42, 411.80, 406.26, 400.79, 395.39, 390.07, 384.82, 379.64, 374.52, 369.43, 364.37, 359.37, 354.44, 349.57, 344.78, 340.05, 335.38, 330.78, 326.24, 321.70, 317.15, 312.66, 308.24, 303.89, 299.59, 295.35, 291.18, 287.06, 283.00, 261.31, 225.35, 193.41, 165.49, 141.03, 120.12, 102.68, 87.82, 75.12, 64.30, 55.08, 47.20, 40.535, 34.79, 29.86, 25.70, 22.14, 19.08, 16.46, 14.20, 12.30, 10.69, 9.29, 8.06, 6.70, 6.11, 5.37, 4.70, 4.10, 3.57, 3.12, 2.74, 2.41, 2.12, 1.87, 1.65, 1.46, 1.29, 1.141, 1.01, 0.89, 0.79, 0.69, 0.61, 0.54, 0.48, 0.42, 0.37, 0.33, 0.29, 0.23, 0.18, 0.13, 0.10, 0.07, 0.05, 0.04, 0.030, 0.020, 0.014, 0.0099, 0.0066, 0.004471, 0.002997, 0.002005, 0.001352, 0.0009193, 0.0006300, 0.0004387, 0.000307 |

and to minimise interpolation errors when looking up the appropriate altitude-dependent AMF. Pixel-specific altitude-dependent AMFs are obtained by using the best estimates for forward model parameters and a 6-D linear interpolation scheme.

Table 14 gives an overview of the reference points for the quantities that make up the 6 dimensions. The dimensions for the LUT are chosen to balance sufficiently accurate 6-dimensional linear interpolation with computational efficiency and resource economy. For Sentinel-5, S5P/TROPOMI and future OMI NO₂ data products the slant to vertical column

| | | |
|--|--------------------|--|
|   | S5L2PP ATBD-NO2 | Reference : KNMI-ESA-S5L2PP-ATBD-001 Version : 5.0 Page Date : 01 September 2023 46/89 |
|--|--------------------|--|

conversion will not be limited in terms of θ_0 ; in practice this means the range will be the same as for the FRESCO-S cloud retrieval: $\theta_0 < 88^\circ$ (i.e. $\cos(\theta_0) = 0.035$), hence the lower limit of $\cos(\theta_0)$ of 0.03 in Table 14. (For practical implementation purposes the LUT contains the altitude-dependent air-mass factor scaled with the geometric AMF, v_l/M^{geo} , rather than v_l directly.) The `qa_value` (see Appendix D) is setup to indicate that observations with $\theta_0 > 81.2$ should not be used. Experience has shown that (observation-forecast) differences increase rapidly above this point.

A proposed innovation for S5, as compared to S5P/TROPOMI, is the inclusion of surface BRDF effects. Inclusion of the BRDF effects implies that three components of the retrieval need to be generalised simultaneously: the surface albedo, the cloud retrieval and the altitude-dependent AMFs as described above.

Several approaches exist to account for the angular dependence of the surface reflectivity. The easiest approach is the generation of a LER database that depends on the viewing angle, based on existing observations from e.g. GOME-2 or OMI. Secondly, surface BRDF information from sensors like MODIS may be translated into an effective LER. This approach has the advantage that the altitude-dependent air mass factor lookup table as described above can still be used. Third, a full surface BRDF treatment could be implemented. In this case also the cloud retrieval code should be modified to use the same surface BRDF information. The number of dimensions in the AMF LUT (Table 14) will be increased to accommodate the three parameters describing the surface BRDF.

The three alternative approaches scetched above are the topic of ongoing studies, e.g. for OMI and GOME-2. A better understanding of the advantages and disadvantages of the various approaches is desirable. The BRDF related innovation will be discussed in more detail in the updates of this ATBD.

Baseline – Altitude-dependent AMFs are computed based on the Lambertian reflectivity approach used also for S5P/TROPOMI

Non-baseline – Altitude-dependent AMFs are computed accounting for angle-dependent surface reflectivity (BRDF effects)

6.7.4 Temperature correction

For the S5 NO₂ retrieval, a temperature correction will be applied in the air-mass factor step (see Eq. (19)). The NO₂ cross-sections used in the DOAS retrieval, taken from Vandaele et al. [1998] [ER6], are valid for NO₂ at a temperature of 220 K. The temperature at which the NO₂ cross-section is evaluated does significantly influence the fit: amplitudes of the differential NO₂ absorption features decrease with increasing temperature, while the overall shape of the differential cross-section is in good approximation independent of temperature.

To account for the temperature sensitivity, a correction factor has been determined for the difference between the effective temperature of the NO₂ (which is derived from the ECMWF temperature profile and the modelled profiles in the data assimilation system) and the temperature of the cross-section, where the temperature dependence is assumed to be linear. For layer l of the NO₂ profile the correction factor c_l is:

$$c_l = 1 - 0.00316(T_l - T_\sigma) + 3.39 \times 10^{-6}(T_l - T_\sigma)^2 \quad (24)$$

with T_l and T_σ the temperature of the profile layer and cross-section, respectively. The function in Eq. (24) is an update [RD19] w.r.t. the correction used for the OMI NO₂ data in DOMINO v2 (Boersma et al. [2002], Boersma et al. [2004], Bucsela et al. [2013]). Note that the temperature sensitivity given in the above equation is determined for the default wavelength window 405 – 465 nm used for the fit; depending on the fit window and on Sentinel-5's spectral resolution details, the function may need to be adapted.

6.7.5 Cloud correction

The AMF formulation accounts for cloud-contaminated pixels. Following Martin et al. [2002] and Boersma et al. [2002], the independent pixel approximation (IPA) is used to express the AMF as a linear combination of a cloudy AMF (M_{cld}) and a clear-sky AMF (M_{clr}), both for the total column and the tropospheric column:

$$M = w_{\text{NO}_2} M_{\text{cld}} + (1 - w_{\text{NO}_2}) M_{\text{clr}}, \quad M^{\text{trop}} = w_{\text{NO}_2} M_{\text{cld}}^{\text{trop}} + (1 - w_{\text{NO}_2}) M_{\text{clr}}^{\text{trop}} \quad (25)$$

with w_{NO_2} the radiance weighted cloud fraction described in Sect. 6.4.1.

In order for data users to be able to analyse the effect of a different cloud radiance fraction, e.g. in case of data product validation, both cloudy and clear-sky AMFs are written to the output product file, as is done for other data products.



| | | |
|--|--------------------|---|
|   | S5L2PP ATBD-NO2 | Reference : KNMI-ESA-S5L2PP-ATBD-001 Version : 5.0 Date : 01 September 2023 |
| | | Page 47/89 |

Table 15: Input of vertical column processing step.

| Parameter | Symbol | Physical Unit | Range / Remark | Source (Sect.) |
|-----------------------------|---|---------------|-------------------|--------------------|
| DOAS fit results | — | — | — | Table 6 |
| cloud (radiance) fraction | — | — | — | Table 10 |
| de-stripping correction | — | — | — | Table 12 |
| external cloud data product | — | — | — | Table 7 |
| CAMS/CTM output | — | — | — | Table 13 |
| AMF LUT | — | — | — | Table 14 |
| ground pixel coordinates | $\vartheta_{\text{geo}}, \delta_{\text{geo}}$ | ° | centre and corner | S5 L1b UVR product |
| viewing geometry | $\theta_0, \theta, \phi_0, \theta$ | ° | — | S5 L1b UVR product |
| measurement time | t | s | — | S5 L1b UVR product |

Table 16: Output of the vertical column processing step.

| Parameter | Symbol | Physical Unit | Range / Remark | Destination |
|------------------------------|--------------------------------|--------------------|--|-----------------------------------|
| stratospheric slant column * | $N_{\text{s}}^{\text{strat}}$ | mol/m ² | — | NO ₂ product: Table 17 |
| stratospheric vert. column * | $N_{\text{v}}^{\text{strat}}$ | mol/m ² | — | NO ₂ product: Table 17 |
| total vertical column * | N_{v} | mol/m ² | N_{s}/M | NO ₂ product: Table 17 |
| summed vertical column * | $N_{\text{v}}^{\text{sum}}$ | mol/m ² | $N_{\text{v}}^{\text{trop}} + N_{\text{v}}^{\text{strat}}$ | NO ₂ product: Table 17 |
| tropospheric AMF | M^{trop} | 1 | — | NO ₂ product: Table 17 |
| stratospheric AMF | M^{strat} | 1 | — | NO ₂ product: Table 17 |
| total AMF | M | 1 | — | NO ₂ product: Table 17 |
| cloudy tropospheric AMF | $M_{\text{cld}}^{\text{trop}}$ | 1 | — | NO ₂ product: Table 17 |
| clear-sky tropospheric AMF | $M_{\text{clr}}^{\text{trop}}$ | 1 | — | NO ₂ product: Table 17 |
| averaging kernel | A | 1 | — | NO ₂ product: Table 17 |
| ghost column | $N_{\text{v}}^{\text{ghost}}$ | mol/m ² | — | NO ₂ product: Table 17 |

6.7.6 Input & Output

Table 15 lists the input for the vertical column processing, which performs the stratosphere / troposphere separation and calculates the NO₂ vertical column products.

The output of this processing step are listed in Table 16 and in the NO₂ product overview Table 17.

6.8 The NO₂ data product

The final Sentinel-5 NO₂ vertical column data product shall have the data sets listed in Table 17. The main product is the tropospheric NO₂ column, but the file also contains all intermediate steps such as the results from the DOAS NO₂ retrieval, output from the data assimilation, cloud information, input database information, flags, uncertainties and the AMF calculation results. The attributes in the file provide full traceability of the data product (including information on processor version, settings, inputs).

Table 18 provides a list of seven main classes of possible S5 NO₂ data users and the data sets that these users will need for their applications. For notes on applying the averaging kernel, see Sect. 6.8.1. More information on the content and usage of the data product can be found in the NO₂ Product User Manual (PUM).

In order to comply with the SI unit definitions, the TROPOMI NO₂ data product file gives trace gas concentrations in mol/m², rather than in the commonly used unit molec/cm². The following multiplication factors – also provided as attributes to the data sets – enabling the user to easily make the conversions, if needed:

- The multiplication factor to convert mol/m² to molec/cm² is 6.02214×10^{19} .
- The multiplication factor to convert mol/m² to DU is 2241.15.
- The O₂-O₂ concentration is given in mol²/m⁵; the multiplication factor to convert this to the commonly used unit



| | | |
|--|--------------------|--|
|   | S5L2PP ATBD-NO2 | Reference : KNMI-ESA-S5L2PP-ATBD-001 Version : 5.0 Page Date : 01 September 2023 48/89 |
|--|--------------------|--|

Table 17: Overview of data sets for each ground pixel in the final NO₂ data product assembled for dissemination via the Sentinel-5 website. Where relevant, the precision $\Delta(\text{parameter})$ of a data set is provided as well. The processing flags at the bottom can be set by any of the process stages. A more detailed overview can be found in the data product list in Tables 23.

| Origin of data set | For each ground pixel | Symbols |
|---|---|---|
| Level-1b spectrum | measurement time ground pixel centre and corner coordinates viewing geometry data | t $\vartheta_{\text{geo}}, \delta_{\text{geo}}$ $\theta_0, \theta, \phi_0, \phi$ |
| Wavelength calibration | irradiance wavelength calibration details radiance wavelength calibration details | $w_s^{E0}, w_q^{E0}, (\chi_w^{E0})^2$ w_s, w_q, χ_w^2 |
| DOAS retrieval | NO ₂ slant column slant columns of secondary trace gases Ring effect coefficients polynomial coefficients intensity offset coefficients number of spectral points degrees of freedom RMS, χ^2 and no. iterations of the fit reflectance at $\lambda_{c,\text{NO}_2} = 440$ nm | N_{s,NO_2} $N_{\text{s},\text{O}_3}, N_{\text{s},\text{O}_2-\text{O}_2}, N_{\text{s},\text{H}_2\text{O}_{\text{vap}}}, N_{\text{s},\text{H}_2\text{O}_{\text{liq}}}$ C_{ring} $a_m [m = 0, 1, \dots, n_p]$ $c_m [m = 0, 1, \dots, n_{\text{off}}]$ n_λ D $R_{\text{RMS}}, \chi^2, n_i$ $R_{\text{mod}}(\lambda_{c,\text{NO}_2})$ |
| NO ₂ cloud fraction | cloud fraction in the NO ₂ window cloud radiance fraction in the NO ₂ window | $f_{\text{eff},\text{NO}_2}$ w_{NO_2} |
| Surface albedo climatology | surface albedo in the NO ₂ window | A_{s,NO_2} |
| S5 cloud product | cloud albedo, fraction and pressure scene pressure and albedo surface albedo used for the cloud retrieval surface pressure | A_c, f_{eff}, p_c $p_{\text{sc}}, A_{\text{sc}}$ A_s p_s |
| S5 auxiliary product | surface elevation snow/ice flag | z_s — |
| S5 AAI product | absorbing aerosol index | — |
| CAMS / CTM | model tropopause layer index model pressure level coefficients | l_{tp} A_l, B_l |
| De-stripping | NO ₂ SCD stripe amplitude | $N_{\text{s},\text{NO}_2}^{\text{corr}}$ |
| Strat / trop separation & AMF calculation | NO ₂ tropospheric vertical column NO ₂ stratospheric vertical column NO ₂ total vertical columns NO ₂ slant column stripe amplitude NO ₂ ghost column tropospheric AMF stratospheric and total AMF clear-sky and cloudy AMF averaging kernel | N_v^{trop} N_v^{strat} $N_v \equiv N_s/M, N_v^{\text{sum}} \equiv N_v^{\text{trop}} + N_v^{\text{strat}}$ $N_{\text{s},\text{NO}_2}^{\text{corr}}$ N_v^{ghost} $M^{\text{trop}}, M_{\text{clr}}^{\text{trop}}, M_{\text{cld}}^{\text{trop}}$ M^{strat}, M $M_{\text{clr}}, M_{\text{cld}}$ A |
| Processing flags | quality assurance value (qa_value) processing quality flags | f_{QA} — |

Table 18: Overview of different user applications of NO₂ data and the data sets from the S5 NO₂ data product the users will need. In addition all users may need pixel related data, such as measurement time, geolocation, viewing geometry, etc., as well as the processing and data quality flags.

| | <i>user application</i> | <i>data sets needed</i> |
|-----|--|---|
| # 1 | Tropospheric chemistry / air quality model evaluation and data assimilation Validation with tropospheric NO ₂ profile measurements (aircraft, balloon, MAX-DOAS) | $N_V^{\text{trop}}, \Delta N_V^{\text{trop, kernel}}$ $M^{\text{trop}}, M, \mathbf{A}^{\dagger}$ $A_l^{\text{TM5}}, B_l^{\text{TM5}}, l_{\text{tp}}^{\text{TM5}}, p_s$ f_{QA} |
| # 2 | Tropospheric column comparisons, e.g. with other NO ₂ column retrievals | $N_V^{\text{trop}}, \Delta N_V^{\text{trop}}$ f_{QA} |
| # 3 | Stratospheric chemistry model evaluation and data assimilation Validation with stratospheric NO ₂ profile measurements (limb/occultation satellite observations) | $N_V^{\text{strat}}, \Delta N_V^{\text{strat}} \ddagger$ $A_l^{\text{TM5}}, B_l^{\text{TM5}}, l_{\text{tp}}^{\text{TM5}}, p_s$ f_{QA} |
| # 4 | Stratospheric column comparisons, e.g. with ground-based remote sensors | $N_V^{\text{strat}}, \Delta N_V^{\text{strat}}$ f_{QA} |
| # 5 | Whole atmosphere (troposphere + stratosphere) data assimilation systems | $N_V, \Delta N_V^{\text{kernel}}, \mathbf{A}^{\S}$ $A_l^{\text{TM5}}, B_l^{\text{TM5}}, l_{\text{tp}}^{\text{TM5}}, p_s$ f_{QA} |
| # 6 | Whole atmosphere (troposphere + stratosphere) comparisons with ground-based remote sensing (e.g. Pandora) | $N_V^{\text{sum}}, \Delta N_V^{\text{sum}} \S$ f_{QA} |
| # 7 | Visualisation of the NO ₂ product, as well as generation of Level-3 gridded and time averaged NO ₂ fields | $N_V^{\text{trop}}, N_V^{\text{strat}}, N_V^{\text{sum}} \S$ f_{QA} |

[†] The tropospheric kernel \mathbf{A}^{trop} is derived from the total kernel \mathbf{A} and the air-mass factors M and M^{trop} .

[‡] The stratospheric kernel $\mathbf{A}^{\text{strat}}$ is derived from the total kernel \mathbf{A} and the air-mass factors M and M^{strat} .



[§] Note that the total NO₂ vertical column $N_V \equiv N_s/M$ is *not* the same as the sum $N_V^{\text{sum}} \equiv N_V^{\text{trop}} + N_V^{\text{strat}}$

molec²/cm⁵ is 3.62662×10^{37} .

The output for each ground pixel is accompanied by two flags indicating the status of the results of the processing and the retrieval. The "quality assurance value" (qa_value of f_{QA}) is a continuous variable, ranging from 0 (no output) to 1 (all is well). Warnings that occur during processing or results of the processing can be reasons to decrease the flag value. The qa_value is the main flag for data usage:

- qa_value > 0.75.
For most users this is the recommended pixel filter. This removes clouds (cloud radiance fraction > 0.5), scenes covered by snow/ice, errors and problematic retrievals.
- qa_value > 0.50.
This adds the good quality retrievals over clouds and over scenes covered by snow/ice. Errors and problematic retrievals are still filtered out. In particular this may be useful for assimilation and model comparison studies.

The determination of the qa_value is described in detail in Appendix D. The qa_value indicates whether the footprint is cloud covered or not, and whether there is snow or ice on the surface. It is set to 0 if anywhere in the processing an error occurred, as indicated by the processing_quality_flags. Warnings related to the South Atlantic Anomaly, sun glint, or missing non-critical input data lower the qa_value. The qa_value depends on the solar zenith angle, tropospheric air-mass factor and quality of the DOAS fit, and filters unrealistic albedo values.

| | | |
|--|--------------------|--|
|   | S5L2PP ATBD-NO2 | Reference : KNMI-ESA-S5L2PP-ATBD-001 Version : 5.0 Page Date : 01 September 2023 50/89 |
|--|--------------------|--|

The "processing quality flags" (`processing_quality_flags`) contains the individual event that led to processing failure, or a precise record of the warnings that occurred during processing. The definitions and usage of this flag is harmonised between the Level-2 data products of S5 and will be documented in the NO₂ Product User Manual (PUM).

The NO₂ data product provides the Absorbing Aerosol Index (AAI; Sect. 6.3.3) and a snow/ice flag (see Sect. 6.4.3) as additional information for the NO₂ data users. The AAI is not yet used in the flags discussed above, but this may be added in an upcoming update.

6.8.1 Averaging kernels

For each ground pixel, the S5 data product will provide the corresponding total NO₂ column averaging kernel. The averaging kernel for DOAS retrievals is equal to the altitude-dependent AMF ratioed (decoupled from the NO₂ vertical distribution) by the total air-mass factor [Eskes and Boersma, 2003]. Furthermore, the height-dependent air-mass factors include a term that corrects for the difference between the temperature of the cross section used in the DOAS fit and the actual temperature in a given layer [RD19] (cf. Sect. 6.7.4). The tropospheric averaging kernel can be obtained by scaling the total-column kernel by M/M^{trop} (see [RD20]) and setting all elements of the kernel to zero above the tropopause layer, i.e. for $l > l_{\text{tp}}$. Note that the stratospheric NO₂ column reported in the product is derived from the model after assimilation of the S5 measurements. Therefore this quantity does not have a corresponding averaging kernel.

Using the averaging kernel is important for data users who wish to minimise the discrepancies between the assumptions in the Sentinel-5 retrieval and their application of interest, for example for validation, data assimilation, or comparison to a model (e.g. Silver et al. [2013]; Boersma et al. [2016]). In particular, comparisons that make use of the kernel are no longer depending on the a-priori TM5-MP profile shape [Eskes and Boersma, 2003].

The averaging kernel should be used in validation exercises, model evaluations, and assimilation or inversion attempts with Sentinel-5 NO₂ columns whenever possible (i.e. whenever independent profile information is available). Not using the averaging kernel may lead to inflated discrepancies between the Sentinel-5 NO₂ columns and independent sources of data, as discussed in Boersma et al. [2016]. The recipe for using the averaging kernel **A** for the purpose of obtaining a model estimate of the tropospheric NO₂ column (N_v^{trop}) that can be compared to Sentinel-5 is as follows:

$$N_v^{\text{trop}} = \mathbf{A} \vec{x}_m = \sum_{l=1}^{n_l} A_l S_l x_{m,l} \quad (26)$$

where S_l are the components at the l -th vertical layer of an operator that executes a mass-conserving vertical interpolation, followed by a conversion to sub-columns (molec/cm²) in case the model vertical distribution $x_{m,l}$ is not given in those units.



Alternatively, the kernels may be used to replace the global TM5-MP a-priori profile used in the retrieval by an alternative modelled NO₂ profile shape, e.g. from a high-resolution regional chemistry-transport model (Griffin et al. [2019], Lin et al. [2014]).

6.9 Near-real time processing vs. off-line / (re-)processing

The processing chain described above reflects the NRT processing of NO₂ data from Sentinel-5 observations taking place at the EUMETSAT processing facility.

In the case of OMI-DOMINO and S5P/TROPOMI various retrieval streams are defined: near-real time processing, off-line processing and reprocessing. These alternative streams differ in their inputs and sometimes in the implementation. Based on past experiences, it is desirable to allow for improvements (upgrades) of the retrieval algorithms, and to re-process the datasets after major algorithm updates.

At the moment of writing it is not known how the off-line (re)processing will be organised for Sentinel-5. A future version of this ATBD may provide more information regarding this point.

| | | |
|--|--------------------|---|
|   | S5L2PP ATBD-NO2 | Reference : KNMI-ESA-S5L2PP-ATBD-001 Version : 5.0 Date : 01 September 2023 |
| | | Page 51/89 |

7 Error analysis

The Sentinel-5 NO₂ retrieval algorithm generates stratospheric and tropospheric vertical column densities for all pixels. Since assumptions differ considerably for stratospheric and tropospheric retrievals, the error budget for each case will be treated separately below.

The overall error for the retrieved tropospheric columns is determined through propagation of the three main error sources: (a) measurement noise and spectral fitting affecting the slant columns, (b) errors related to the separation of stratospheric and tropospheric NO₂, and (c) systematic errors due to uncertainties in model parameters such as clouds, surface albedo, and a priori profile shape, affecting the tropospheric air-mass factor. For the stratospheric NO₂ column, the errors are driven by slant column errors, errors in the estimate of the stratospheric contribution to the slant column, and stratospheric AMF (observation operator) errors.

For NO₂, the overall error budget thus consists of several different error source terms. Errors in the slant columns will be driven in part by instrumental noise (random errors), and in part by necessary choices on the physical model and reference spectra used (systematic errors). Errors in the AMF will be mostly systematic (e.g. assumptions on albedo) but will also have random contributions (e.g. from observed cloud parameters, or sampling / interpolation errors). It is thus not possible to make a clear distinction between these error types in the total error reported in the S5 NO₂ data product. This implies that by averaging S5 pixels over time or over a larger area, the random part of the overall error can be largely eliminated, but systematic effects may still persist in averaged retrievals.

Experience with errors in OMI NO₂ over polluted regions, largely stemming from theoretical error analysis and practical validation studies, indicates that overall errors on the order of 25% for individual tropospheric NO₂ column retrievals may be expected. Validation studies show that the systematic part of this error is on the order of 10-15% (e.g. Hains et al. [2010]; Irie et al. [2012]; Ma et al. [2013]). For stratospheric NO₂ columns, the errors are considerably smaller and depend mostly on the absolute accuracy of the slant columns, and on the separation of the stratospheric and tropospheric contributions. The stratospheric NO₂ column error is expected to have errors on the order of 5-10% (e.g. Hendrick et al. [2012]).

7.1 Slant column errors

Instrument noise is the main source of errors in the spectral fitting of S5 Level-1b spectra. The anticipated radiometric SNR of S5 in the 400 – 500 nm range is 1250 for an individual Level-1b spectrum [RD1]. Experience with OMI spectral fitting in the 405 – 465 nm spectral domain showed that the uncertainty in OMI NO₂ slant column densities of about 0.75×10^{15} molec/cm² in 2005 (when the SNR of OMI was 900 – 1000) to about 0.90×10^{15} molec/cm² in 2015. [Boersma et al., 2007], [Zara et al., 2018]. The quoted OMI uncertainty contains contributions from striping effects that may not occur for the S5 sensor, so 0.7×10^{15} molec/cm² is adopted as a conservative estimate for the S5 slant column error. Other, potentially systematic, errors include inaccuracies in the NO₂ cross-section spectrum (Vandaele et al. [1998]; [ER6]), in other reference spectra, notably in the Ring spectrum, and in the temperature dependence of the NO₂ cross section, but these have been shown to be of little concern for the slant column errors [Boersma et al., 2002].

Figure 11 shows as function of the SNR an estimate of the uncertainty of the retrieved slant column density determined by a DOAS fit in the wavelength window 405 – 465 nm with polynomial degree 5. Spectra were simulated with a radiative transfer code using an atmosphere with two NO₂ profiles, taken from the CAMELOT study [RD10], with the same profile shape in the stratosphere:

- (a) European background profile, simulated with a total vertical column $N_v = 2.5 \times 10^{15}$ molec/cm²
- (b) European polluted profile, simulated with a total vertical column $N_v = 7.5 \times 10^{15}$ molec/cm²

The simulations are performed with surface albedo $A_s = 0.05$, no clouds, solar zenith angle $\theta_0 = 50^\circ$, and looking down in nadir. The legend of Fig. 11 gives the total slant column N_s in 10^{15} molec/cm². The retrieved N_s varies very little with the SNR: about 3×10^{12} molec/cm² between SNR = 700 and 1100. For profile (a) the retrieved N_s is within 5% of the initial N_s and for profile (b) it is within 3%. Given this a good accuracy of the DOAS fits can be expected, with uncertainties in the range of 10 – 15% for background NO₂ cases and 5 – 10% for polluted cases.

7.2 Errors in the stratospheric (slant) columns

The analysis below is based on TM5. The analysis will have to be repeated when CAMS analyses/forecasts are used.

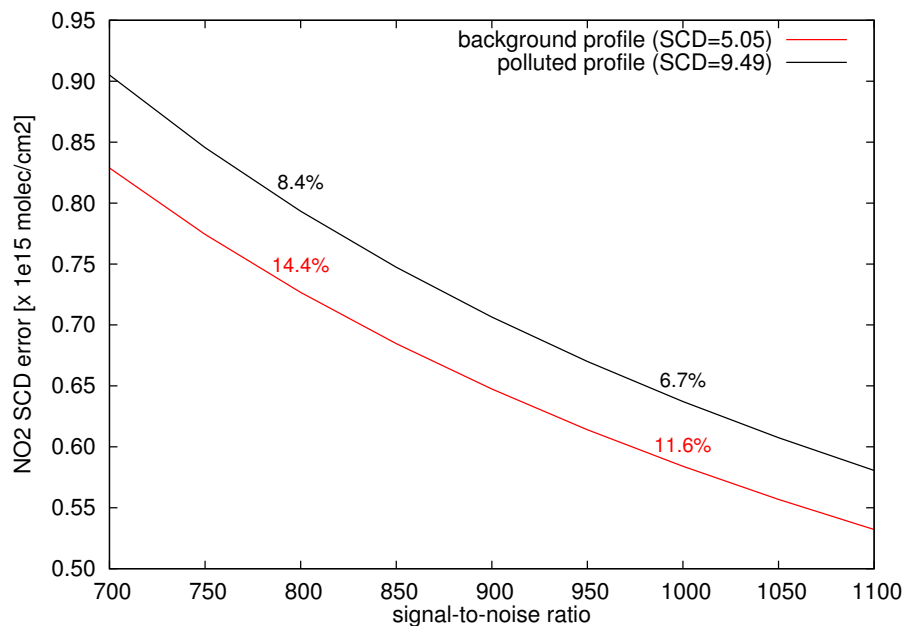


Figure 11: DOAS retrieval slant column uncertainty estimate [in 10^{15} molec/cm²] as function of the SNR for two NO₂ profiles. The plot legend gives the retrieved slant column in 10^{15} molec/cm². At SNR equal 800 and 1000 the relative slant column uncertainty is indicated. For further details see the text.

Data assimilation of S5 NO₂ slant columns in TM5 provides the estimate of the stratospheric contribution to the NO₂ slant columns. The accuracy of these estimates is largely determined by the accuracy of the slant columns, as the TM5 stratospheric NO₂ distributions are scaled to become consistent with the retrieved slant columns. Random error estimates are derived from the assimilation approach: a considerable advantage of the assimilation scheme is that it provides a statistical estimate of the uncertainties in the stratospheric (slant) columns through the standard deviation of the differences between the TM5 model analysis and forecast stratospheric NO₂ ("A-F"). Generally, the uncertainty for the stratospheric NO₂ columns is of the order of $0.1 - 0.2 \times 10^{15}$ molec/cm² similar to OMI [Dirksen et al., 2011]. This similarity with OMI is partly the result of using superobservations, which reduces the random contribution to the errors in the stratospheric slant column estimates. Fig. 9, right panel, shows the average A-F difference for 1 April 2018 in the data assimilation system based on TM5-MP. The A-F differences are on average 0.15×10^{15} molec/cm², and O-F over unpolluted scenes are about 0.2×10^{15} molec/cm². The latter is used as estimate of the uncertainties of the stratospheric NO₂ columns.

Forward (radiative transfer) model calculations are important for, but contribute little to errors in the assimilation procedure. The observation operator (see Sect. 6.7.1) is proportional to the averaging kernel [Eskes and Boersma, 2003], the vector that contains the vertical sensitivity of S5 to NO₂ in each layer. The scalar product of the observation operator vector and the TM5 NO₂ profile at the location of the individual S5 observations yields the slant column that would be observed by S5 given the modeled profile. Stratospheric radiative transfer calculations around 435 nm are relatively straightforward compared to those for the troposphere, where multiple scattering occurs, and the effects of clouds and aerosols interact with the vertical distribution of NO₂. The main forward model parameter influencing errors in the stratospheric estimate is the a priori stratospheric NO₂ profile shape (and associated temperature correction), but sensitivity tests suggest that uncertainties in the exact shape of this profile are of little influence to the overall error of the stratospheric NO₂ column.

One potential source of error is the sphericity correction in the radiative transfer model. These errors are negligible for most viewing geometries, but need to be considered for far off-nadir viewing angles and high solar zenith angles. Lorente et al. [2017] investigated the differences between stratospheric NO₂ AMFs calculated with a model simulating radiative transfer for an atmosphere spherical for incoming, single-scattered, and multiple-scattered light (McArtim), and a model with an atmosphere that is spherical for incoming light, but plane-parallel for scattered sunlight. When solar and viewing zenith angles are both large, the DAK model overestimates the stratospheric AMFs by 5-10%, which would explain the negative tropospheric NO₂ columns often encountered at high latitudes in DOMINO v2. For

Table 19: Estimate of the error in the AMF due to several error sources ('BL' stands for Boundary Layer.) The estimated AMF errors are considered to be representative of 'typical' retrieval scenarios over regions of interest, i.e. with substantial NO₂ pollution for mostly clear-sky situations, and non-extreme boundary conditions for surface albedo and pressure. Note that the uncertainties can be substantially larger for specific condition, e.g. for very small albedo and large SZA.

| Error type | Estimated error | Corresponding AMF error |
|--|----------------------------|-------------------------|
| Cloud fraction | ± 0.02 | $\pm 10\%$ |
| Cloud pressure | ± 50 hPa | $\pm [0 - 10]\%$ |
| Surface albedo | ± 0.015 | $\pm 10\%$ |
| Surface pressure | ± 20 hPa | $\pm [0 - 5]\%$ |
| A priori NO ₂ profile shape | BL height & mixing schemes | $\pm 10\%$ |
| A priori NO _x emissions | $\pm [0 - 25]\%$ | $\pm [0 - 10]\%$ |
| Aerosol-related errors | | $\pm [0 - 10]\%$ |
| Overall error | | $\pm [15 - 25]\%$ |

S5P/TROPOMI and Sentinel-5, we will therefore use an AMF LUT that is based on DAK radiative transfer simulations, but whose values for extreme viewing geometries have been made consistent with the McArtim simulations. This is the same AMF LUT that is being used in the QA4ECV retrievals of NO₂ from OMI and GOME-2A ([RD6], [ER2]).

7.3 Errors in the tropospheric air-mass factors

The tropospheric AMF is calculated with a forward model (here version 3.2 of the DAK radiative transfer model) and depends on the a priori assumed profile shape and forward model parameters (cloud fraction, cloud pressure, surface albedo, surface pressure and aerosol properties). The AMF also depends on the solar zenith, viewing zenith and relative azimuth angles, but the measurement geometry is known with high accuracy and therefore does not contribute significantly to the AMF errors. The forward model itself is assumed to represent the physics of the measurement accurately, so that forward model errors can be characterised in terms of model parameters only.

The most important AMF errors are cloud fraction, surface albedo, and a priori profile shape. Cloud parameters are obtained from S5 observations, and these will have random as well as systematic components. Surface albedo and NO₂ profile shape are obtained from a priori assumptions (i.e. a pre-calculated climatology and CTM simulations, respectively), and much depends on the accuracy of these assumptions that will be different for different retrieval situations (e.g. season, surface type etc.). Because the retrieved cloud fraction depend on similar (if not the same) surface albedo assumptions as the NO₂ air-mass factors, errors will be dampened to some extent [Boersma et al., 2004].

In Table 19 the most probable uncertainties of the forward model parameters to provide a cautious error prediction for S5 NO₂ AMFs are listed. For this the theoretical error propagation framework used in Boersma et al. [2004] is followed. This approach takes into account the sensitivity of the AMF to uncertainties around the actual value of a particular forward model parameter (e.g. the AMF is much more sensitive to albedo errors for dark surfaces than for brighter surfaces).

Aerosol-related errors are intimately coupled to cloud parameter errors. The O₂ A-band cloud algorithm currently does not correct for the presence of aerosols, so that an effective cloud fraction and cloud pressure will be retrieved. It is a matter of ongoing research whether or not the disentanglement of aerosol and cloud effects will improve the quality of the AMFs (Leitão et al. [2010]; Boersma et al. [2011]; Lin et al. [2014]).

The results in Table 19 provide a general estimate of overall retrieval uncertainties that may be expected for S5 NO₂ data under polluted conditions. In these conditions, AMF uncertainties contribute most to the retrieval uncertainties. But error analysis for individual retrievals show considerable variability on these estimates [Boersma et al., 2004]. For instance, regions with a low surface albedo are very sensitive to albedo uncertainties, and this can be reflected in AMF errors of more than 50%. For S5 NO₂ a full error propagation that takes these sensitivities into account will be provided, and as well as a unique error estimate for every pixel.



| | | |
|--|--------------------|--|
|   | S5L2PP ATBD-NO2 | Reference : KNMI-ESA-S5L2PP-ATBD-001 Version : 5.0 Page Date : 01 September 2023 54/89 |
|--|--------------------|--|

Table 20: Relative tropospheric NO₂ vertical column per pixel uncertainty due to the tropospheric AMF uncertainty only. Estimates based on QA4ECV OMI NO₂ data for selected regions for the year 2005, taken from Boersma et al. [2018].

| Region | Average AMF uncertainty | box size ranges | |
|--------------|----------------------------|-----------------|-----------|
| | | longitude | latitude |
| China | 17 - 22 % | 110 : 140 | 35 : 45 |
| USA | 17 - 27 % | −100 : −75 | 35 : 45 |
| Europe | 18 - 26 % | −10 : 15 | 40 : 55 |
| Johannesburg | 15 - 20 % | 26 : 30 | −28 : −24 |

7.4 Total errors in the tropospheric NO₂ columns

The overall error in the S5 tropospheric NO₂ columns is driven by error propagation of the error terms discussed before, i.e. (1) slant column errors, (2) errors associated with the separation of the stratospheric and tropospheric contributions to the slant column, and (3) tropospheric air-mass factor errors.

The overall error variance for each pixel is written as in Boersma et al. [2004]:

$$\langle \varepsilon^2 \rangle = \left(\frac{\sigma(N_s)}{M^{\text{trop}}} \right)^2 + \left(\frac{\sigma(N_s^{\text{strat}})}{M^{\text{trop}}} \right)^2 + \left(\frac{(N_s - N_s^{\text{strat}}) \cdot \sigma(M^{\text{trop}})}{(M^{\text{trop}})^2} \right)^2 \quad (27)$$

with $\sigma(N_s)$ the slant column error (0.7×10^{15} molec/cm²), $\sigma(N_s^{\text{strat}})$ the stratospheric slant column error (0.2×10^{15} molec/cm²) and $\sigma(M^{\text{trop}})$ the estimated error in the tropospheric air-mass factor ($\pm 25\%$). We see immediately that the total error depends on details in the retrieval and therefore differs from one pixel to the next. For small tropospheric excess slant columns, the overall retrieval uncertainty is dominated by the random errors in spectral fitting, whereas for large tropospheric slant columns, the retrieval uncertainty is dominated by air-mass factor uncertainties (the last term in Eq. (27)).

Figure 12 shows the absolute and relative error in the tropospheric NO₂ column retrieved for clear-sky scenes from S5P/TROPOMI data on 1 April 2018. We see that over the oceans and the remote continental regions, the overall tropospheric retrieval uncertainty is dominated by errors in the spectral fitting and the stratospheric column estimate and is more than 100% (indicated by purple colours in the bottom panel of Fig. 12). For larger columns over continental areas, the relative uncertainty in the retrieved column reduces to 20 – 50%, and is dominated by the uncertainty in the tropospheric air-mass factor. Retrieval results are generally best for regions with strong NO₂ sources and/or high surface albedos.

Based on the instrumental performance expectations for S5, and our experience with OMI and S5P/TROPOMI tropospheric NO₂ retrievals (see Fig. 12 and Table 20), the overall error budget for individual S5 tropospheric NO₂ retrievals can tentatively be approximated as $\varepsilon = 0.5 \times 10^{15}$ molec/cm² + [0.25 to 0.50] · N_v^{trop} . This is a more complete and realistic error statement than the requirements from [RD7] ($\varepsilon = 1.3 \times 10^{15}$ molec/cm² + 0.1 · N_v^{trop} for a horizontal resolution of 5 – 20 km; cf. Table 1).

The error components can be split in two classes: input parameter plus DOAS related uncertainties (cloud, albedo, aerosol, stratosphere, slant column) and a-priori related uncertainties (profile shape). In Rodgers optimal estimation formalism the latter may be called the smoothing error. It depends on the use of the data which uncertainty should be used. When the NO₂ vertical columns are used without knowledge of the NO₂ profiles, then the uncertainty, $\Delta N_{v, \text{NO}_2}^{\text{trop, kernel}}$, is the sum of input parameter, DOAS and smoothing. When profile information is available (e.g. when comparisons with models are performed) and the kernels are used, the uncertainty, $\Delta N_{v, \text{NO}_2}^{\text{trop}}$, is the sum of input parameter and DOAS only, without the smoothing error contribution. Both uncertainty estimates for the tropospheric vertical column will be made available in the product: one for applications with the kernel, one for applications without.

The individual components of the total uncertainty of the tropospheric column are available in the code and provided in the NO₂ data files of the QA4ECV project ([RD6], [ER2]). In the current S5P/TROPOMI NO₂ processor only the total error is made available in the data product. In the next upgrade we consider to add the tropospheric column error components due to the slant column uncertainties, stratospheric estimate and the air-mass factor, and contributions of this AMF uncertainty due to cloud fraction, cloud pressure, albedo and profile shape uncertainties.

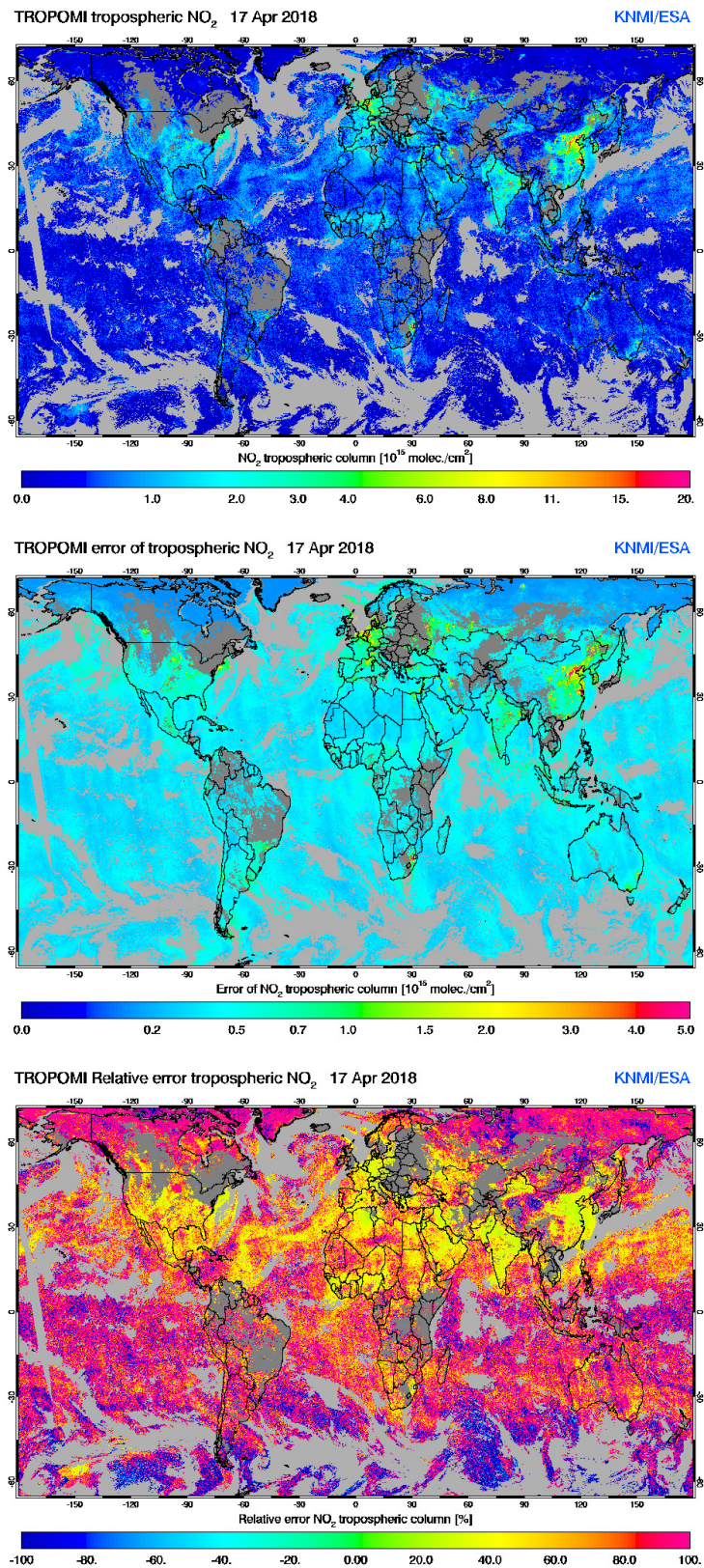



Figure 12: Tropospheric NO₂ vertical column values (*top panel*; in 10^{15} molec/cm²), the corresponding absolute error estimate (*middle panel*; in 10^{15} molec/cm²), and the relative error (*bottom panel*; in %) for 17 April 2018, based on S5P/TROPOMI data. Large relative errors are seen mostly over areas with small NO₂ column values: oceans and remote continental regions.

| | | |
|---|--------------------|---|
|  | S5L2PP ATBD-NO2 | Reference : KNMI-ESA-S5L2PP-ATBD-001 Version : 5.0 Date : 01 September 2023 |
| | | Page 56/89 |

8 Validation

8.1 Validation requirements

The most important validation need for S5 NO₂ is for tropospheric NO₂ under polluted and clean conditions. Under polluted NO₂ conditions, column and profile information in the lower troposphere is essential for column density validation. The NO₂ data from OMI has been validated in several studies over the past years, based on satellite inter-comparisons (e.g. GOME-2, SCIAMACHY) as well as comparisons against ground-based (e.g. MAX-DOAS, Lidar) and in-situ (e.g. aircraft, balloon) measurements. And these validation activities have covered both tropospheric and stratospheric NO₂ data.

Despite these validation activities large uncertainties remain. These uncertainties are partly related to the quality of the independent NO₂ data used for the validation. And they are partly related to the issue of representativity of the often point-size ground-based and in-situ measurements w.r.t. the finite-sized satellite ground pixels.

KNMI is involved in a number of NO₂ validation activities, ranging from satellite intercomparisons to MAX-DOAS measurements [Peters et al., 2012] and the development of a special balloon-borne NO₂ sonde [Sluis et al., 2010]. Some of the validation activities are performed within the framework of dedicated international validation campaigns. Furthermore, KNMI has a close collaboration with other institutes involved in NO₂ validation activities.

For the validation of the S5 NO₂ data we advise to extend the validation activities, concentration on a better characterisation of the quality of the independent NO₂ data and any difference between these data sets and the S5 NO₂ data. These validation activities should make a distinction between stratospheric and tropospheric NO₂.

There is also a need for correlative surface albedo data to investigate the accuracy of the OMI-based surface albedo climatology. Retrieval of S5 NO₂ depends on cloud information, thus cloud properties (from the FRESCO-S retrieval and cloud fraction retrieval in the NO₂ window) must be validated carefully with correlative measurements.

Below plans for pre-launch (algorithm testing) and post-launch activities related to validation of the S5 NO₂ data product are listed. Post-launch activities include comparisons of geophysical data comparisons between S5 and correlative NO₂ data from a variety of sources.

More details of the validation work will be provided in updates of this ATBD.

8.2 Algorithm testing and verification



This important activity provides confidence in the retrieval algorithms, including forward and inverse models, based on simulations, and comparisons between different techniques and software programs. Much of S5's verification phase will address this issue in a thorough way. This activity also includes reviews and updates of the S5 NO₂ ATBD.

In the (pre-launch) verification phase, the intention is to test the TROPOMI retrieval algorithm on data from existing satellite instruments, especially OMI. This has actually already been done for this ATBD but this effort will be extended.

Furthermore, we anticipate that an extensive comparison of the TROPOMI NO₂ with the TROPOMI verification algorithm will provide useful validation and verification of the retrieval algorithm proposed here. Similar activities have already taken place for GOME-2A and OMI in the framework of the FP7 QA4ECV project ([RD6], [ER2]). These efforts demonstrated that the OMNO2A v2 (KNMI; VanGeffen et al. [2015]) and QA4ECV (Bremen, BIRA; [RD13]) spectral fitting approaches lead to consistent results, but with better precision for the QA4ECV spectral fitting algorithm including so-called intensity offset correction terms [Zara et al., 2018]. In the early stages of the TROPOMI mission we will test and evaluate both approaches on the TROPOMI Level-1b spectra. If the QA4ECV algorithm performs better, we will replace the default OMNO2A v2 algorithm.

During the QA4ECV project, the representation of stratospheric NO_y in the model has been improved by nudging ODIN HNO₃:O₃ ratios, leading to more realistic NO₂ concentrations in the free-running mode. These improvements will be applied to TROPOMI as well. The profile shape in the stratosphere is crucial for a good quality stratospheric column estimate. This profile shape should be monitored on a regular basis, and should be compared with (satellite limb) observations and climatology. Increasing the number of stratospheric layers in the TM5 model is something that will be tested, and the modelled diurnal cycle of stratospheric NO₂ will be investigated.

The QA4ECV-project led to the generation of a new NO₂ AMF LUT for QA4ECV NO₂ retrievals for OMI, GOME-2A, etc. This LUT was generated with DAK, and now includes a simple sphericity correction based on detailed comparisons

| | | |
|--|--------------------|--|
|   | S5L2PP ATBD-NO2 | Reference : KNMI-ESA-S5L2PP-ATBD-001 Version : 5.0 Page Date : 01 September 2023 57/89 |
|--|--------------------|--|

between DAK and McArtim as described in Lorente et al. [2017]. We intend to include this LUT also for the TROPOMI NO₂ algorithms.

8.3 Stratospheric NO₂ validation

For stratospheric NO₂ columns, correlative (column and profile) measurements are needed in regions that are representative for a complete zonal band, and hence need to be relatively unpolluted. The currently operational NDACC network covers this need in principle, although there are concerns about the accuracy of the standard SAOZ and FTIR measurements techniques for some stations (e.g. Dirksen et al. [2011]). Nevertheless, the measurements of stratospheric NO₂ concentrations taken from high-altitude ground stations such as the Jungfraujoch station in Switzerland, are particularly valuable for validation (e.g. Hendrick et al. [2012]). Other useful sources of stratospheric NO₂ data are satellite instruments that measure in limb view. Past and present examples are SCIAMACHY (Beirle et al. [2010], Hilboll et al. [2013b]), HIRDLS and MLS [Belmonte et al., 2014]. These measurements can provide vertical profiles of NO₂ in the stratosphere, but there are difficulties in using them for direct validation as they are often only sparsely validated themselves.

In our view the main priority of the validation efforts should lie on a better characterisation of the vertical profile of stratospheric NO₂, as these profiles are an essential input to the data assimilation system in use for the separation between tropospheric and stratospheric NO₂ columns from the S5 measurements. To this end the validation measurements should be well characterised, in terms of the quality of the data and of estimates of the error on the data. Improving the knowledge of spatial and seasonal variations in the stratospheric NO₂ profiles is also important.

Stratospheric NO₂ measurements near the Arctic vortex in late winter and early spring would be useful to better test the capability of the data assimilation scheme (and other stratosphere-troposphere separation schemes) in capturing the influence of stratospheric air masses low in NO_x on stratospheric NO₂ at lower latitudes. Such excursions are known to occur and may lead to systematic errors in the separation scheme (e.g. Dirksen et al. [2011]; Bucsela et al. [2013]). Independent measurements may provide important information on how to improve these issues.

8.4 Tropospheric NO₂ validation



For validation of tropospheric NO₂ data, correlative (column and profile) measurements are needed in the highly populated polluted regions at mid-latitudes, and also in regions with natural sources of nitrogen oxides, e.g. from biomass burning, microbial soil activity and lightning. NDACC-instruments unfortunately do not meet this need, as they are often located in relatively remote and clear areas.

Information on tropospheric NO₂ concentrations – with the NO₂ in the planetary boundary layer and/or in the free troposphere – comes from in-situ instruments (at the ground, in masts, or on low-flying balloons) and from remote-sensing instruments at the ground, on balloons or aircraft. The emerging suite of MAX-DOAS and PANDORA instruments are particularly valuable for validation of S5 measurements, but homogenisation and cross-calibration of these measurements should remain a priority for successful validation.

An important issue when comparing independent NO₂ measurements with data derived from satellite-based instruments is the question of representativity. We recommend a careful investigation into the spatial representativity of any independent NO₂ measurement, in order to facilitate a meaningful comparison with the 7×3.5 km² S5 pixel. Flying NO₂ mapping instruments on airplanes will be an important source of information to tackle in particular this representativity issue.

Important for the validation as well as for the data assimilation system in use for the separation between tropospheric and stratospheric NO₂ columns from the S5 measurements is a good understanding of the vertical profile of the tropospheric NO₂. The best source of information on vertical profiles of NO₂ is still from incidental aircraft campaigns. Alternatively, experimental NO₂ profiles from (tethered) balloon sondes, and measurement towers, will provide valuable information on the vertical distribution of NO₂.

Since tropospheric retrievals depend on the concept of the air-mass factor, which has to rely on a priori information, it is important to also validate the inputs and assumptions that go into the air-mass factor calculation. This mostly concerns cloud parameters – cloud fraction and cloud pressure – that should be well characterised. Another critical issue, about which very little is known as yet, is the effect of the presence of aerosols on the NO₂ retrieval. Collocated information on the aerosol profile – e.g. coming from the S5 Aerosol Layer Height data product – could be useful for this.

| | | |
|--|--------------------|--|
|   | S5L2PP ATBD-NO2 | Reference : KNMI-ESA-S5L2PP-ATBD-001 Version : 5.0 Page Date : 01 September 2023 58/89 |
|--|--------------------|--|

9 Feasibility

9.1 Estimated computational effort

An estimate of the computational effort is based on a system with the following hardware specification:

- Intel(R) Xeon(R) CPU E5-2637 v3 @ 3.50GHz, 8 core (16 cores with HT), 128 GB Memory.
- SPEC CPU2006 CFP rate: 437/425 [URL01]
- OS: Red Hat Enterprise Linux Server release 7.3 (Maipo)
- Kernel: 3.10.0-514.10.2.el7.x86_64
- CFP2006 Result: Hewlett-Packard Company ProLiant DL380 Gen9 (3.50 GHz, Intel Xeon E5-2637 v3),
- url: <http://www.spec.org/cpu2006/results/res2014q4/cpu2006-20141118-33146.html>

On this system the full NO₂ retrieval with the S5P/TROPOMI Level-2 processor, which serves as the breadboard code for Sentinel-5, on S5P/TROPOMI orbit 00657 using 14 cores takes 496 seconds. There are 1189635 succesful retrievals, with an average of $0.004000s \pm 0.000042s$. Since $1189635 \times 0.004000/14 = 340s$, 156s was spend on initialisation (94s), output generation and pixels without a successful retrieval (e.g. because the SZA is too large).

9.2 Static and dynamic input

The processing of Sentinel-5 NO₂ data poses different demands for different retrieval steps. As described in Sect. 6.1 and illustrated in Fig. 4, the main processing will take place at EUMETSAT, which processes incoming Level-1b data as well as data from two other Sentinel-5 data products (Clouds and AUI), and ingests information of a data assimilation / CTM system running elsewhere in order to convert the NO₂ slant column data into the respective tropospheric and stratospheric vertical column data.

9.2.1 Static input

Table 21 lists the static input needed for the processing at EUMETSAT, depicted in Fig. 4.

Table 21: Overview of the static input data needed for the Sentinel-5 NO₂ processing at EUMETSAT. The reference spectra will be delivered by KNMI to the processor pre-convolved with the Sentinel-5 slit function (see column 5) and given at 0.01 nm resolution. The usage of the data is marked by: U = used in computation; F = used for filtering for processing; C = copied to output only. The table does not list the input needed by the data assimilation system, which runs elsewhere.

| Parameter | Symbol | Physical unit | Source | Pre-process needs | Usage & comments |
|---------------------------------|---|----------------------------------|---|-------------------|------------------|
| absorption cross sections | | | | | |
| NO ₂ | $\sigma_{\text{NO}_2}(\lambda)$ | m ² /mol | Vandaele et al. [1998] | convolution | U |
| O ₃ | $\sigma_{\text{O}_3}(\lambda)$ | m ² /mol | Gorshchev et al. [2014] & Serdyuchenko et al. [2014] | convolution | U |
| O ₂ -O ₂ | $\sigma_{\text{O}_2-\text{O}_2}(\lambda)$ | m ⁵ /mol ² | Thalman and Volkamer [2013] | convolution | U |
| H ₂ O _{vap} | $\sigma_{\text{H}_2\text{O}_{\text{vap}}}(\lambda)$ | m ² /mol | HITRAN 2012 data | convolution | U [†] |
| H ₂ O _{liq} | $\sigma_{\text{H}_2\text{O}_{\text{liq}}}(\lambda)$ | 1/m | Pope and Frey [1997] | convolution | U |
| Ring reference spectrum | $I_{\text{ring}}(\lambda)$ | mol/s/m ² /nm | Chance and Spurr [1997] | convolution | U [†] |
| high-res. solar spectrum | $E_{\text{ref}}(\lambda)$ | mol/s/m ² /nm | Chance and Kurucz [2010] | convolution | U |
| air-mass factor lookup table | — | — | KNMI | — | U |
| cloud fraction lookup table | — | — | KNMI | — | U [‡] |
| surface albedo database | $A_{\text{s,NO}_2}$ | 1 | or Tilstra et al. [2017]; [ER9] or Kleipool et al. [2008]; [ER8] | — | U (Sect. 6.4.2) |
| co-registration data | — | — | S5 procedure/product | — | U (Sect. 6.3.1) |
| retrieval input settings | — | — | KNMI | — | U (App. E.1) |

[†] These reference spectra are created as in Van Geffen et al. [2015]; see also [RD14].

[‡] For the cloud fraction retrieval in the NO₂ fit window and for the cloud radiance fraction; see Sect. 6.4.1.

If not available via the Sentinel-5 cloud product.



| | | |
|--|--------------------|--|
|   | S5L2PP ATBD-NO2 | Reference : KNMI-ESA-S5L2PP-ATBD-001 Version : 5.0 Page Date : 01 September 2023 59/89 |
|--|--------------------|--|

Table 22: Overview of the dynamic input data needed for the Sentinel-5 NO₂ processing at EUMETSAT. The usage of the data is marked by: U = used in computation; F = used for filtering for processing; C = copied to output only. The table does not list the input needed by the data assimilation system, which runs elsewhere.

| Parameter | Symbol | Physical unit | Source | Pre-process needs | Backup if not available | Usage & comments |
|---------------------------|---|-----------------------------|--------------------------------|-------------------|-------------------------|------------------|
| earth radiance VIS band | $I(\lambda), \Delta I(\lambda)$ | mol/s/m ² /nm/sr | S5 L1b UVR product | per pixel | no retrieval | U |
| solar irradiance VIS band | $E_0(\lambda), \Delta E_0(\lambda)$ | mol/s/m ² /nm | S5 L1b UVR product | per pixel | use previous | U |
| cloud & scene data | $f_{\text{eff}}, A_c, A_{\text{sc}}, A_s$ | 1 | S5 L2 cloud product | — | no VCD product | C & U ‡ |
| absorbing aerosol index | p_c, p_{sc}, p_s | Pa | — | — | — | — |
| snow/ice cover flag | — | 1 | S5 L2 AUI product | — | set fill value | C [U] ‡# |
| meteo data | — | — | S5 L2 AUX product (NSDIC NISE) | per pixel | latest available | U |
| NO ₂ profile | n_{I,NO_2} | mixing ratio | S5 L2 AUX product (CAMS) | — | latest available | U † |
| stripe amplitude | $N_{\text{s},\text{NO}_2}^{\text{corr}}$ | mol/m ² | S5 L2 SBG product | — | latest available | U † |
| surface albedo | A_{s,NO_2} | 1 | S5 L2 AUX product (GOME2 LER) | pixel average | latest available | U |
| surface elevation | z_{s} | m | S5 L2 AUX product (GMTED2010) | pixel average | latest available | U |

† Latest available value for that day.

‡ Data co-registered to the NO₂ data before usage (see Sect. 6.3.1)

Currently only passed on to the output, but may be used at some later stage in the determination of the qa_value.

9.2.2 Dynamic input

Table 22 lists the dynamic input needed for the processing at EUMETSAT, depicted in Fig. 4.

9.3 Output product overview

The Sentinel-5 NO₂ data output product consists of the retrieved tropospheric and stratospheric NO₂ columns, along with error estimates, AMFs and the averaging kernel. A general overview of the data product contents is given in Sect. 6.8 and Table 17. Table 23 provides a more detailed overview of the data sets, their unit, type, etc. in the main output data product. The file size per orbit for the S5P/TROPOMI NO₂ data product is estimated at 455 MB (uncompressed). Sentinel-5 has about half the amount of ground pixels of S5P/TROPOMI, but there may be a few more datasets in the file. First estimate of filesize therefore 250 MB.

The averaging kernel describes how the retrieved NO₂ columns relate to the true NO₂ profile [Eskes and Boersma, 2003]. The averaging kernel should be used in validation exercises, model evaluations, and assimilation or inverse modelling attempts with TROPOMI NO₂ data. The output product will also contain the necessary information (surface pressure and CTM sigma coordinates) to construct the pressure grid to which the averaging kernel values correspond.

The S5P/TROPOMI data product consists of two files: one with the main retrieval results – similar to the one for S5 described above – and a separate TM5-MP model data file with vertical information on atmospheric NO₂, SO₂ and HCHO profile and temperature at the 1° × 1° grid of TM5-MP on a half-hourly basis. The additional "support output product file" is large and will probably not be used by most NO₂ data users, but some advanced users the model profiles have shown to be useful. (The OMI-DOMINO processing provides a similar, but less extensive, support product file.) It remains to be decided whether for S5 we will also provide such a support output file, which then comes from the CAMS system, and in what form this will be: on the CAMS grid like is done for S5P/TROPOMI on an hourly bases or regridded to the S5 ground pixel coordinates. Like for S5P/TROPOMI, the S5 support file could contain the a-priori profiles of different data products, so that one file can be shared with among the data products.








| | | |
|--|--------------------|--|
|        | S5L2PP ATBD-NO2 | Reference : KNMI-ESA-S5L2PP-ATBD-001 Version : 5.0 Page Date : 01 September 2023 60/89 |
|--|--------------------|--|

Table 23: Overview of the datasets, units, types and sizes in the main data output product file, listed alphabetically; cf. Table 17. All quantities followed by a * in the "symbol" column consist of the value and the associated precision $\Delta(\text{parameter})$ (for these the number of data per pixel is doubled in the 6th column).

| Parameter | Symbol | Physical unit | Description | Type | Data per pixel | Comments |
|--|---|----------------------------------|--|-------|---------------------------------|-------------------------|
| aerosol absorbing index | — | 1 | L2 354/388 nm wavel. pair | float | 1 | cf. Sect. 6.3.3 |
| air-mass factor | M^{trop} | 1 | tropospheric AMF | float | 1 | — |
| | M^{strat} | 1 | stratospheric AMF | float | 1 | — |
| | M | 1 | total AMF | float | 1 | — |
| | $M_{\text{clr}}^{\text{trop}}$ | 1 | clear-sky tropospheric AMF | float | 1 | — |
| | $M_{\text{cld}}^{\text{trop}}$ | 1 | cloudy tropospheric AMF | float | 1 | — |
| averaging kernel | \mathbf{A} | 1 | — | float | n_l | \dagger |
| chi-squared | χ^2 | 1 | χ^2 of the NO ₂ DOAS fit | float | 1 | cf. Eq. (3) |
| cloud albedo | A_c | 1 | used in the cloud retrieval | float | 1 | — |
| cloud pressure | p_c | Pa | from the cloud retrieval | float | 1×2 | — |
| cloud fraction | f_{eff} | 1 | from the cloud retrieval | float | 1×2 | — |
| cloud fraction NO ₂ | $f_{\text{eff}, \text{NO}_2}$ | 1 | for the NO ₂ VCD | float | 1 | cf. Sect. 6.4 |
| cloud radiance fraction | w_{NO_2} | 1 | for the NO ₂ VCD | float | 1 | cf. Sect. 6.4 |
| degrees of freedom | D | 1 | of the DOAS fit | float | 1 | — |
| DOAS fit results | $N_{\text{s}, \text{NO}_2}^*$ | mol/m ² | total NO ₂ SCD | float | 1×2 | — |
| | $N_{\text{s}, \text{H}_2\text{O}_{\text{liq}}}^*$ | m | H ₂ O _{liq} coeff. in NO ₂ window | float | 1×2 | — |
| | $N_{\text{s}, \text{H}_2\text{O}_{\text{vap}}}^*$ | mol/m ² | H ₂ O _{vap} SCD in NO ₂ window | float | 1×2 | — |
| | $N_{\text{s}, \text{O}_2-\text{O}_2}^*$ | mol ² /m ⁵ | O ₂ -O ₂ SCD in NO ₂ window | float | 1×2 | — |
| | $N_{\text{s}, \text{O}_3}^*$ | mol/m ² | O ₃ SCD in NO ₂ window | float | 1×2 | — |
| | C_{ring}^* | 1 | Ring coeff. in NO ₂ window | float | 1×2 | — |
| ghost column | $N_{\text{V}}^{\text{ghost}}$ | mol/m ² | NO ₂ column below the clouds | float | 1 | \ddagger |
| ground pixel coordinates | δ_{geo} | ° | VIS pixel – latitude | float | 5 | centre, 4 corners |
| | ϑ_{geo} | ° | VIS pixel – longitude | float | 5 | centre, 4 corners |
| ground pixel index | — | 1 | across-track pixel index | int | 1 | — |
| intensity off. coefficients | c_m^* | 1 | in the NO ₂ DOAS fit | float | $(n_{\text{off}} + 1) \times 2$ | cf. Eq. (8) |
| measurement time | t | s | VIS pixel | float | 2 | — |
| model pressure level | A_l | Pa | — | float | 0 | \P |
| coefficients | B_l | 1 | — | float | 0 | \P |
| model tropopause layer index | l_{tp} | 1 | — | int | 1 | — |
| model NO ₂ slant column | $N_{\text{s}, \text{NO}_2}^{\text{mod}}$ | mol/m ² | from model a-priori | float | 1 | — |
| number of wavelengths | n_λ | 1 | in the NO ₂ fit window | int | 1 | # |
| number of iterations | n_i | 1 | from the DOAS fit | int | 1 | — |
| polynomial coefficients | a_m^* | 1 | in the NO ₂ DOAS fit | float | $(n_p + 1) \times 2$ | cf. Eq. (7) \S |
| processing quality flags | — | 1 | — | int | 1 | cf. TBD |
| qa_value | f_{QA} | 1 | quality assurance value | float | 1 | cf. TBD |
| reflectance at $\lambda_{\text{c}, \text{NO}_2}$ | $R_{\text{mod}}(\lambda_{\text{c}, \text{NO}_2})$ | 1 | default: $\lambda_{\text{c}, \text{NO}_2} = 440$ nm | float | 1 | cf. Sect. 6.4 |
| root-mean-square | R_{RMS} | 1 | RMS of the NO ₂ DOAS fit | float | 1 | cf. Eq. (5) |
| satellite coordinates | z_{sat} | m | altitude of the satellite | float | 1 | — |
| | δ_{sat} | ° | latitude sub satellite point | float | 1 | — |
| | ϑ_{sat} | ° | longitude sub satellite point | float | 1 | — |
| | φ_{sat} | 1 | relative offset in orbit | float | 1 | — |
| scanline index | — | 1 | along-track pixel index | int | 1 | — |
| scene albedo | A_{sc}^* | 1 | from the cloud retrieval | float | 1×2 | — |
| scene pressure | p_{sc}^* | Pa | from the cloud retrieval | float | 1×2 | — |
| snow-ice flag | — | 1 | snow/ice case flagging | int | 1 | — |
| stripe amplitude | $N_{\text{s}, \text{NO}_2}^{\text{corr}}$ | mol/m ² | NO ₂ SCD stripe amplitude | float | 0 | cf. Sect. 6.5 \otimes |
| surface albedo | A_{s} | 1 | for the cloud retrieval | float | 1 | — |
| surface albedo NO ₂ | $A_{\text{s}, \text{NO}_2}$ | 1 | for cloud fraction NO ₂ window | float | 1 | — |
| surface classification | — | 1 | land/water classification | int | 1 | — |
| surface elevation | z_{s}^* | m | VIS pixel | float | 1×2 | — |
| surface pressure | p_{s} | Pa | VIS pixel | float | 1 | — |

Table continues on next page








| | | |
|--|--------------------|--|
|        | S5L2PP ATBD-NO2 | Reference : KNMI-ESA-S5L2PP-ATBD-001 Version : 5.0 Page Date : 01 September 2023 61/89 |
|--|--------------------|--|

Table 23: — *continued*.

| Parameter | Symbol | Physical unit | Description | Type | Data per pixel | Comments |
|-------------------------|------------------------------------|--------------------|-----------------------------------|-------|----------------|-----------------------------------|
| vertical column density | N_{v,NO_2}^{trop} | mol/m ² | tropospheric NO ₂ VCD | float | 1 | — |
| | $\Delta N_{v,NO_2}^{trop}$ | mol/m ² | averaging kernel not applied | float | 1 | cf. Sect. 7.4 |
| | $\Delta N_{v,NO_2}^{trop, kernel}$ | mol/m ² | averaging kernel applied | float | 1 | cf. Sect. 7.4 |
| | N_{v,NO_2}^{strat} | mol/m ² | stratospheric NO ₂ VCD | float | 1 × 2 | — |
| | N_{v,NO_2} | mol/m ² | total NO ₂ VCD | float | 1 × 2 | $\equiv N_s/M$ |
| | N_{v,NO_2}^{sum} | mol/m ² | total NO ₂ VCD | float | 1 × 2 | $\equiv N_v^{trop} + N_v^{strat}$ |
| viewing geometry data | θ_0 | ° | solar zenith angle | float | 1 | at surface |
| | ϕ_0 | ° | solar azimuth angle | float | 1 | at surface |
| | θ | ° | viewing zenith angle | float | 1 | at surface |
| | ϕ | ° | viewing azimuth angle | float | 1 | at surface |
| wavelength calibration | w_s | nm | wavelength shift | float | 1 × 2 | cf. Eq. (2) |
| | w_q | 1 | wavelength stretch | float | 1 × 2 | cf. Eq. (2) |
| | χ_w^2 | 1 | χ^2 of the calibration | float | 1 | cf. Eq. (2) |
| wavelength calibration | w_s^{E0} | nm | wavelength shift | float | 0 × 2 | cf. Eq. (2) ⊗ |
| | w_q^{E0} | 1 | wavelength stretch | float | 0 × 2 | cf. Eq. (2) ⊗ |
| | $(\chi_w^{E0})^2$ | 1 | χ^2 of the calibration | float | 0 | cf. Eq. (2) ⊗ |

† The number of TM5 layers is $n_l = 34$ for the DOMINO-v2 processing; this may change when the layer distribution is optimised.

‡ The NO₂ ghost column is the NO₂ profile shape from TM5 integrated from the surface to the cloud pressure level.

The actual number of wavelengths n_λ used in the fit (cf. Eq. (3)), i.e. after removal of, for example, bad pixels within the fit window.

§ The degree of the DOAS polynomial is $n_p = 5$ in the current OMNO2A; there will be room in the data product to change this.

¶ One set of $n_l + 1$ (see note †) TM5 pressure level coefficients per data granule.

⊗ One set per spatial channel.

9.4 Breakpoint output parameters

The NO₂ data product file, described above, contains the main output of the individual processing steps. Each of the intermediate output data fields serves as breakpoint output data of the processing. Apart from that, additional diagnostic output of some input to and intermediate results of the DOAS fit (cf. Sect. 6.2 for details) as is possible in the S5P/TROPOMI processors. An overview is given in Table 24. Several quantities are given as function of the wavelength at which the DOAS fit is performed, i.e. the common wavelength grid (Sect. 6.2.2). Wavelength pixels that have been skipped, e.g. because they were flagged as bad pixel, saturated pixel, or that were removed from the fit by the spike removal algorithm in the DOAS fit routine (Sect. 6.2.7), may be skipped from the output as long as the output shows the correct common wavelength grid, or be marked by a very large reflectance precision (as is the case on the S5P/TROPOMI processor, where the reflectance precision of these wavelength pixels is set to 10⁴ times the signal). The additional output may be split in two diagnostic categories, if so desired from a software and/or data output (e.g. file size) point of view.

9.5 Open issues

The following is a list of open issues that will be relevant for the implementation in a prototype or operational processor:

- The details of the explicit implementation of the surface BRDF (cf. Sect. 6.4) is still an open issue, and is the topic of active research. This influences also the air mass factor computations (extended lookup tables) and the cloud fractions and height retrievals. Also the satelliet source of the BRDF information is not yet fixed. The use of GOME-2 or OMI LER datasets has the disadvantage that the resolution does not match the small footprints of Sentinel-5.
- The use of CAMS model outputs as a-priori for the Sentinel-5 retrievals needs to be studied. Currently a full chemistry treatment of NO_x in the stratosphere in CAMS (ECMWF-IFS) does not yet exist. However, the upgrade of CAMS to include stratospheric chemistry may be expected within one year, and first experiments with stratospheric chemistry in IFS look promising. In particular the quality of the resulting stratospheric NO₂ distributions is important for determining the tropospheric part of the column with sufficient precision. The fallback-option to use the TM5 assimilation approach is available, but that will require additional resources.
- It remains to be decided whether for S5 we will also provide such a support output file, as discussed above, at



| | | |
|--|--------------------|--|
|   | S5L2PP ATBD-NO2 | Reference : KNMI-ESA-S5L2PP-ATBD-001 Version : 5.0 Page Date : 01 September 2023 62/89 |
|--|--------------------|--|

Table 24: Overview of the diagnostic datasets, units, types and sizes in the main data output product file, listed alphabetically. Wavelength dependent quantities are given at the common wavelength grid after wavelength calibration (Sect. 6.2.2). All quantities followed by a * in the "symbol" column consist of the value and the associated precision $\Delta(\text{parameter})$; for these the number of data per pixel is doubled in the 6th column. The last column indicates whether the parameter is present in the current operational S5P/TROPOMI debug output. An overview of the main output data is given in Table 23.

| Parameter | Symbol | Physical unit | Description | Type | Data per pixel | Presence & comments |
|---|--|-----------------------------|---------------------------------------|-------|--|---------------------|
| <i>Primary diagnostics: main details</i> | | | | | | |
| fit residual | $R_{\text{meas}}(\lambda) - R_{\text{mod}}(\lambda)$ | 1 | residual of fit (observation – model) | float | n_λ | Y |
| number of outliers | — | 1 | from spike removal (Sect. 6.2.7) | int | 1 | Y |
| reflectance measured | $R_{\text{meas}}(\lambda) *$ | 1 | — | float | $n_\lambda \times 2$ | Y |
| reflectance modelled | $R_{\text{mod}}(\lambda)$ | 1 | — | float | n_λ | Y |
| start index in L1B | — | 1 | start index within input spectrum | int | 1 | Y |
| wavelength grid | λ | nm | common wavelength grid | float | n_λ | Y |
| <i>Secondary diagnostics: further details</i> | | | | | | |
| covariance matrix | — | 1 | result of the DOAS fit | float | $n_{\text{fit}} \times n_{\text{fit}}$ | N [†] |
| DOAS fit time | — | s | time taken by the DOAS fit | float | 1 | Y |
| DOAS polynomial | $P(\lambda)$ | 1 | — | float | n_λ | N |
| irradiance | $E_0(\lambda) *$ | mol/s/m ² /nm | irradiance at common grid | float | $n_\lambda \times 2$ | N |
| irradiance calibration: polynomial coeff. | $a_j *$ | 1 | — | float | $n_p \times 2$ | Y |
| radiance | $I(\lambda) *$ | mol/s/m ² /nm/sr | radiance at common grid | float | $n_\lambda \times 2$ | N |
| radiance calibration : polynomial coeff. | $a_j *$ | 1 | — | float | $n_p \times 2$ | Y |
| Ring fit coeff. | $W_{\text{ring}} *$ | 1 | named C_{ring} in App. B | float | 1×2 | Y |
| wavelength calib. time | — | s | wavelength calib. processing time | float | 1 | Y |

[†] n_{fit} is the number of DOAS fit parameters: slant columns, Ring and intensity offset coefficients, and polynomial coefficients. The diagonal elements of the covariance matrix represent the precision $\Delta(\text{parameter})$ of each fit parameter, which are reported in the main output product, while the off-diagonal elements represent cross-correlations between the fit parameters. The latter elements are thus the actual secondary diagnostics meant here. Whether they are written out as $n_{\text{fit}} \times n_{\text{fit}}$ matrix or in another way is up to the software developer. It may further be necessary to supply an additional dataset explaining the meaning of the elements of the covariance matrix.

the end of Sect. 9.3.

- Whether we will actually use the intensity offset correction (Sect. 6.2.4, Eq. (8)) will be investigated using S5P/TROPOMI data. If that study shows that such an intensity offset correction actually accounts for some physical effect, notably vibrational Raman scattering (VRS), we will opt to include a specific reference spectrum for that effect, which will require additional data variables in the output product.

A Effective cloud fraction in the NO₂ window

The effective cloud fraction in the NO₂ window, $f_{\text{eff},\text{NO}_2}$, discussed in Sect. 6.4, can be computed from a look-up table (LUT) with the top-of-atmosphere (TOA) reflectance at $\lambda_{c,\text{NO}_2} = 440$ nm as a function of viewing geometry, surface & cloud albedo, and surface & cloud pressure. The approach is very similar to FRESCO+ [RD17] and explicitly accounts for Rayleigh scattering. The following description is adapted from [RD21].

The LUT assumes that the measured reflectance at TOA is defined as:

$$R_{\text{TOA}}(\lambda) = \frac{\pi I(\lambda)}{\mu_0 E_0(\lambda)} \quad (28)$$

In the independent pixel approximation the cloud fraction, f_c , for a given wavelength is given by:

$$f_c = \frac{R_{\text{TOA}} - R_s}{R_c - R_s} \quad (29)$$

and the cloud radiance fraction, the fraction of the total radiation that comes from the clouds, is given by:

$$w_{\text{NO}_2} = \frac{f_c R_c}{R_{\text{TOA}}} = \frac{f_c R_c}{f_c R_c + (1 - f_c) R_s} \quad (30)$$

where R_s and R_c are the reflectances at surface and cloud, respectively. These are computed from a limited LUT, based on Chandrasekhar (Chandrasekhar et al. [1950], Sect. 72). For bounding surface 'b', i.e. either surface ('s') or cloud ('c'):

$$R_b(\lambda, A_b(\lambda)) = R_0(\lambda) + \frac{A_b(\lambda) T(\lambda)}{1 - A_b(\lambda) s(\lambda)} \quad (31)$$

where:

- $R_b(\lambda, A_b(\lambda))$ = The reflectance of the combined atmosphere-surface system related to the light coming from the boundary 'b', i.e. either surface ('s') or cloud ('c').
- $R_0(\lambda)$ = The reflectance of the atmosphere if the surface is perfectly black: $A_b = 0$.
- $A_b(\lambda)$ = The albedo at the bounding surface, either cloud (A_c) or surface (A_s).
- $T(\lambda)$ = The transmittance of the atmosphere, a measure for the probability that photons travel through the atmosphere, are reflected by a surface with unit albedo, and travel back to the sensor (reflections by the atmosphere back towards the surface are ignored here).
- $s(\lambda)$ = The spherical albedo of the atmosphere for illumination at its lower boundary; $1/[1 - A_b(\lambda)s(\lambda)]$ is the sum of a geometrical series accounting for the reflections between the atmosphere and the surface.

The transmittance of the atmosphere $T(\lambda)$ is a product of two terms depending on the viewing and solar zenith angles:

$$T(\lambda) = t(\lambda; \mu) t(\lambda; \mu_0) \quad (32)$$

where $\mu = \cos(\theta)$ and $\mu_0 = \cos(\theta_0)$ and:

$$t(\lambda; \mu) = \exp\left(-\frac{\tau(\lambda)}{\mu}\right) + \int_0^1 2\mu' T_0(\lambda; \mu, \mu') d\mu' \quad (33)$$

In Eq. (33) we assume a plane parallel atmosphere; for a spherical shell atmosphere the factor $1/\mu$ in $\exp(-\tau/\mu)$ has to be replaced by a different expression.

The TOA reflectance related to the light coming from the boundary 'b', i.e. either surface ('s') or cloud ('c'), is a function of solar and viewing geometries and surface properties: $R_b(\lambda, A_b(\lambda)) = R_b(\lambda; \theta_0, \theta, \phi - \phi_0; p_b, A_b(\lambda))$, where p_b is the pressure at the boundary 'b'. In addition extra dependencies may be needed to account for absorbing species, in particular at shorter wavelengths where absorption by ozone (O₃) is significant. A more detailed study is needed to determine if O₃ is needed for the cloud fraction, but for NO₂ we estimate that ignoring O₃ absorption leads to an error of 0.01 – 0.02 in the cloud fraction. Raman scattering is ignored here.

Table 25: Look-up tables and dimensions for reflectance calculations; no trace gas column entries included.

| | |
|-----------------|---|
| R_0 | Reflectance of the black surface |
| λ | For all wavelengths where a cloud fraction must be computed $[1, \dots, n]$ |
| μ_0 | For $\mu_0 = [0.0012141231 : 1.0]$, i.e. $\theta_0 = [89.93^\circ : 0^\circ]$, in 42 steps of $2 - 5^\circ$ |
| μ | For $\mu = [0.0012141231 : 1.0]$, i.e. $\theta = [89.93^\circ : 0^\circ]$, in 42 steps of $2 - 5^\circ$ |
| $\phi - \phi_0$ | Dependency stores in three Fourier terms |
| p_b | Pressure of the bounding surface (cloud or surface) for $p_b = [1076 \text{ hPa} : 95 \text{ hPa}]$ in 69 steps * |
| T | Transmittance of the atmosphere |
| λ | For all wavelengths where a cloud fraction must be computed $[1, \dots, n]$ |
| μ_0 | For $\mu_0 = [0.0012141231 : 1.0]$, i.e. $\theta_0 = [89.93^\circ : 0^\circ]$, in 42 steps of $2 - 5^\circ$ |
| μ | For $\mu = [0.0012141231 : 1.0]$, i.e. $\theta = [89.93^\circ : 0^\circ]$, in 42 steps of $2 - 5^\circ$ |
| p_b | Pressure of the bounding surface (cloud or surface) for $p_b = [1076 \text{ hPa} : 95 \text{ hPa}]$ in 69 steps * |
| s | Spherical albedo of the atmosphere |
| λ | For all wavelengths where a cloud fraction must be computed $[1, \dots, n]$ |
| p_b | Pressure of the bounding surface (cloud or surface) for $p_b = [1076 \text{ hPa} : 95 \text{ hPa}]$ in 69 steps * |

*) Through a fixed scale height p_b is linked to the elevation of the bounding surface: $z_b = [-55 \text{ m} : 16500 \text{ m}]$.

The terms used in Eq. (31) have the same or less dependencies: $R_0(\lambda) = R_0(\lambda; \theta_0, \theta, \phi - \phi_0; p_b)$, but crucially not on $A_b(\lambda)$. Further: $T(\lambda) = T(\lambda; \theta_0, \theta; p_b)$ and $s(\lambda) = s(\lambda; p_b)$. The dependency of $R_b(\lambda)$ and $R_0(\lambda)$ on $\phi - \phi_0$ can be expressed as a Fourier sum, in case of a Rayleigh atmosphere with three terms. All in all this gives a small set of LUTs for $R_0(\lambda)$, $T(\lambda)$ and $s(\lambda)$; see the overview in Table 25. For use in the NO_2 retrieval, the set of LUTs has been computed using DAK at $\lambda_{c, \text{NO}_2} = 440 \text{ nm}$, the wavelength used for the air-mass factor calculations.

From these LUTs we can calculate the reflectance of the cloudy part of the pixel, R_c , using the cloud pressure, p_c , and cloud albedo, A_c , from the cloud product. And the reflectance of the cloud-free part of the pixel, R_s , using the surface pressure, p_s , from meteorology or a fixed scale height and the surface elevation, z_s , and the surface albedo, A_s , from a climatology. Note that either p_s or z_s can be used as entry to the LUT: they are "linked" through the fixed scale height.

A.1 Adjusting albedo to respect physical limits to the cloud fraction



In order to limit the cloud fraction to the range $[0, 1]$, the albedo of the boundary can be adjusted. From Eq. (29) it is clear that a negative cloud fraction results when $R_s > R_{\text{TOA}}$. Rewriting Eq. (31) to set $R_s = R_{\text{TOA}}$ provides an adjusted value for A_s :

$$A_s(\lambda) = \frac{R_{\text{TOA}}(\lambda) - R_0(\lambda, p_s)}{T(\lambda, p_s) + s(\lambda, p_s) [R_{\text{TOA}}(\lambda) - R_0(\lambda, p_s)]} \quad (34)$$

In a similar fashion it is clear from Eq. (28) that a cloud fraction larger than 1 results when $R_{\text{TOA}} > R_c$. Rewriting Eq. (31) to set $R_c = R_{\text{TOA}}$ provides an adjusted value for A_c :

$$A_c(\lambda) = \frac{R_{\text{TOA}}(\lambda) - R_0(\lambda, p_c)}{T(\lambda, p_c) + s(\lambda, p_c) [R_{\text{TOA}}(\lambda) - R_0(\lambda, p_c)]} \quad (35)$$

Note that in FRESKO-S (Sect. 6.3.2) the surface albedo is adjusted ignoring Rayleigh scattering, which simplifies Eq. (34) to $A_s(\lambda) = R_{\text{TOA}}(\lambda)$, and Eq. (35) to $A_c(\lambda) = R_{\text{TOA}}(\lambda)$.

| | | |
|--|--------------------|--|
|   | S5L2PP ATBD-NO2 | Reference : KNMI-ESA-S5L2PP-ATBD-001 Version : 5.0 Page Date : 01 September 2023 65/89 |
|--|--------------------|--|

B Wavelength calibration

For S5 a wavelength calibration of the radiance and irradiance spectra in the fitting window specific to the algorithm will be performed, always starting from the nominal (i.e. uncalibrated) wavelength grid provided for the Level-1b spectra. In the unlikely case this wavelength calibration fails, the retrieval will be performed using the nominal wavelength grid. If the calibration is done in the Level 0-to-1b processor, it is done for the whole band instead of a selected wavelength window, and this may or may not meet the science requirements for the wavelength calibration for Level-2 trace gas retrievals. For the wavelength calibration of the radiances an atmosphere model is needed, especially at the shorter wavelengths where ozone absorption is significant, but also the Ring effect modifies the radiance spectra in ways that have to be taken into account when calibrating the wavelength.

For the calibration of a complete band or a complete detector, the calibration is split up in micro-windows, and a polynomial is drawn through the micro-windows to cover the whole band. When fitting for a specific retrieval window, a single fit covering the retrieval window is more appropriate. The model function that is used for the radiance wavelength calibration is a modified version of a DOAS fit. Sections B.1 and B.2 describe the generic wavelength fit used in most retrieval algorithms for S5, in section B.3 the actual application to NO₂ retrieval is discussed.

Note that during phase E1 the Level-1b irradiance data will not be calibrated, so this has to be done by the NO₂ processor. For this the procedure described in below for the radiance data is used, except that atmosphere related effects should be disabled, specifically the Ring effect should *not* be included in this fit. The polynomial order N is set to 1 for the irradiance fit.

B.1 Description of the problem

The S5 Level-1b radiance spectra have a nominal wavelength scale (λ_{nom}), but this wavelength grid is not corrected for inhomogeneous slit illumination [RD22, section 28]. The measurements are also not temperature corrected, but because the instrument itself is temperature stabilized it is expected that this effect can be ignored. The Level-2 processors must correct the nominal wavelength scale of the radiance measurements for inhomogeneous slit illumination due to the presence of clouds in the field of view.

One would like to follow the calibration of the irradiance spectra, for a short wavelength interval. The range $\lambda_{\text{fit}} = [\lambda_-, \lambda_+]$ is the approximate range on which to do the wavelength calibration. To avoid non-linearities this wavelength range is tailored to the specific Level-2 algorithm. For each ground pixel the nominal wavelength λ_{nom} is adjusted with a wavelength offset (or: shift) w_s and a wavelength stretch w_q to find the calibrated wavelength λ_{cal} :

$$\lambda_{\text{cal}} = \lambda_{\text{nom}} + w_s + w_q \left(2 \frac{\lambda_{\text{nom}} - \lambda_0}{\lambda_+ - \lambda_-} \right) + \dots \quad (36)$$

with λ_0 the center of the fit window, λ_- the beginning of the fit window and λ_+ the end of the fit window. In the third term the factor 2 is used to ensure that the wavelength factor of the stretch lies in the range $[-1 : +1]$. The higher order terms in Eq. (36) are ignored, even fitting w_q is optional.



B.2 Non-linear model function and Jacobian

The model function in the fit is similar to a non-linear DOAS equation. Instead of fitting the reflectance R , we fit the radiance I directly, bringing the (model) irradiance E_{mod} to the other side of the equation. The model function \mathcal{M} is given by:

$$\mathcal{M}(\lambda_{\text{nom}}; a_0, \dots, a_N, C_{\text{ring}}, w_s, w_q, N_{s,0}, \dots, N_{s,M}) = P_N(\lambda^*) \cdot \exp \left(\sum_{k=0}^M -N_{s,k} \sigma_k(\lambda_{\text{cal}}) \right) \cdot (E_{\text{mod}}(\lambda_{\text{cal}}) + C_{\text{ring}} I_{\text{ring}}(\lambda_{\text{cal}})) \quad (37)$$

with λ_{cal} the calibrated wavelength as given by the first three terms in Eq. (36),

$$P_N(\lambda^*) = \sum_{j=0}^N a_j (\lambda^*)^j, \quad \lambda^* \equiv 2 \frac{\lambda_{\text{nom}} - \lambda_0}{\lambda_+ - \lambda_-} \quad (38)$$

| | | |
|--|--------------------|--|
|   | S5L2PP ATBD-NO2 | Reference : KNMI-ESA-S5L2PP-ATBD-001 Version : 5.0 Page Date : 01 September 2023 66/89 |
|--|--------------------|--|

a polynomial of order N , E_{mod} the reference irradiance spectrum, and I_{ring} the Ring spectrum; both E_{mod} and I_{ring} are convolved with the instrument slit function (ISRF). The spectra σ_k ($k = 0, \dots, M$) are optional absorption spectra that have a relevant impact on the radiance, for instance the O_3 absorption cross section. These additional reference spectra have also been convolved with the ISRF, but note that the DOAS assumption still applies: this merit function is not applicable to line absorbers such as $\text{H}_2\text{O}_{\text{vap}}$, CH_4 , CO or O_2 , and will fail at wavelengths below ~ 320 nm because the profile shape of O_3 is relevant at those wavelengths. The order of the polynomial is $1 \leq N \leq 5$, depending on the length of the fit window.

The wavelength calibration fit adjusts the parameters $a_0, \dots, a_N, C_{\text{ring}}, w_s, w_q, N_{s,0}, \dots, N_{s,M}$ to minimize χ^2 :

$$\chi^2 = \frac{1}{m-n} \sum_{i=0}^{m-1} \left(\frac{I_i - \mathcal{M}(a_0, \dots, a_N, C_{\text{ring}}, w_s, w_q, N_{s,0}, \dots, N_{s,M})}{\Delta I_i} \right)^2 \quad (39)$$

with I_i the measured radiance at spectral pixel index i , ΔI_i the precision of this radiance, and m the number of spectral points between λ_- and λ_+ . The number of degrees of freedom is m minus the number of fit parameters:

$$n = N + 1 + M + 1 + 3 \quad (40)$$

The additional 3 here is when fitting C_{ring} , w_s and w_q ; if C_{ring} and/or w_q are not fitted, the number of degrees of freedom increases.

To minimize the number of function calls in the optimisation routine derivatives with respect to the fit parameters as a Jacobian matrix need to be supplied, with i the spectral pixel index: The components of the Jacobian are given by Eqs. (41–45) below.



$$\frac{\partial \mathcal{M}_i}{\partial a_j} = (\lambda_i^*)^j \cdot \exp \left(\sum_{k=0}^M -N_{s,k} \sigma_k(\lambda_{\text{cal},i}) \right) \cdot [E_{\text{mod}}(\lambda_{\text{cal},i}) + C_{\text{ring}} I_{\text{ring}}(\lambda_{\text{cal},i})] \quad (41)$$

$$\frac{\partial \mathcal{M}_i}{\partial C_{\text{ring}}} = P_N(\lambda_i^*) \cdot \exp \left(\sum_{k=0}^M -N_{s,k} \sigma_k(\lambda_{\text{cal},i}) \right) \cdot I_{\text{ring}}(\lambda_{\text{cal},i}) \quad (42)$$

$$\begin{aligned} \frac{\partial \mathcal{M}_i}{\partial w_s} = P_N(\lambda_i^*) \cdot \exp \left(\sum_{k=0}^M -N_{s,k} \sigma_k(\lambda_{\text{cal},i}) \right) \times \\ \left\{ \left(- \sum_{k=0}^M N_{s,k} \frac{d\sigma_k}{d\lambda} \right)_{\lambda=\lambda_{\text{cal},i}} \cdot (E_{\text{mod}}(\lambda_{\text{cal},i}) + C_{\text{ring}} I_{\text{ring}}(\lambda_{\text{cal},i})) \right. \\ \left. + \left(\frac{dE_{\text{mod}}}{d\lambda} \right)_{\lambda=\lambda_{\text{cal},i}} + C_{\text{ring}} \left(\frac{dI_{\text{ring}}}{d\lambda} \right)_{\lambda=\lambda_{\text{cal},i}} \right\} \quad (43) \end{aligned}$$

$$\begin{aligned} \frac{\partial \mathcal{M}_i}{\partial w_q} = P_N(\lambda_i^*) \cdot \exp \left(\sum_{k=0}^M -N_{s,k} \sigma_k(\lambda_{\text{cal},i}) \right) \times \\ \left\{ \left(- \sum_{k=0}^M N_{s,k} \lambda_i^* \frac{d\sigma_k}{d\lambda} \right)_{\lambda=\lambda_{\text{cal},i}} \cdot (E_{\text{mod}}(\lambda_{\text{cal},i}) + C_{\text{ring}} I_{\text{ring}}(\lambda_{\text{cal},i})) \right. \\ \left. + \left(\lambda_i^* \frac{dE_{\text{mod}}}{d\lambda} \right)_{\lambda=\lambda_{\text{cal},i}} + C_{\text{ring}} \lambda_i^* \left(\frac{dI_{\text{ring}}}{d\lambda} \right)_{\lambda=\lambda_{\text{cal},i}} \right\} \quad (44) \end{aligned}$$

$$\frac{\partial \mathcal{M}_i}{\partial N_{s,k}} = -P_N(\lambda_i^*) \cdot \sigma_k(\lambda_{\text{cal},i}) \cdot \exp \left(\sum_{k=0}^M -N_{s,k} \sigma_k(\lambda_{\text{cal},i}) \right) \cdot (E_{\text{mod}}(\lambda_{\text{cal},i}) + C_{\text{ring}} I_{\text{ring}}(\lambda_{\text{cal},i})) \quad (45)$$

| | | |
|--|--------------------|--|
|   | S5L2PP ATBD-NO2 | Reference : KNMI-ESA-S5L2PP-ATBD-001 Version : 5.0 Page Date : 01 September 2023 67/89 |
|--|--------------------|--|

The reference spectra $E_{\text{mod}}(\lambda)$, $I_{\text{ring}}(\lambda)$ and $\sigma_k(\lambda)$ are pre-convolved with the ISRF. During the fitting 4th degree splines are used to represent these spectra. An interesting feature is that a spline of the derivative with respect to the independent variable can be calculated from the parameters of the original spline (given that the derivatives are w.r.t. the wavelength, the resulting spline for these derivatives is 3rd degree).

These equation can be used with various optimization routines, for instance Levenberg-Marquardt or Gauss-Newton, with or without constraints or regularization methods. After thorough testing the optimal estimation method as implemented in DISAMAR, which uses an unmodified Gauss-Newton to find the state vector for the next iteration, was selected for S5.

B.2.1 Prior information for the optimal estimation fit

Optimal estimation needs prior information for the regularisation process during the fitting procedure, both a starting value and a covariance value. For input only the diagonal elements of the covariance matrix are specified, on output a full posteriori error covariance matrix is available. The polynomial coefficients are not important, the values and variance were estimated from a large number of retrievals. The Ring coefficient was taken from the same data set. The value for w_s is taken from the spacing of the nominal grid. A 1- σ error of a third of the spacing of the wavelength grid seems reasonable: $\sigma_{\text{prior}}(w_s) = \Delta\lambda/3$. This value will mostly prevent fitting a shift w_s that is larger than half of the grid spacing, which basically means the wavelength is not known at all. The prior value for w_q is 0 (zero), i.e. no stretch or squeeze. The range depends on the size of the fitting window, a consequence of the use of λ^* , as defined in Eq. (38). The current value is a deliberate overestimation. The slant column of O_3 is typically 0.18 mol/m² (about 600 DU); other trace gases are not included. An overview of the prior information used for S5 is given in Table 26.

Table 26: A priori values and a priori error for the optimal estimation wavelength fit for S5. The ozone slant column is expressed in mol/m²; the other quantities are dimensionless.

| Names | a_0 | a_1 | $a_{2,\dots,N}$ | C_{ring} | w_s | w_q | N_{s,O_3} |
|------------|---------|-----------|-----------------|------------------------|-----------------------|-----------|---------------------------|
| Prior | 1 | -0.5 | 0.01 | 6×10^{-2} | 0 | 0 | 0.25 |
| Covariance | $(1)^2$ | $(0.5)^2$ | $(0.1)^2$ | $(6 \times 10^{-2})^2$ | $(\Delta\lambda/3)^2$ | $(0.1)^2$ | $(0.18)^2$ |
| Optional | no | no | yes | yes | no | yes | yes |

B.3 Application of the wavelength calibration in NO₂

For the retrieval of NO₂ the N_{s,O_3} is not fitted, as O₃ shows little structure in the NO₂ and it is a weak absorber in the NO₂ fit window (405 – 465 nm).

Testing with OMI [RD23] has shown that there is no significant amount of stretch in the wavelength of the spectra of that instrument. Given the similarities of OMI, S5P/TROPOMI and S5, the initial baseline is to not fit w_q . After launch the need to include w_q in the fit can be investigated; turning it on is a simple configuration change. The order of the polynomial N is set to 2 and the Ring effect is included in the fit. The a priori error of w_s is set to 0.07 nm.

C High-sampling interpolation

After the wavelength calibration of the radiance spectrum, discussed in Appendix B, the irradiance and radiance observations need to be brought to the same wavelength grid in order to be able to compute the reflectance in Eq. (1). Because of the geometry of the solar observations, these measurements are shifted with respect to the radiance observations due to the Doppler shift caused by the motion of the satellite relative to the sun. Given that the irradiance spectrum is known better than the radiance spectrum, the irradiance spectrum is shifted to the radiance grid and the radiance observations are left without modification:

$$E_0(\lambda_{i,\text{earth}}) = \frac{E_{\text{high}}(\lambda_{i,\text{earth}})}{E_{\text{high}}(\lambda_{i,\text{solar}})} E_0(\lambda_{i,\text{solar}}) \quad (46)$$

with E_0 the observed irradiance, E_{high} a high resolution solar reference spectrum, convolved with the instrument spectral response function, $\lambda_{i,\text{earth}}$ the wavelength of the earth radiance spectrum for pixel i , and $\lambda_{i,\text{solar}}$ the wavelength of the solar irradiance spectrum for pixel i . The index i is synchronized between the radiance and irradiance observations, such that they refer to the same physical pixel on the detector. On E_{high} 4th degree spline interpolation is used to find the value at the indicated wavelengths. The input data for the splines have sufficient spectral resolution to allow for this.

Figure 13 shows the procedure graphically. Panel (d) shows the effect of spline interpolation on the irradiance data to

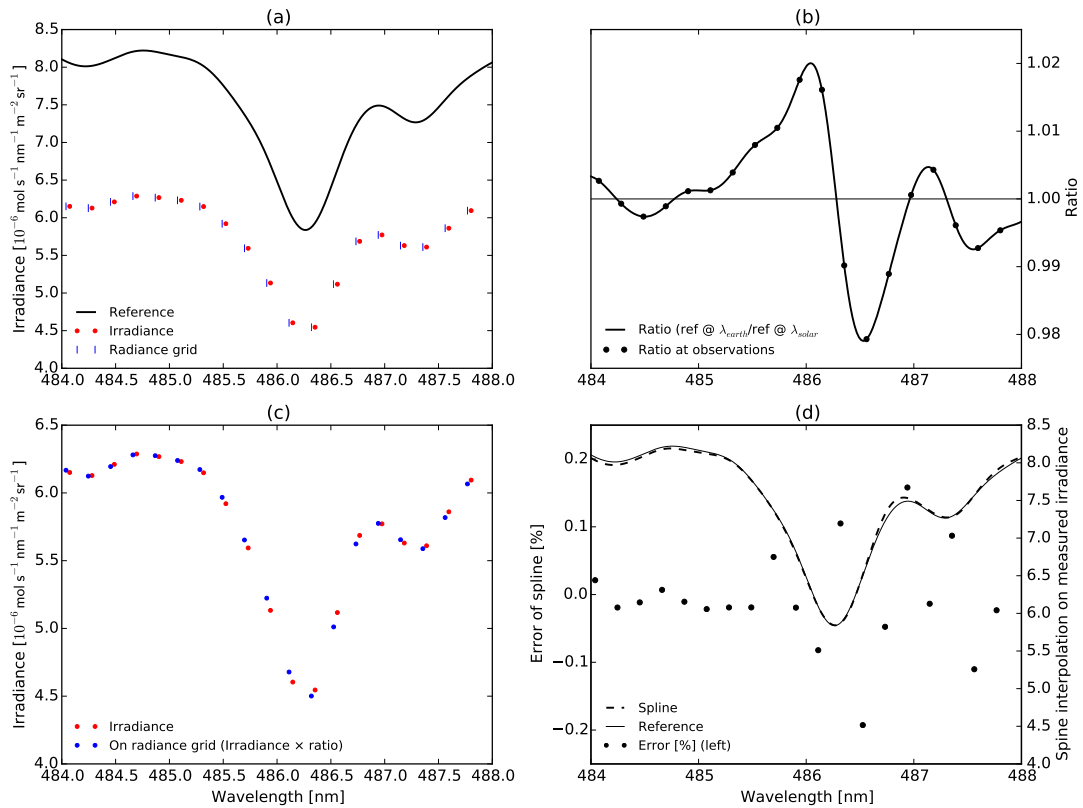




Figure 13: High sampling interpolation on part of a solar observation. (a) The red dots show the actual observation (taken from GOME-2A). The blue vertical lines indicate the wavelength grid of the radiance observation. The solid line shows a high resolution solar reference spectrum that has been convolved with the instrument spectral response function of the instrument (in this case GOME-2A). (b) The ratio $E_{\text{high}}(\lambda_{i,\text{earth}})/E_{\text{high}}(\lambda_{i,\text{solar}})$. (c) In red $E_0(\lambda_{i,\text{solar}})$, in blue $E_0(\lambda_{i,\text{earth}})$. (d) The solid line is the solar reference spectrum. The dash-dotted line is a high resolution irradiance spectrum created by spline interpolation directly on the observed irradiances, brought to the same average level of the window shown here to ease comparisons. The black dots indicate the error in % that are caused by using spline interpolation directly on the irradiance observations. Clear artifacts are caused by this, especially because noise on the observations becomes correlated between nearby points in the spectrum.

| | | |
|--|--------------------|---|
|   | S5L2PP ATBD-NO2 | Reference : KNMI-ESA-S5L2PP-ATBD-001 Version : 5.0 Date : 01 September 2023 |
| | | Page 69/89 |

find the values at the earth radiance wavelength grid. Errors are small but systematic. Note that these errors appear directly in the reflectance data. The reflectance in Eq. (1) is then be calculated a at the radiance wavelenth grid:

$$R_{\text{meas}}(\lambda_{i,\text{earth}}) = \pi I(\lambda_{i,\text{earth}}) / \mu_0 E_0(\lambda_{i,\text{earth}}).$$

D Data quality value: the qa_value flags

To make the use of the S5 data product files easier, a so-called *qa_value* (where 'qa' stands for 'quality assurance') is assigned to each ground pixel. The *qa_value* is intended to serve as an easy filter of the observations (dividing the dataset in useful versus not useful observations), depending on how the data is used.

The data files have for each ground pixel the so-called *processing_quality_flags*, which provides the user information on processing issues, such as errors that were encountered in the processing, as well as a number of warnings. Some of these warnings have been included in the *qa_value*.

The following differentiation of the *qa_value*, f_{QA} , for usage of the NO₂ data product has been made:



| | |
|------------------------------|--|
| $0.75 \leq f_{QA} \leq 1.00$ | The ground pixel is recommended for all applications, including column comparisons, visualisation, trends, monthly/seasonal averages. The data is restricted to cloud-free observations (cloud radiance fraction < 0.5), and snow-ice free observations. |
| $0.50 \leq f_{QA} < 0.75$ | The ground pixel is recommended for use in data assimilation and comparisons against models or vertical profile observations, given that the averaging kernel is used to specify the sensitivity profile in cloudy situations; this includes good quality retrievals over clouds and snow/ice. |
| $0 < f_{QA} < 0.50$ | The ground pixel is not recommended for use due to serious retrieval issues. |
| $f_{QA} = 0$ | A processing error occurred so that the ground pixel cannot be used at all, or the solar zenith angle exceeds the limit set in the data assimilation |

The determination of the *qa_value* is done as follows. Starting from the initial value $f_{QA} = 1$, f_{QA} is multiplied by the modification factor f_{QA}^i of each of the criteria i listed in Table 27 that have been met (i.e. if criterion i is not met then $f_{QA}^i = 1$). The thresholds for the criteria and their multiplication factor are configuration parameters; see App. E.1.3).

Table 27: Overview of the selection criteria for the *qa_value*, f_{QA} . currently in use for S5P/TROPOMI and proposed S5. Some quantities have a minimum or maximum value; these values are configuration parameters in the processing. In this table f_{NISE} stands for the NISE snow/ice flags listed in Table 8. And f_{AAI} represents the aerosol index 354/388 nm pair, which is passed on to the NO₂ data product file as added flag.

| i | criterion | f_{QA}^i |
|-----|---|------------|
| 0 | if fatal error encountered according to <i>processing_quality_flags</i> | 0.00 |
| 1 | if south_atlantic_anomaly_warning set in <i>processing_quality_flags</i> | 0.95 |
| 2 | if sun_glint_warning set in <i>processing_quality_flags</i> over water | 0.93 |
| 3 | if pixel_level_input_data_missing_warning set in <i>processing_quality_flags</i> | 0.90 |
| 4 | if interpolation_warning set in <i>processing_quality_flags</i> | 0.90 |
| 5 | if solar_eclipse set in <i>geolocation_flags</i> | 0.20 |
| 6 | if $\theta_0 > \theta_0^{\max,1} = 81.2^\circ$ | 0.30 |
| 7 | if $\theta_0 > \theta_0^{\max,2} = 84.5^\circ$ | 0.10 |
| 8 | if $M^{\text{trop}}/M^{\text{geo}} < M_{\min}^{\text{trop}} = 0.1$ | 0.45 |
| 9 | if $\Delta N_s > (\Delta N_s)^{\max} = 33.0 \times 10^{-6} \text{ mol/m}^2 (= 2 \times 10^{15} \text{ molec/cm}^2)$ | 0.15 |
| 10 | if $f_{NISE} < f_{NISE}^{\max} = 1$ * or $f_{NISE} = 252$ or $f_{NISE} = 255$ then [no snow or ice] | 0.20 |
| 11 | $A_{s,NO_2} > A_s^{\max} = 0.3$ $w_{NO_2} > w_{NO_2}^{\max} = 0.5$ | 0.74 |
| | else-if ($f_{NISE} \neq 253$ and $f_{NISE} \neq 254$) [snow/ice case] | |
| 12 | if ($f_{NISE} > 80$ and $f_{NISE} < 104$ and $p_{sc} > 0.98 \cdot p_s$) [cloud-free snow/ice] | 0.88 |
| 13 | else [cloudy snow/ice] | 0.73 |
| 14 | if $p_{sc} < p_{sc}^{\min} = 3.0 \times 10^4 \text{ Pa}$ | 0.25 |
| 15 | else [snow/ice error] | 0.00 |
| 16 | $f_{AAI} > f_{AAI}^{\max} = 1.0 \times 10^{10}$ [for future use] | 0.40 |

*) Note that this criterion means that the system switches to the scene mode if there is 1% or more snow/ice.

| | | |
|--|--------------------|---|
|   | S5L2PP ATBD-NO2 | Reference : KNMI-ESA-S5L2PP-ATBD-001 Version : 5.0 Date : 01 September 2023 |
| | | Page 71/89 |

E Overview of process configuration parameters of S5P/TROPOMI NO₂

This appendix gives an overview of the configuration settings as used in v1.3.0 (February/March 2019) of the S5P/TROPOMI NO₂ processor, the prototype of the Sentinel-5 processor depicted in Figure 4. The processing is configured via two files: the settings specifically for the NO₂ processing (App. E.1) and the joborder XML file for the processor (App. E.2) essentially listing the names of the input, configuration and output files of the processing.

E.1 NO₂ process configuration

Below follows the NO₂ process configuration options of the S5P/TROPOMI v1.3.0 processor (see App. E.1.1–E.1.6) which are given via the configuration file that is mentioned in the joborder XML file for the processor (App. E.2). In addition there are default configuration options set in the code and that are thus not manually configurable (see App. E.1.7).

Note that both the wavelength calibration and the DOAS slant column retrieval are performed with an Optimal Estimation (OE) algorithm, which requires an initial guess and an a-priori error estimate for each of the fit parameters.

E.1.1 Wavelength calibration configuration

Both the irradiance and the radiance Level-1B input spectra are wavelength calibrated against a reference solar spectrum; see Sect. 6.2.2 & Table 2 & Appendix B

In case of the radiance spectra, the Ring effect is taken into account and a polynomial is included in the fit to account of smooth atmospheric absorption features in the calibration window.

General settings:

```
wavelength_calibration.convergence_threshold = "1.0"
wavelength_calibration.max_iterations = "12"
wavelength_calibration.window = "405.0, 465.0"
wavelength_calibration.polynomial_order = "2"
```

Include Ring effect or not:

```
wavelength_calibration.irr.perform_wavelength_fit = "yes"
wavelength_calibration.irr.include_ring = "no"



wavelength_calibration.perform_wavelength_fit = "yes"
wavelength_calibration.include_ring = "yes"
wavelength_calibration.include_stretch = "no"
```

Settings for the OE algorithm:

```
wavelength_calibration.initial_guess.shift = "0.0"
wavelength_calibration.initial_guess.stretch = "0.0"
wavelength_calibration.sigma.shift = "0.07"
wavelength_calibration.sigma.stretch = "0.07"

wavelength_calibration.initial_guess.a0 = "1.0"
wavelength_calibration.initial_guess.a1 = "0.1"
wavelength_calibration.initial_guess.a2 = "0.01"
wavelength_calibration.sigma.a0 = "1.0"
wavelength_calibration.sigma.a1 = "0.1"
wavelength_calibration.sigma.a2 = "0.01"

wavelength_calibration.initial_guess.ring = "0.06"
wavelength_calibration.sigma.ring = "0.06"
```

| | | |
|--|--------------------|--|
|   | S5L2PP ATBD-NO2 | Reference : KNMI-ESA-S5L2PP-ATBD-001 Version : 5.0 Page Date : 01 September 2023 72/89 |
|--|--------------------|--|

E.1.2 DOAS retrieval configuration

The DOAS retrieval is described in Sect. 6.2 & Table 2.

In the S5P/TROPOMI processing framework, the key 'NO2DOAS' identifies which the processor to use, i.e. that NO₂ is the main trace gas.

General settings:

```
NO2DOAS.wavelength_start = "405.0"
NO2DOAS.wavelength_end = "465.0"
NO2DOAS.convergence_threshold = "0.99"
NO2DOAS.max_iterations = "20"
NO2DOAS.scale_precision_with_chisq = "true"
NO2DOAS.include_ring = "true"
NO2DOAS.polynomial_order = "5"
```

Trace gas specification and id for the file containing the reference cross sections (the cross sections are given for fixed temperatures, but the option is there to include a temperature dependence for NO₂ and O₃):

```
NO2DOAS.species = "NO2, O3, O2O2, H2O_vapor, H2O_liquid"
NO2DOAS.reference_cross_sections_key = "REF_XS_NO2"
NO2DOAS.NO2.reference_temperature = "-1.0"
NO2DOAS.O3.reference_temperature = "-1.0"
```

Settings for the OE algorithm:



```
NO2DOAS.initial_guess.H2O_liquid = "0.0"
NO2DOAS.initial_guess.H2O_vapor = "1.5e+3"
NO2DOAS.initial_guess.NO2 = "1.2e-5"
NO2DOAS.initial_guess.O2O2 = "8.0e+5"
NO2DOAS.initial_guess.O3 = "3.6e-1"
NO2DOAS.sigma.H2O_liquid = "20.0"
NO2DOAS.sigma.H2O_vapor = "1.0e+4"
NO2DOAS.sigma.NO2 = "1.0e-2"
NO2DOAS.sigma.O2O2 = "2.0e+6"
NO2DOAS.sigma.O3 = "5.0e0"

NO2DOAS.initial_guess.ring = "0.06"
NO2DOAS.sigma.ring = "0.2"
```

```
NO2DOAS.initial_guess.a0 = "1.0"
NO2DOAS.initial_guess.a1 = "0.125"
NO2DOAS.initial_guess.a2 = "0.015625"
NO2DOAS.initial_guess.a3 = "0.015625"
NO2DOAS.initial_guess.a4 = "0.015625"
NO2DOAS.initial_guess.a5 = "0.015625"
NO2DOAS.sigma.a0 = "1.0"
NO2DOAS.sigma.a1 = "0.125"
NO2DOAS.sigma.a2 = "0.015625"
NO2DOAS.sigma.a3 = "0.015625"
NO2DOAS.sigma.a4 = "0.015625"
NO2DOAS.sigma.a5 = "0.015625"
```

Settings for the intensity offset correction, which is implemented but not yet fully tested.

```
NO2DOAS.include_offset = "false"
NO2DOAS.intensity_offset_scalefactor = "1.0"
NO2DOAS.background_offset.polynomial_order = "1"
NO2DOAS.initial_guess.c0 = "1.0"
NO2DOAS.initial_guess.c1 = "0.125"
```

| | | |
|--|--------------------|--|
|   | S5L2PP ATBD-NO2 | Reference : KNMI-ESA-S5L2PP-ATBD-001 Version : 5.0 Page Date : 01 September 2023 73/89 |
|--|--------------------|--|

```

NO2DOAS.initial_guess.c2 = "0.015625"
NO2DOAS.initial_guess.c3 = "0.015625"
NO2DOAS.sigma.c0 = "1.0"
NO2DOAS.sigma.c1 = "0.125"
NO2DOAS.sigma.c2 = "0.015625"
NO2DOAS.sigma.c3 = "0.015625"

```

Specification of variable names to use in the output file:

```

NO2DOAS.NO2.output.name = "nitrogendioxide"
NO2DOAS.O2O2.output.name = "oxygen_oxygen_dimer"
NO2DOAS.O3.output.name = "ozone"
NO2DOAS.H2O_liquid.output.name = "water_liquid"
NO2DOAS.H2O_vapor.output.name = "water"

```

Configuration of the spike (i.e. outlier) removal in the DOAS fit (Sect. 6.2.7) includes: *a*) turn it on or off, *b*) set the fraction of the spectrum that must be flagged as outlier before the DOAS fit is performed again (where zero means always redo the fit, which is the most likely setting), *c*) set the Q_f threshold for detecting outliers, and *d*) set the maximum number of outliers that is allowed to be in a spectrum before an error (`max_num_outlier_exceeded_error` in the `processing_quality_flags`) is raised (use -1 to disable this limit).

```

NO2DOAS.filter_outliers = true
NO2DOAS.filter_outliers_fraction = 0.0
NO2DOAS.filter_outliers_threshold = 3.0
NO2DOAS.filter_outliers_maximum_number_allowed_outliers = 15

```

E.1.3 Quality value configuration

The `qa_value` is introduced in Sect. 6.8 and the set of criteria is presented in Appendix D.

Both the threshold and the modification factor (multiplied by 100) of the criteria are configuration parameters, where the number at the beginning of each line identifies the criteria number in Appendix D:



```

1  qa_value.south_atlantic_anomaly_warning = "95.0"
2  qa_value.sun_glint_warning = "93.0"
3  qa_value.pixel_level_input_data_missing = "90.0"
4  qa_value.interpolation_warning = "90.0"
5  qa_value.eclipse_modification_percent = "20.0"

6  qa_value.sza_max_1_modification_percent = "30.0"
6  qa_value.sza_max_1_threshold = "81.2"
7  qa_value.sza_max_2_modification_percent = "10.0"
7  qa_value.sza_max_2_threshold = "84.5"
8  qa_value.amf_trop_geo_ratio_modification_percent = "45.0"
8  qa_value.amf_trop_geo_ratio_threshold = "0.1"
9  qa_value.no2_scd_precision_modification_percent = "15.0"
9  qa_value.no2_scd_precision_threshold = "33.0e-6"

10 qa_value.surface_albedo_modification_percent = "20.0"
10 qa_value.surface_albedo_threshold = "0.3"
11 qa_value.cloud_radiance_fraction_modification_percent = "74.0"
11 qa_value.cloud_radiance_fraction_threshold = "0.5"
13 qa_value.snow_ice_max_modification_percent = "73.0"
13 qa_value.snow_ice_max_threshold = "1"
14 qa_value.minimum_scene_pressure_modification_percent = "25.0"
14 qa_value.minimum_scene_pressure_threshold = "30000.0"
15 qa_value.maximum_aerosol_index_modification_percent = "40.0"
15 qa_value.maximum_aerosol_index_threshold = "1.0e10"

```

| | | |
|--|--------------------|--|
|   | S5L2PP ATBD-NO2 | Reference : KNMI-ESA-S5L2PP-ATBD-001 Version : 5.0 Page Date : 01 September 2023 74/89 |
|--|--------------------|--|

Note that criterion #12 in the qa_value list is a processor internal default setting and is therefore not available as configuration option (see App. E.1.7: qa_value.snow_ice_nocloud_...).

Modification factors for treating warnings from the processing_quality_flags that are currently not used in the S5P/TROPOMI NO₂ processing but appear in the metadata as possible configuration options:

```
qa_value.AAI_warning = "100.0"
qa_value.altitude_consistency_warning = "100.0"
qa_value.cloud_warning = "100.0"
qa_value.data_range_warning = "100.0"
qa_value.deconvolution_warning = "100.0"
qa_value.extrapolation_warning = "100.0"
qa_value.input_spectrum_warning = "100.0"
qa_value.low_cloud_fraction_warning = "100.0"
qa_value.signal_to_noise_ratio_warning = "100.0"
qa_value.snow_ice_warning = "100.0"
qa_value.so2_volcanic_origin_certain_warning = "100.0"
qa_value.so2_volcanic_origin_likely_warning = "100.0"
qa_value.sun_glint_correction = "100.0"
qa_value.wavelength_calibration_warning = "100.0"
```

Note that qa_value.sun_glint_correction is a flag used by DLR in their S5P/TROPOMI cloud product; for the NO₂ processing, the qa_value.sun_glint_warning is used (#2 in the list).

E.1.4 General process configuration

Allow the framework and the processor to verify that the configuration file is up to date:

```
configuration.version.framework = "1.3.0"
configuration.version.algorithm = "1.3.0"
```

Define the algorithm that is to be loaded:

```
processing.algorithm = "NO2_--"
```

Set some limits on the viewing geometry of ground pixels to process:

```
processing.szaMax = "88.0"
processing.szaMin = "0.0"
processing.vzaMax = "75.0"
processing.vzaMin = "0.0"
```

Wavelength pixels in the NO₂ fit window that are flagged as "saturated" are handled via two config parameters. The first one specifies the maximum fraction wavelength pixels allowed to be flagged saturated before deciding to skip the ground pixel from processing. The second one sets a limit on the fraction of saturated pixels before raising a warning; if this is set to zero, any saturation event is flagged.



```
processing.saturationMaxFraction = "0.12"
processing.saturationMaxWarningFraction = "0.00"
```

Specify, based on the Level-1B flags, the minimum fraction of wavelength pixels in the NO₂ fit window that must be valid wavelength pixels (40% of 305 is 122) for fitting to proceed, as well as a minimum fraction of valid wavelength pixels (80% of 305 is 244) that must be valid before generating a warning:

```
processing.radianceFractionMinError = "0.4"
processing.radianceFractionMinWarning = "0.8"
```

Set a lower limit to the NO₂ slant column in case that is negative:

```
processing.NO2_scd_limit = "-20.0e-6"
```


| | | |
|--|--------------------|--|
|   | S5L2PP ATBD-NO2 | Reference : KNMI-ESA-S5L2PP-ATBD-001 Version : 5.0 Page Date : 01 September 2023 75/89 |
|--|--------------------|--|

Set an upper limit to the noise ratio on the reflectance (if the noise is larger than this limit, it is adjusted upwards), and specify whether only noise ("false") or both noise and error ("true") on the Level-1B data is used for the error on the reflectance:

```
processing.reflectance_noise_floor = "2500.0"
processing.use_error_in_l1b = "false"
```

Specify whether the surface pressure is to be adapted based on the local orography:

```
processing.correct_surface_pressure_for_altitude = "true"
```

Specify the name of the irradiance and Ring reference spectra variables in the REF_SOLAR_ file (the _cf means that spectra are specified using the CF convention of using SI units):

```
processing.irradFluxVarName = "irradiance_flux_cf"
processing.radRingFluxVarName = "radiance_ring_flux_cf"
```

Specify how far, to be on the safe side, the retrieved spectra need to extend outside the fit window:

```
processing.fitWindowExtent = "3"
```

Wavelength at which the cloud (radiance) fraction calculation (see Sect. 6.4, App. A) is done in band 4 (this should be equal to the value in the 'Wavelength' variable in the LUT_N02CLD look-up table file), whether to obtain the reflectance at that wavelength from the modelled reflectance ("true") or not ("false"), and in the latter case what interval to average the measured reflectance over:

```
processing.cloud_wavelength = "440.0"
processing.reflectance_from_model = "true"
processing.cloud_wavelength_delta = "1.0"
```

Specify which digital elevation map (DEM) of the surface altitude and which surface albedo (LER) database to use in the respective files.

```
processing.groupDem = "DEM_RADIUS_05000"
processing.groupLer = "OMI"
```



E.1.5 Input specifications

Define the number of input files – in case of S5P/TROPOMI NO₂ processing this is 4: radiance RA_BD4, irradiance IR_UVN, clouds (either FRESCO, the O₂-O₂ cloud product 022CLD, or the DLR cloud product CLOUD_) – and the wavelength bands associated with this input:

```
input.count = "4"
input.1.band = "4"
input.1.irrType = "L1B_IR_UVN"
input.1.type = "L1B_RA_BD4"
input.2.band = "6"
input.2.required = "false"
input.2.type = "L2__FRESCO"
input.3.band = "3"
input.3.type = "L2__AER_AI"
input.4.band = "3"
input.4.required = "false"
input.4.type = "L2__CLOUD_"
input.5.band = "4"
input.5.required = "false"
input.5.type = "L2__022CLD"
```

E.1.6 Output specifications

Define the number of output products (should be 1), the output product short name, the band from which to include the geolocation information, and the output level (0 = nominal, 1 = stats, 2 = full):

| | | |
|--|--------------------|--|
|   | S5L2PP ATBD-NO2 | Reference : KNMI-ESA-S5L2PP-ATBD-001 Version : 5.0 Page Date : 01 September 2023 76/89 |
|--|--------------------|--|

```

output.count = "1"
output.1.band = "4"
output.1.config = "cfg/product/product.NO2_...xml"
output.1.level = "0"
output.1.type = "L2__NO2__"

```

Settings for compression and filtering to be used for the output netCDF file:

```

output.compressionLevel = "3"
output.useCompression = "true"
output.useFletcher32 = "true"
output.useShuffleFilter = "true"

```

Settings for the data histograms in the metadata:

```

output.histogram.nitrogen dioxide_stratospheric_column.logarithmic = "false"
output.histogram.nitrogen dioxide_stratospheric_column.range = "0,0.000166054"
output.histogram.nitrogen dioxide_total_column.logarithmic = "true"
output.histogram.nitrogen dioxide_total_column.range = "1.66054e-06,0.00166054"
output.histogram.nitrogen dioxide_tropospheric_column.logarithmic = "true"
output.histogram.nitrogen dioxide_tropospheric_column.range = "1.66054e-06,0.00166054"

```



E.1.7 Fixed configuration settings in the code

The S5P/TROPOMI NO₂ code contains a number of configuration settings in the code that have a fixed (default) value which cannot be altered via the configuration file. The following is a list of these fixed configuration settings given in the same order as those in the above subsections, without further information.

```

wavelength_calibration.irr.convergence_threshold = 1.000000
wavelength_calibration.irr.include_stretch = 0
wavelength_calibration.irr.initial_guess.a0 = 1.000000
wavelength_calibration.irr.initial_guess.a1 = 0.100000
wavelength_calibration.irr.initial_guess.a2 = 0.010000
wavelength_calibration.irr.initial_guess.shift = 0.000000
wavelength_calibration.irr.max_iterations = 12
wavelength_calibration.irr.polynomial_order = 2
wavelength_calibration.irr.sigma.a0 = 1.000000
wavelength_calibration.irr.sigma.a1 = 0.100000
wavelength_calibration.irr.sigma.a2 = 0.010000
wavelength_calibration.irr.sigma.shift = 0.070000
wavelength_calibration.irr.window = UNDEFINED
wavelength_calibration.rad.convergence_threshold = 1.000000
wavelength_calibration.rad.include_ring = 1
wavelength_calibration.rad.include_stretch = 0
wavelength_calibration.rad.initial_guess.a0 = 1.000000
wavelength_calibration.rad.initial_guess.a1 = 0.100000
wavelength_calibration.rad.initial_guess.a2 = 0.010000
wavelength_calibration.rad.initial_guess.ring = 0.060000
wavelength_calibration.rad.initial_guess.shift = 0.000000
wavelength_calibration.rad.max_iterations = 12
wavelength_calibration.rad.perform_wavelength_fit = 1
wavelength_calibration.rad.polynomial_order = 2
wavelength_calibration.rad.sigma.a0 = 1.000000
wavelength_calibration.rad.sigma.a1 = 0.100000
wavelength_calibration.rad.sigma.a2 = 0.010000
wavelength_calibration.rad.sigma.ring = 0.060000
wavelength_calibration.rad.sigma.shift = 0.070000
wavelength_calibration.rad.window = UNDEFINED

```

| | | |
|--|--------------------|---|
|   | S5L2PP ATBD-NO2 | Reference : KNMI-ESA-S5L2PP-ATBD-001 Version : 5.0 Date : 01 September 2023 |
| | | Page 77/89 |

```

NO2DOAS.H2O_liquid.reference_temperature = -1.000000
NO2DOAS.H2O_vapor.reference_temperature = -1.000000
NO2DOAS.O2O2.reference_temperature = -1.000000

```

```

qa_value.snow_ice_nocloud_modification_percent = 88.000000
qa_value.snow_ice_nocloud_scene_pressure_fraction_threshold = 0.980000
qa_value.snow_ice_nocloud_snow_threshold = 80

```

```



configuration.outputfile =
coregistration.fraction.minimum = 0.000000
coregistration.maxDeltaTime = 60
l2dp_home = /usr/people/sneep/tropnll2dp/
processing.albedo_wavelength = 440.000000
processing.bypassAlgo = 0
processing.bypassCloud = 0
processing.bypassSmallPixelVariance = 0
processing.ctm.maximum_age = 5.000000
processing.deadline.finalize = 20.000000
processing.groupDem2 = ECMWF_DEM_N640
processing.latMax = UNDEFINED
processing.latMin = UNDEFINED
processing.lonMax = UNDEFINED
processing.lonMin = UNDEFINED
processing.nPasses = 1
processing.nprogress = 25000
processing.nthreads.pass1 = 1
processing.pixelMax = 999999
processing.pixelMin = 0
processing.pixelStep = 1
processing.pixels = UNDEFINED
processing.radiancePixelsMinError = 0
processing.radiancePixelsMinWarning = 0
processing.saaMax = 180.000000
processing.saaMin = -180.000000
processing.saturationMask = 16
processing.scanlineMax = 999999
processing.scanlineMin = 0
processing.scanlineStep = 1
processing.scanlines = UNDEFINED
processing.sgaLimit = 30.000000
processing.signal_to_noise.test = 0
processing.signal_to_noise.threshold = 12
processing.signal_to_noise.window.end = -1.000000
processing.signal_to_noise.window.range =
processing.signal_to_noise.window.start = 0.000000
processing.snowIceAgeMax = 7
processing.testPixelNr = 1
processing.threadStackSize = 0
processing.threadTimeOut = 60
processing.vaaMax = 180.000000
processing.vaaMin = -180.000000
processing.writeTestData = 0
test.latitude = -4.069229

```

```

input.1.data_group.irradiance = STANDARD_MODE

```

| | | |
|--|--------------------|--|
|   | S5L2PP ATBD-NO2 | Reference : KNMI-ESA-S5L2PP-ATBD-001 Version : 5.0 Page Date : 01 September 2023 78/89 |
|--|--------------------|--|

```

input.1.data_group.radiance = STANDARD_MODE
input.1.required = 1
input.3.required = 0
input.5.checkBand = 1
input.5.checkOverlap = 1
input.5.checkProcessingMode = 1
input.5.checkType = 1
input.coadd.count = 1

debug.level = 0
debug.productwriter = 0
debug.vcd = 0
metadata.atbd.date = 2015-11-30
metadata.atbd.doi = N/A
metadata.atbd.title = TROPOMI ATBD of the total and tropospheric NO2 data products; \
                      S5P-KNMI-L2-0005-RP; release 1.0
metadata.creator_url = http://www.tropomi.eu
metadata.credit = The Sentinel 5 Precursor TROPOMI Level 2 products are developed with \
                  funding from the European Space Agency (ESA), the Netherlands Space \
                  Office (NSO), the Belgian Science Policy Office, the German \
                  Aerospace Center (DLR) and the Bayerisches Staatsministerium für \
                  Wirtschaft und Medien, Energie und Technologie (StMWi).
metadata.keywords.agu = 0345 Pollution, Urban and Regional; \
                        0365 Troposphere, Composition and Chemistry; \
                        0368 Troposphere, Constituent Transport and Chemistry; \
                        3360 Remote Sensing; \
                        3363 Stratospheric Dynamics
metadata.naming_authority = nl.knmi
metadata.product.doi = 10.5270/S5P-s4ljg54
metadata.pum.date = 2015-11-30
metadata.pum.doi = N/A
metadata.pum.title = Sentinel-5 precursor/TROPOMI Level 2 Product User Manual Nitrogen \
                    Dioxide; S5P-KNMI-L2-0021-MA; release 1.0
metadata.references = http://www.tropomi.eu/data-products/nitrogen-dioxide
output.nPixels = 450

```



E.2 Example XML process control file

The following is a listing of one of an S5P/TROPOMO NO₂ process XML file, the so-called joborder file, which essentially specifies the names of the input, configuration and output files.

In the following the names of the files have been removed for brevity and some open lines have been added for clarity.

Some notes, with links to related sections and tables:

- Sensing_Time can be used to process a slice of a granule
- CFG_NO2___ = configuration file with NO₂ process specifications (App. E.1)
- REF_SOLAR_ and REF_XS_NO2 = reference spectrum files (Sect. 6.2.6; Table 21)
- REF_DEM___ = surface altitude file (Sect. 6.3.4; Table 22)
- REF_LER___ = surface albedo files (Sect. 6.4.2; Table 21)
- LUT_COREG_ = inter-band co-registration data file (Sect. 6.3.1)
- LUT_NO2AMF = AMF look-up table (Sect. 6.7.2-6.7.3; Table 14; Table 21)
- LUT_NO2CLD = NO₂ cloud (radiation) fraction look-up table (Sect. 6.4; Table 21; App. A)
- AUX_CTMFCT or AUX_CTMANA = CTM / data assimilation forecast (FCT) or analysis (ANA) file (Sect. 6.6; Table 22)
- AUX_MET_2D and AUX_NISE__ = ECMWF meteo and NISE snow/ice data files (Sect. 6.4.3; Table 22)
- L2__FRESCO and L2__AER_AI = cloud and AAI Level-2 data files (Sect. 6.3.2; Sect. 6.3.3; Table 22)
- L1B_IR_UVN and L1B_RA_BD4 = Level-1b input files (Sect. 6; Table 22)

| | | |
|--|--------------------|--|
|   | S5L2PP ATBD-NO2 | Reference : KNMI-ESA-S5L2PP-ATBD-001 Version : 5.0 Page Date : 01 September 2023 79/89 |
|--|--------------------|--|

- L2__NO2__ = Level-2 output file (Sect. 6.8; Table 23)

Note that setting the Stdout_Log_Level keys to DEBUG results in a logfile that specifies each file, data variable, and config value that is read, including the configuration settings that are internal defaults (), as well as debug output of the retrieval per ground pixel.

```
<?xml version='1.0' encoding='utf-8'?>
<Ipf_Job_Order>

  <Ipf_Conf>
    <Processor_Name>NO2__</Processor_Name>
    <Version>1.3.0</Version>
    <Stdout_Log_Level>INFO</Stdout_Log_Level>
    <Stderr_Log_Level>INFO</Stderr_Log_Level>
    <Test>false</Test>
    <Breakpoint_Enable>false</Breakpoint_Enable>
    <Processing_Station>KNMI</Processing_Station>
    <Config_Files/>

    <Sensing_Time>
      <Start>00000000_000000000000</Start>
      <Stop>99999999_999999999999</Stop>
    </Sensing_Time>



    <Dynamic_Processing_Parameters>
      <Processing_Parameter>
        <Name>Processing_Mode</Name>
        <Value>OFFL</Value>
      </Processing_Parameter>
      <Processing_Parameter>
        <Name>Threads</Name>
        <Value>1</Value>
      </Processing_Parameter>
      <Processing_Parameter>
        <Name>Deadline_Time</Name>
        <Value>99999999_999999999999</Value>
      </Processing_Parameter>
    </Dynamic_Processing_Parameters>

  </Ipf_Conf>

  <List_of_Ipf_Procs count="1">
    <Ipf_Proc>
      <Task_Name>TROPNLL2DP</Task_Name>
      <Task_Version>1.3.0</Task_Version>

      <List_of_Inputs count="15">

        <Input>
          <File_Type>CFG_NO2__</File_Type>
          <File_Name_Type>Physical</File_Name_Type>
          <List_of_File_Names count="1">
            <File_Name>....</File_Name>
          </List_of_File_Names>
        </Input>
      </List_of_Inputs>
    </Ipf_Proc>
  </List_of_Ipf_Procs>
</Ipf_Job_Order>
```


| | | |
|--|--------------------|--|
|   | S5L2PP ATBD-NO2 | Reference : KNMI-ESA-S5L2PP-ATBD-001 Version : 5.0 Page Date : 01 September 2023 80/89 |
|--|--------------------|--|



```

<Input>
  <File_Type>REF_SOLAR_</File_Type>
  <File_Name_Type>Physical</File_Name_Type>
  <List_of_File_Names count="1">
    <File_Name>.....</File_Name>
  </List_of_File_Names>
</Input>
<Input>
  <File_Type>REF_XS_NO2</File_Type>
  <File_Name_Type>Physical</File_Name_Type>
  <List_of_File_Names count="1">
    <File_Name>.....</File_Name>
  </List_of_File_Names>
</Input>

<Input>
  <File_Type>REF_DEM__</File_Type>
  <File_Name_Type>Physical</File_Name_Type>
  <List_of_File_Names count="1">
    <File_Name>.....</File_Name>
  </List_of_File_Names>
</Input>
<Input>
  <File_Type>REF_LER__</File_Type>
  <File_Name_Type>Physical</File_Name_Type>
  <List_of_File_Names count="1">
    <File_Name>.....</File_Name>
  </List_of_File_Names>
</Input>
<Input>
  <File_Type>LUT_COREG</File_Type>
  <File_Name_Type>Physical</File_Name_Type>
  <List_of_File_Names count="1">
    <File_Name>.....</File_Name>
  </List_of_File_Names>
</Input>
<Input>
  <File_Type>LUT_NO2AMF</File_Type>
  <File_Name_Type>Physical</File_Name_Type>
  <List_of_File_Names count="1">
    <File_Name>.....</File_Name>
  </List_of_File_Names>
</Input>
<Input>
  <File_Type>LUT_NO2CLD</File_Type>
  <File_Name_Type>Physical</File_Name_Type>
  <List_of_File_Names count="1">
    <File_Name>.....</File_Name>
  </List_of_File_Names>
</Input>

<Input>
  <File_Type>AUX_CTMFCT</File_Type>
  <File_Name_Type>Physical</File_Name_Type>
  <List_of_File_Names count="1">
    <File_Name>.....</File_Name>

```

| | | |
|--|--------------------|--|
|   | S5L2PP ATBD-NO2 | Reference : KNMI-ESA-S5L2PP-ATBD-001 Version : 5.0 Page Date : 01 September 2023 81/89 |
|--|--------------------|--|

```

    </List_of_File_Names>
</Input>
<Input>
  <File_Type>AUX_MET_2D</File_Type>
  <File_Name_Type>Physical</File_Name_Type>
  <List_of_File_Names count="1">
    <File_Name>.....</File_Name>
  </List_of_File_Names>
</Input>
<Input>
  <File_Type>AUX_NISE__</File_Type>
  <File_Name_Type>Physical</File_Name_Type>
  <List_of_File_Names count="1">
    <File_Name>.....</File_Name>
  </List_of_File_Names>
</Input>



<Input>
  <File_Type>L2__FRESCO</File_Type>
  <File_Name_Type>Physical</File_Name_Type>
  <List_of_File_Names count="1">
    <File_Name>.....</File_Name>
  </List_of_File_Names>
</Input>
<Input>
  <File_Type>L2__AER_AI</File_Type>
  <File_Name_Type>Physical</File_Name_Type>
  <List_of_File_Names count="1">
    <File_Name>.....</File_Name>
  </List_of_File_Names>
</Input>

<Input>
  <File_Type>L1B_IR_UVN</File_Type>
  <File_Name_Type>Physical</File_Name_Type>
  <List_of_File_Names count="1">
    <File_Name>.....</File_Name>
  </List_of_File_Names>
</Input>
<Input>
  <File_Type>L1B_RA_BD4</File_Type>
  <File_Name_Type>Physical</File_Name_Type>
  <List_of_File_Names count="1">
    <File_Name>.....</File_Name>
  </List_of_File_Names>
</Input>

</List_of_Inputs>



<List_of_Outputs count="1">
  <Output>
    <File_Type>L2__NO2___</File_Type>
    <File_Name_Type>Physical</File_Name_Type>
    <File_Name>.....</File_Name>
  </Output>
</List_of_Outputs>

```

| | | | |
|--|--------------------|---|---------------|
|   | S5L2PP ATBD-NO2 | Reference : KNMI-ESA-S5L2PP-ATBD-001 Version : 5.0 Date : 01 September 2023 | Page 82/89 |
|--|--------------------|---|---------------|



</Ipf_Proc>
</List_of_Ipf_Procs>

</Ipf_Job_Order>



| | | |
|--|--------------------|--|
|   | S5L2PP ATBD-NO2 | Reference : KNMI-ESA-S5L2PP-ATBD-001 Version : 5.0 Page Date : 01 September 2023 83/89 |
|--|--------------------|--|

F References



- [Adams et al., 2016] Adams, C., Normand, E. N., McLinden, C. A., Bourassa, A. E., Lloyd, N. D., Degenstein, D. A., Krotkov, N. A., Rivas, M. B., Boersma, K. F., and Eskes, H. (2016). Limb-nadir matching using non-coincident no2 observations: proof of concept and the omi-minus-osisis prototype product. *Atmos. Meas. Tech.*, 9:4103–4122.
- [Adams et al., 2013] Adams, C., Strong, K., Zhao, X., Bourassa, A. E., Daffer, W. H., Degenstein, D., Drummond, J. R., Farahani, E. E., Fraser, A., Lloyd, N. D., Manney, G. L., McLinden, C. A., Rex, M., Roth, C., Strahan, S. E., Walker, K. A., and Wohltmann, I. (2013). The spring 2011 final stratospheric warming above Eureka: anomalous dynamics and chemistry. *Atmos. Chem. Phys.*, 13:611–624.
- [Bak et al., 2013] Bak, J., Kim, J. H., Liu, X., Chance, K., and Kim, J. (2013). Evaluation of ozone profile and tropospheric ozone retrievals from GEMS and OMI spectra. *Atmos. Meas. Tech.*, 6:239–249.
- [Beirle et al., 2011] Beirle, S., Boersma, K. F., Platt, U., Lawrence, M. G., and Wagner, T. (2011). Megacity emissions and lifetimes of nitrogen oxides probed from space. *Science*, 333:1737–1739.
- [Beirle et al., 2016] Beirle, S., Hörmann, C., P., J., Liu, S., Penning de Vries, M., Pozzer, A., Sihler, H., Valks, P., and Wagner, T. (2016). The STRatospheric Estimation Algorithm from Mainz (STREAM): estimating stratospheric NO₂ from nadir-viewing satellites by weighted convolution. *Atmos. Meas. Tech.*, 9:2753–2779.
- [Beirle et al., 2010] Beirle, S., Kühl, S., Pukite, J., and Wagner, T. (2010). Retrieval of tropospheric column densities of NO₂ from combined SCIAMACHY nadir/limb measurements. *Atmos. Meas. Tech.*, 3:283–299.
- [Belmonte-Rivas et al., 2014] Belmonte-Rivas, M., Veefkind, P., Boersma, F., P., Eskes, H., and Gille, J. (2014). Intercomparison of daytime stratospheric NO₂ satellite retrievals and model simulations. *Atmos. Meas. Tech.*, 7:2203–2225.
- [Bernath et al., 2005] Bernath, P. F., McElroy, C. T., Abrams, M. C., Boone, C. D., and M. Butler, e. a. (2005). Atmospheric Chemistry Experiment (ACE): Mission overview. *Geophys. Res. Lett.*, 32(L15S01):5 pp.
- [Boersma et al., 2002] Boersma, K. F., Bucsela, E., Brinksma, E., and Gleason, J. F. (2002). NO₂. In *OMI Algorithm Theoretical Basis Document – Vol. 4: OMI Trace Gas Algorithms, ATBD-OMI-02 Vers. 2.0*, pages 13–28. NASA Goddard Space Flight Cent., Greenbelt, Md.
- [Boersma et al., 2004] Boersma, K. F., Eskes, H. J., and Brinksma, E. J. (2004). Error analysis for tropospheric NO₂ retrieval from space. *J. Geophys. Res.*, 109(D04311):20 pp.
- [Boersma et al., 2011] Boersma, K. F., Eskes, H. J., Dirksen, R. J., Van der A, R. J., Veefkind, J. P., Stammes, P., Huijnen, V., Kleipool, Q. L., Sneep, M., Claas, J., Leitão, J., Richter, A., Zhou, Y., and Brunner, D. (2011). An improved retrieval of tropospheric NO₂ columns from the Ozone Monitoring Instrument. *Atmos. Meas. Tech.*, 4:1905–1928.
- [Boersma et al., 2018] Boersma, K. F., Eskes, H. J., Richter, A., Smedt, I. D., Lorente, A., Beirle, S., van Geffen, J. H. G. M., Zara, M., Peters, E., Roozendael, M. V., Wagner, T., Maasakkers, J. D., van der A, R. J., Nightingale, J., Rudder, A. D., Irie, H., Pinardi, G., Lambert, J.-C., and Compennolle, S. (2018). Improving algorithms and uncertainty estimates for satellite NO₂ retrievals: Results from the Quality Assurance for Essential Climate Variables (QA4ECV) project Variables (QA4ECV) project. *Atmos. Meas. Tech.*, 11:6651–6678.
- [Boersma et al., 2007] Boersma, K. F., Eskes, H. J., Veefkind, J. P., Brinksma, E. J., Van der A, R. J., Sneep, M., Van den Oord, G. H. J., P. F., Stammes, P., F., G. J., and Bucsela, E. J. (2007). Near-real time retrieval of tropospheric NO₂ from OMI. *Atmos. Chem. Phys.*, 7:2013–2128.
- [Boersma et al., 2009] Boersma, K. F., Jacob, D. J., Trainic, M., Rudich, Y., DeSmedt, I., Dirksen, R., and Eskes, H. J. (2009). Validation of urban NO₂ concentrations and their diurnal and seasonal variations observed from the SCIAMACHY and OMI sensors using in situ surface measurements in israeli cities. *Atmos. Chem. Phys.*, 9:3867–3879.
- [Boersma et al., 2016] Boersma, K. F., Vinken, G. C. M., and Eskes, H. J. (2016). Representativeness errors in comparing chemistry transport and chemistry climate models with satellite UV-Vis tropospheric column retrievals. *Geosci. Model Dev.*, 9:875–898.

| | | |
|--|--------------------|--|
|   | S5L2PP ATBD-NO2 | Reference : KNMI-ESA-S5L2PP-ATBD-001 Version : 5.0 Page Date : 01 September 2023 84/89 |
|--|--------------------|--|



- [Bovensmann et al., 1999] Bovensmann, H., Burrows, J. P., Buchwitz, M., Frerick, J., Noel, S., Rozanov, V. V., Chance, K. V., and Goede, A. P. H. (1999). SCIAMACHY: mission objectives and measurement modes. *J. Atmos. Sci.*, 56:127–150.
- [Bucsela et al., 2006] Bucsela, E. J., Celarier, E. A., Wenig, M. O., Gleason, J. F., Veefkind, J. P., Boersma, K. F., and Brinkma, E. J. (2006). Algorithm for NO₂ vertical column retrieval from the ozone monitoring instrument. *IEEE Trans. Geosci. Rem. Sens.*, 44:1245–1258.
- [Bucsela et al., 2013] Bucsela, E. J., Krotkov, N. A., Celarier, E. A., Lamsal, L. N., Swartz, W. H., Bhartia, P. K., Boersma, K. F., Veefkind, J. P., Gleason, J. F., and Pickering, K. E. (2013). A new stratospheric and tropospheric NO₂ retrieval algorithm for nadir-viewing satellite instruments: applications to OMI. *Atmos. Meas. Tech.*, 6:2607–2626.
- [Burrows et al., 1999] Burrows, J. P., Weber, M., Buchwitz, M., Rozanov, V., Ladstätter-Weissenmayer, A., Richter, A., Debeek, R., Hoogen, R., Bramstedt, K., Eichmann, K.-U., Eisinger, M., and Perner, D. (1999). The Global Ozone Monitoring Experiment (GOME): Mission concept and first results. *J. Atmos. Sci.*, 56:151–175.
- [Castellanos and Boersma, 2012] Castellanos, P. and Boersma, K. F. (2012). Reductions in nitrogen oxides over Europe driven by environmental policy and economic recession. *Scientific Reports*, 2:7 pp.
- [Chance and Kurucz, 2010] Chance, K. V. and Kurucz, R. L. (2010). An improved high-resolution solar reference spectrum for earth's atmosphere measurements in the ultraviolet, visible, and near infrared. *J. Quant. Spectrosc. Radiat. Transfer*, 111:1289–1295.
- [Chance and Spurr, 1997] Chance, K. V. and Spurr, R. J. D. (1997). Ring effect studies: Rayleigh scattering, including molecular parameters for rotational Raman scattering and the Fraunhofer spectrum. *Appl. Opt.*, 36(21):5224–5230.
- [Chandrasekhar, 1960] Chandrasekhar, S. (1960). *Radiative Transfer*. Dover Publications, New York.
- [Chu and McCormick, 1986] Chu, W. P. and McCormick, M. P. (1986). Sage observations of stratospheric nitrogen dioxide. *J. Geophys. Res.*, 91(D5):5465–5476.
- [Crutzen, 1970] Crutzen, P. J. (1970). The influence of nitrogen oxides on the atmospheric ozone content. *Quart. J. R. Meteorol. Soc.*, 96:320–325.
- [De Haan et al., 1987] De Haan, J. F., Bosma, P. B., and Hovenier, J. W. (1987). The adding method for multiple scattering in a non-homogeneous Rayleigh atmosphere. *Astron. & Astroph.*, 183:371–391.
- [De Ruyter de Wildt et al., 2012] De Ruyter de Wildt, M., Eskes, H., and Boersma, K. F. (2012). The global economic cycle and satellite-derived NO₂ trends over shipping lanes. *Geophys. Res. Lett.*, 39(L01802):6 pp.
- [Dentener et al., 2006] Dentener, F., Drevet, J., Lamarque, J. F., Bey, I., Eickhout, B., Fiore, A. M., Hauglustaine, D., Horowitz, L. W., Krol, M., Kulshrestha, U. C., Lawrence, M., Galy-Lacaux, C., Rast, S., Shindell, D., Stevenson, D., Noije, T. V., Atherton, C., Bell, N., Bergman, D., Butler, T., Cofala, J., Collins, B., Doherty, R., Ellingsen, K., Galloway, J., Gauss, M., Montanaro, V., Müller, J. F., Pitari, G., Rodriguez, J., Sanderson, M., Solomon, F., Strahan, S., Schultz, M., Sudo, K., Szopa, S., and Wild, O. (2006). Nitrogen and sulfur deposition on regional and global scales: A multimodel evaluation. *Global Biogeochem. Cycles*, 20(GB4003):21 pp.
- [Dentener et al., 2003] Dentener, F., Van Weele, M., Krol, M., Houweling, S., and van Velthoven, P. (2003). Trends and inter-annual variability of methane emissions derived from 1979-1993 global CTM simulations. *Atmos. Chem. Phys.*, 3:73–88.
- [Dirksen et al., 2011] Dirksen, R. J., Boersma, K. F., Eskes, H. J., Ionov, D. V., Bucsela, E. J., P. F., and Kelder, H. M. (2011). Evaluation of stratospheric NO₂ retrieved from the Ozone Monitoring Instrument: Intercomparison, diurnal cycle, and trending. *J. Geophys. Res.*, 116(D08305):22 pp.
- [Eskes and Boersma, 2003] Eskes, H. J. and Boersma, K. F. (2003). Averaging kernels for DOAS total-column satellite retrievals. *Atmos. Chem. Phys.*, 3:1285–1291.
- [Eskes et al., 2023] Eskes, H. J., Tsikerdekis, A., Benedictow, A., Bennouna, Y., Blake, L., Bouarar, I., Errera, Q., Griesfeller, J., Ilic, L., Kapsomenakis, J., Langerock, B., Mortier, A., Pison, I., Pitkänen, M. R. A., Richter, A., Schoenhardt, A., Schulz, M., Thouret, V., Warneke, T., and Zerefos, C. (2023). Upgrade verification note for the CAMS near-real time global atmospheric composition service: Evaluation of the e-suite for the CAMS Cy48R1 upgrade of 27 June 2023. Technical report, Copernicus Atmosphere Monitoring Service (CAMS), June 2023, doi:10.24380/rzg1-8f3l.

| | | |
|--|--------------------|--|
|   | S5L2PP ATBD-NO2 | Reference : KNMI-ESA-S5L2PP-ATBD-001 Version : 5.0 Page Date : 01 September 2023 85/89 |
|--|--------------------|--|



- [Fuglestad et al., 1999] Fuglestad, J. S., Berntsen, T., Isaksen, I. S. A., Mao, H., Liang, X.-Z., and Wang, W.-C. (1999). Climatic forcing of nitrogen oxides through changes in tropospheric ozone and methane. *Atmos. Environ.*, 33(3):961–977.
- [Gordley et al., 1996] Gordley, L. L., III, J. M. R., Mickley, L. J., Frederick, J. E., Park, J. H., Stone, K. A., Beaver, G. M., McInerney, J. M., Deaver, L. E., Toon, G. C., Murcray, F. J., Blatherwick, R. D., Gunson, M. R., Abbatt, J. P. D., III, R. L. M., Mount, G. H., Sen, B., and Blavier, J.-F. (1996). Validation of nitric oxide and nitrogen dioxide measurements made by the Halogen Occultation Experiment for UARS platform. *J. Geophys. Res.*, 101(D6):10241–10266.
- [Gorshchev et al., 2014] Gorshchev, V., Serdyuchenko, A., Weber, M., and Burrows, J. P. (2014). High spectral resolution ozone absorption cross-sections: Part I. Measurements, data analysis and comparison around 293K. *Atmos. Meas. Tech.*, 7:609–624.
- [Griffin et al., 2019] Griffin, D., Zhao, X., McLinden, C. A., Boersma, F., Bourassa, A., Dammers, E., Degenstein, D., Eskes, H., Fehr, L., Fioletov, V., Hayden, K., Kharol, S. K. Li, S.-M., Makar, P., Martin, R. V., Mihele, C., Mittermeier, R. L., Krotkov, N., Snee, M., Lamsal, L. N., ter Linden, M., van Geffen, J., Veefkind, P., and Wolde, M. (2019). High resolution mapping of nitrogen dioxide with TROPOMI: First results and validation over the Canadian oil sands. *Geophys. Res. Lett.*, 46:1049–1060.
- [Gruzdev and Elokhov, 2009] Gruzdev, A. N. and Elokhov, A. S. (2009). Validating NO₂ measurements in the vertical atmospheric column with the OMI instrument aboard the EOS Aura satellite against ground-based measurements at the Zvenigorod Scientific Station. *Izv. Atmos. Oceanic Phys.*, 45(4):444–455.
- [Hains et al., 2010] Hains, J. C., Boersma, K. F., Kroon, M., Dirksen, R. J., Cohen, R. C., Perring, A. E., Bucsela, E., Volten, H., Swart, D. P. J., Richter, A. and Wittrock, F., Schoenhardt, A., Wagner, T., Ibrahim, O. W., Roozendael, V., M., Pinardi, G., Gleason, J. F., Veefkind, J. P., and , P. (2010). Testing and improving OMI DOMINO tropospheric NO₂ using observations from the DANDELIONS and INTEx-B validation campaigns. *J. Geophys. Res.*, 115(D05301):20 pp.
- [Hakkarainen et al., 2016] Hakkarainen, J., Jalongo, I., and Tamminen, J. (2016). Direct space-based observations of anthropogenic CO₂ emission areas from OCO-2. *Geophys. Res. Lett.*, 43(21):11,400–11,406.
- [Hendrick et al., 2012] Hendrick, F., Mahieu, E., Bodeker, G. E., Boersma, K. F., Chipperfield, M. P., De Mazière, M., De Smedt, I., Demoulin, P., Fayt, C., Hermans, C., Kreher, K., Lejeune, B., Pinardi, G., Servais, C., Stübi, R., Van der A, R., Vernier, J.-P., and Van Roozendael, M. (2012). Analysis of stratospheric NO₂ trends above Jungfraujoch using ground-based UV-visible, FTIR, and satellite nadir observations. *Atmos. Chem. Phys.*, 12:8851–8864.
- [Hilboll et al., 2013a] Hilboll, A., Richter, A., and Burrows, J. P. (2013a). Long-term changes of tropospheric NO₂ over megacities derived from multiple satellite instruments. *Atmos. Chem. Phys.*, 13:4145–4169.
- [Hilboll et al., 2013b] Hilboll, A., Richter, A., Rozanov, A., Hodnebrog, O., Heckel, A., Solberg, S., Stordal, F., and Burrows, J. P. (2013b). Improvements to the retrieval of tropospheric NO₂ from satellite – stratospheric correction using SCIAMACHY limb/nadir matching and comparison to Oslo CTM2 simulations. *Atmos. Meas. Tech.*, 6:565–584.
- [Huijnen et al., 2010a] Huijnen, V., Eskes, H. J., Poupkou, A., Elbern, H., Boersma, K. F., Foret, G., Sofiev, M., Valdebenito, A., Flemming, J., Stein, O., Gross, A., Robertson, L., D’Isidoro, M., Kioutsioukis, I., Friese, E., Amstrup, B., Bergstrom, R., Strunk, A., Vira, J., Zyryanov, D., Maurizi, A., Melas, D., Peuch, V.-H., and Zerefos, C. (2010a). Comparison of OMI NO₂ tropospheric columns with an ensemble of global and European regional air quality models. *Atmos. Chem. Phys.*, 10:3273–3296.
- [Huijnen et al., 2016] Huijnen, V., Flemming, J., Chabrilat, S., Errera, Q., Christophe, Y., Blechschmidt, A.-M., Richter, A., and Eskes, H. (2016). C-IFS-CB05-BASCOE: stratospheric chemistry in the Integrated Forecasting System of ECMWF. *Geosci. Model Dev.*, 9:3071–3091.
- [Huijnen et al., 2010b] Huijnen, V., Williams, J., Van Weele, M., Van Noije, T., Krol, M., Dentener, F., Segers, A., Houweling, S., Peters, W., De Laat, J., Boersma, F., Bergamaschi, P., Van Velthoven, P., Le Sager, P., Eskes, H., Alkemade, F., Scheele, R., Nédélec, P., and Pätz, H.-W. (2010b). The global chemistry transport model tm5: description and evaluation of the tropospheric chemistry version 3.0. *Geosci. Model Dev.*, 3(2):445–473.
- [Ingmann et al., 2012] Ingmann, P., Veihelmann, B., Langen, J., Lamarre, D., Stark, H., and Courrèges-Lacoste, G. B. (2012). Requirements for the GMES Atmosphere Service and ESA’s implementation concept: Sentinels-4/-5 and -5p. *Rem. Sens. Environment*, 120:58–69.

| | | |
|--|--------------------|--|
|   | S5L2PP ATBD-NO2 | Reference : KNMI-ESA-S5L2PP-ATBD-001 Version : 5.0 Page Date : 01 September 2023 86/89 |
|--|--------------------|--|



- [Irie et al., 2012] Irie, H., Boersma, K. F., Kanaya, Y., Takashima, H., Pan, X., and Wang, Z. F. (2012). First quantitative bias estimates for tropospheric NO₂ columns retrieved from SCIAMACHY, OMI, and GOME-2 using a common standard. *Atmos. Meas. Tech.*, 5:2403–2411.
- [Jacob, 1999] Jacob, D. J. (1999). *Introduction to Atmospheric Chemistry*. Princeton University Press.
- [Kim et al., 2020] Kim, J., Jeong, U., Ahn, H.-H., Kim, J. H., Park, R. J., and et al., H. L. (2020). New era of air quality monitoring from space: Geostationary Environment Monitoring Spectrometer (GEMS). *Bulletin of the American Meteorological Society*, 101:22 pp.
- [Kleipool et al., 2008] Kleipool, Q. L., Dobber, M. R., De Haan, J. F., and , P. F. (2008). Earth surface reflectance climatology from 3 years of OMI data. *J. Geophys. Res.*, 113(D18308):22 pp.
- [Koelemeijer et al., 2001] Koelemeijer, R. B. A., Stammes, P., W., H. J., and De Haan, J. F. (2001). A fast method for retrieval of cloud parameters using oxygen A band measurements from the Global Ozone Monitoring Experiment. *J. Geophys. Res.*, 106(D4):3475–3490.
- [Lampel et al., 2015] Lampel, J., Frieß, U., and U., P. (2015). The impact of vibrational raman scattering of air on doas measurements of atmospheric trace gases. *Atmos. Meas. Tech.*, 8:3767–3787.
- [Lamsal et al., 2010] Lamsal, L. N., Martin, R. V., Van Donkelaar, A., Celarier, E. A., Bucsela, E. J., Boersma, K. F., Dirksen, R., Luo, C., and Wang, Y. (2010). Indirect validation of tropospheric nitrogen dioxide retrieved from the OMI satellite instrument: Insight into the seasonal variation of nitrogen oxides at northern midlatitudes. *J. Geophys. Res.*, 115(D05302):15 pp.
- [Leitão et al., 2010] Leitão, J., Richter, A., Vrekoussis, M., Kokhanovsky, A., Zhang, Q., Beekmann, M., and Burrows, J. P. (2010). On the improvement of NO₂ satellite retrievals – aerosol impact on the air mass factors. *Atmos. Meas. Tech.*, 3:475–493.
- [Leue et al., 2001] Leue, C., Wenig, M., Wagner, T., Klimm, O., Platt, U., and Jähne, B. (2001). Quantitative analysis of NO_x emissions from Global Ozone Monitoring Experiment satellite image sequences. *J. Geophys. Res.*, 106(D6):5493–5505.
- [Levelt et al., 2006] Levelt, P. F., van den Oord, G. H. J., Dobber, M. R., Mäkki, A., Visser, H., de Vries, J., Stammes, P., Lundell, J. O. V., and Saari, H. (2006). The Ozone Monitoring Instrument. *IEEE Trans. Geosci. Rem. Sens.*, 44:1093–1101.
- [Liley et al., 2000] Liley, J. B., Johnston, P. V., McKenzie, R. L., Thomas, A. J., and Boyd, I. S. (2000). Stratospheric NO₂ variations from a long time series at Lauder, New Zealand. *J. Geophys. Res.*, 105(D9):11,633–11,640.
- [Lin et al., 2014] Lin, J., Martin, R. V., Boersma, K. F., Sneep, M., Stammes, P., Spurr, R., Wang, P., Roozendael, M. V., Clémer, K., and Irie, H. (2014). Retrieving tropospheric nitrogen dioxide over China from the Ozone Monitoring Instrument: Effects of aerosols, surface reflectance anisotropy and vertical profile of nitrogen dioxide. *Atmos. Chem. Phys.*, 14:1441–1461.
- [Lin et al., 2010] Lin, J.-T., McElroy, M. B., and Boersma, K. F. (2010). Constraint of anthropogenic NO_x emissions in china from different sectors: a new methodology using multiple satellite retrievals. *Atmos. Chem. Phys.*, 10:63–78.
- [Llewellyn et al., 2004] Llewellyn, E. J., Lloyd, N. D., Degenstein, D. A., Gattinger, R. L., and S. V. Petelina, e. a. (2004). The OSIRIS instrument on the Odin spacecraft. *Canadian Journal of Physics*, 82(6):411–422.
- [Lorente et al., 2017] Lorente, A., Folkert Boersma, K., Yu, H., Dörner, S., Hilboll, A., Richter, A., Liu, M., Lamsal, L. N., Barkley, M., De Smedt, I., Van Roozendael, M., Wang, Y., Wagner, T., Beirle, S., Lin, J.-T., Krotkov, N., Stammes, P., Wang, P., Eskes, H. J., and Krol, M. (2017). Structural uncertainty in air mass factor calculation for NO₂ and HCHO satellite retrievals. *Atmos. Meas. Tech.*, 10:759–782.
- [Ma et al., 2013] Ma, J. Z., Beirle, S., Jin, J. L., Shaiganfar, R., Yan, P., and Wagner, T. (2013). Tropospheric NO₂ vertical column densities over Beijing: results of the first three years of ground-based MAX-DOAS measurements (2008–2011) and satellite validation. *Atmos. Chem. Phys.*, 13:1547–1567.
- [Maasakkers et al., 2013] Maasakkers, J. D., Boersma, K. F., Williams, J. E., Van Geffen, J., Vinken, G. C. M., Sneep, M., Hendrick, F., Van Roozendael, M., and Veefkind, J. P. (2013). Vital improvements to the retrieval of tropospheric NO₂ columns from the Ozone Monitoring Instrument. *Geophys. Res. Abstracts*, 15(EGU2013-714):1. EGU General Assembly 2013.

| | | |
|--|--------------------|--|
|   | S5L2PP ATBD-NO2 | Reference : KNMI-ESA-S5L2PP-ATBD-001 Version : 5.0 Page Date : 01 September 2023 87/89 |
|--|--------------------|--|

- [Martin et al., 2002] Martin, R. V., Chance, K., Jacob, D. J., Kurosu, T. P., Spurr, R. J. D., Bucsela, E., Gleason, J. F., Palmer, P. I., Bey, I., Fiore, A. M., Li, Q., Yantosca, R. M., and Koelemeijer, R. B. A. (2002). An improved retrieval of tropospheric nitrogen dioxide from GOME. *J. Geophys. Res.*, 107(D20):4437–4457.
- [Mijling and Van der A, 2012] Mijling, B. and Van der A, R. J. (2012). Using daily satellite observations to estimate emissions of short-lived air pollutants on a mesoscopic scale. *J. Geophys. Res.*, 117(D17302):20 pp.
- [Mount et al., 1984] Mount, G. H., Rusch, D. W., Noxon, J. F., Zawodny, J. M., and Barth, C. A. (1984). Measurements of stratospheric NO₂ from the Solar Mesosphere Explorer Satellite: 1. An overview of the results. *J. Geophys. Res.*, 89(D1):1327–1340.
- [Munro et al., 2006] Munro, R., Eisinger, M., Anderson, C., Callies, J., Corpaccioli, E., Lang, R., Lefebvre, A., Livschitz, Y., and Albinana, A. P. (2006). GOME-2 on MetOp. In *Proceedings of the Atmospheric Science Conference 2006*, SP 628. ESA, ESA, Paris.
- [Murphy et al., 1993] Murphy, D. M., Fahey, D. W., Proffitt, M. H., Liu, S. C., Chan, K. R., Eubank, C. S., Kawa, S. R., and Kelly, K. K. (1993). Reactive nitrogen and its correlation with ozone in the lower stratosphere and upper troposphere. *J. Geophys. Res.*, 98(D5):8751–8773.
- [Ott et al., 2010] Ott, L. E., Pickering, K. E., Stenchikov, G. L., Allen, D. J., DeCaria, A. J., Ridley, B., Lin, R.-F., Lang, S., and Tao, W.-K. (2010). Production of lightning NO and its vertical distribution calculated from three-dimensional cloud-scale chemical transport model simulations. *J. Geophys. Res.*, 115(D04301):19 pp.
- [Palmer et al., 2001] Palmer, P. I., Jacob, D., Chance, K., Martin, R. V., Spurr, R. J. D., Kurosu, T. P., Bey, I., Yantosca, R., Fiore, A., and Li, Q. (2001). Air-mass factor formulation for spectroscopic measurements from satellite: applications to formaldehyde retrievals from the Global Ozone Monitoring Experiment. *J. Geophys. Res.*, 106:14539–14550.
- [Peters et al., 2012] Peters, A. J. M., Boersma, K. F., Kroon, M., Hains, J. C., and Van Roozendael M., et al. (2012). The Cabauw Intercomparison campaign for Nitrogen Dioxide measuring Instruments (CINDI): design, execution, and early results. *Atmos. Meas. Tech.*, 5:457–485.
- [Platt, 1994] Platt, U. (1994). Differential Optical Absorption Spectroscopy (DOAS). *Air monitoring by spectroscopic techniques, Chem. Anal.*, 127:27–76. edited by M.W. Sigrist.
- [Platt and Stutz, 2008] Platt, U. and Stutz, Z. (2008). *Differential Optical Absorption Spectroscopy, Principles and Applications*. Springer, Heidelberg, Germany.
- [Pope and Fry, 1997] Pope, R. M. and Fry, E. S. (1997). Absorption spectrum (380–700 nm) of pure water. II. Integrating cavity measurements. *Appl. Opt.*, 36(33):8710–8723.
- [Randall et al., 1998] Randall, C. E., Rusch, D. W., Bevilacqua, R. M., Hoppel, K. W., and Lumpe, J. D. (1998). Polar Ozone and Aerosol Measurement (POAM) II stratospheric NO₂ 1993–1996. *J. Geophys. Res.*, 103(D21):28361–28371.
- [Ravishankara et al., 2009] Ravishankara, A. R., Daniel, J. S., and Portmann, R. W. (2009). Nitrous Oxide (N₂O): The Dominant Ozone-Depleting Substance Emitted in the 21st Century. *Science*, 326(5949):123–125.
- [Richter et al., 2011] Richter, A., Begoin, M., Hilboll, A., and Burrows, J. P. (2011). An improved NO₂ retrieval for the GOME-2 satellite instrument. *Atmos. Meas. Tech.*, 4:1147–1159.
- [Richter and Burrows, 2002] Richter, A. and Burrows, J. P. (2002). Tropospheric NO₂ from GOME measurements. *Adv. Space Res.*, 29(11):1673–1683.
- [Rodgers, 2000] Rodgers, C. D. (2000). *Inverse Methods for Atmospheric Sounding: Theory and Practice*. World Scientific Publishing.
- [Schaub et al., 2007] Schaub, D., Brunner, D., Boersma, K. F., Keller, J., Folini, D., Buchmann, B., Berresheim, H., and Staehelin, J. (2007). SCIAMACHY tropospheric NO₂ over Switzerland: estimates of NO_x lifetimes and impact of the complex Alpine topography on the retrieval. *Atmos. Chem. Phys.*, 7:5971–5987.
- [Seinfeld and Pandis, 2006] Seinfeld, J. H. and Pandis, S. N. (2006). *Atmospheric Chemistry and Physics - From Air Pollution to Climate Change (2nd Edition)*. John Wiley & Sons.

| | | |
|--|--------------------|--|
|   | S5L2PP ATBD-NO2 | Reference : KNMI-ESA-S5L2PP-ATBD-001 Version : 5.0 Page Date : 01 September 2023 88/89 |
|--|--------------------|--|

- [Serdyuchenko et al., 2014] Serdyuchenko, A., Gorshelev, V., Weber, M., Chehade, W., and Burrows, J. P. (2014). High spectral resolution ozone absorption cross-sections: Part II. Temperature dependence. *Atmos. Meas. Tech.*, 7:625–636.
- [Shindell et al., 2009] Shindell, D. T., Faluvegi, G., Koch, D. M., Schmidt, G. A., Unger, N., and Bauer, S. E. (2009). Improved attribution of climate forcing to emissions. *Science*, 326(5953):716–718.
- [Sierk et al., 2006] Sierk, B., Richter, A., Rozanov, A., Von Savigny, C., Schmoltner, A. M., Buchwitz, M., Bovensmann, H., and Burrows, J. P. (2006). Retrieval and monitoring of atmospheric trace gas concentrations in nadir and limb geometry using the space-borne SCIAMACHY instrument. *Environmental Monitoring and Assessment*, 120:65–73.
- [Sillman et al., 1990] Sillman, S., Logan, J. A., and Wofsy, S. C. (1990). The sensitivity of ozone to nitrogen oxides and hydrocarbons in regional ozone episodes. *J. Geophys. Res.*, 95(D2):1837–1851.
- [Silver et al., 2013] Silver, J. D., Brandt, J., Hvidberg, M., Frydendall, J., and Christensen, J. H. (2013). Assimilation of OMI NO₂ retrievals into the limited-area chemistry-transport model DEHM (V2009.0) with a 3-D OI algorithm. *Geosc. Model Dev.*, 6:1–16.
- [Sluis et al., 2010] Sluis, W. W., Allaart, M. A. F., M., P. A. J., and Gast, L. F. L. (2010). The development of a nitrogen dioxide sonde. *Atmos. Meas. Tech.*, 3:1753–1762.
- [Solomon, 1999] Solomon, S. (1999). Stratospheric ozone depletion: A review of concepts and history. *Rev. Geophys.*, 37(3):275–316.
- [Stammes, 2001] Stammes, P. (2001). Spectral radiance modeling in the UV-visible range. In Smith, W. and Timofeyev, Y., editors, *IRS 2000: Current Problems in Atmospheric Radiation*, pages 385–388. A. Deepak, Hampton, Va.
- [Stammes et al., 2008] Stammes, P., Sneep, M., De Haan, J. F., Veefkind, J. P., Wang, P., and , P. F. (2008). Effective cloud fractions from the Ozone Monitoring Instrument: Theoretical framework and validation. *J. Geophys. Res.*, 113(D16S38):12 pp.
- [Stavrakou et al., 2008] Stavrakou, T., Müller, J.-F., Boersma, K. F., De Smedt, I., and Van der A, R. J. (2008). Assessing the distribution and growth rates of NO₂ emission sources by inverting a 10-year record of NO₂ satellite columns. *Geophys. Res. Lett.*, 35(L10801):5 pp.
- [Thalman and Volkamer, 2013] Thalman, R. and Volkamer, R. (2013). Temperature dependant absorption cross-sections of O₂-O₂ collision pairs between 340 and 630 nm at atmospherically relevant pressure. *Phys. Chem. Chem. Phys.*, 15:15371–15381.
- [Tilstra et al., 2017] Tilstra, L. G., Tuinder, O. N. E., Wang, P., and Stammes, P. (2017). Surface reflectivity climatologies from UV to NIR determined from Earth observations by GOME-2 and SCIAMACHY. *J. Geophys. Res.*, 122:4084–4111.
- [Valks et al., 2011] Valks, P., Pinardi, G., Richter, A., Lambert, J.-C., Hao, N., Loyola, D., Van Roozendael, M., and Emmadi, S. (2011). Operational total and tropospheric NO₂ column retrieval for GOME-2. *Atmos. Meas. Tech.*, 4:1491–1514.
- [Van der A et al., 2008] Van der A, R. J., Eskes, H. J., Boersma, K. F., Van Noije, T. P. C., Van Roozendael, M., De Smedt, I., Peters, D. H. M. U., Kuenen, J. J. P., and Meijer, E. W. (2008). Trends, seasonal variability and dominant NO_x source derived from a ten year record of NO₂ measured from space. *J. Geophys. Res.*, 113(D04302):12 pp.
- [Van Diedenhoven et al., 2007] Van Diedenhoven, B., Hasekamp, O. P., and Landgraf, J. (2007). Retrieval of cloud parameters from satellite-based reflectance measurements in the ultraviolet and the oxygen A-band. *J. Geophys. Res.*, 112(D15208):15 pp.
- [Van Geffen et al., 2020] Van Geffen, J. H. G. M., Boersma, K. F., Eskes, H., Sneep, M., ter Linden, M., Zara, M., and Veefkind, J. P. (2020). S5P/TROPOMI NO₂ slant column retrieval: method, stability, uncertainties, and comparisons with OMI. *Atmos. Meas. Tech.*, 13:1315–1335.
- [Van Geffen et al., 2015] Van Geffen, J. H. G. M., Boersma, K. F., Van Roozendael, M., Hendrick, F., Mahieu, E., De Smedt, I., M., S., and Veefkind, J. P. (2015). Improved spectral fitting of nitrogen dioxide from OMI in the 405 – 465 nm window. *Atmos. Meas. Tech.*, 8:1685–1699.

| | | |
|--|--------------------|--|
|   | S5L2PP ATBD-NO2 | Reference : KNMI-ESA-S5L2PP-ATBD-001 Version : 5.0 Page Date : 01 September 2023 89/89 |
|--|--------------------|--|

- [Vandaele et al., 1998] Vandaele, A. C., Hermans, C., Simon, P. C., Carleer, M., Colin, R., Fally, S., Mérienne, M. F., Jenouvrier, A., and Coquart, B. (1998). Measurements of the NO₂ absorption cross-section from 42000 cm⁻¹ to 10000 cm⁻¹ (238-1000 nm) at 220 K and 294 K. *J. Quant. Spectrosc. & Radiat. Transfer*, 59:171–184.
- [Veefkind et al., 2012] Veefkind, J. P., Aben, I., McMullan, K., Förster, H., De Vries, J., Otter, G., Claas, J., Eskes, H. J., De Haan, J. F., Kleipool, Q., Van Weele, M., Hasekamp, O., Hoogeveen, R., Landgraf, J., Snel, R., Tol, P., Ingmann, P., Voors, R., Kruizinga, B., Vink, R., Visser, H., and P. F. (2012). TROPOMI on the ESA Sentinel-5 Precursor: A GMES mission for global observations of the atmospheric composition for climate, air quality and ozone layer applications. *Rem. Sens. Environment*, 120:70–83.
- [Vermote and Tanré, 1992] Vermote, E. and Tanré, D. (1992). Analytic expressions for radiative properties of planar Rayleigh scattering media, including polarization contributions. *J. Quant. Spectrosc. & Radiat. Transfer*, 47:305–314.
- [Wang et al., 2008] Wang, P., Stammes, P., Van der A, R., Pinardi, G., and Van Roozendaal, M. (2008). FRESCO+: an improved O₂ A-band cloud retrieval algorithm for tropospheric trace gas retrievals. *Atmos. Chem. Phys.*, 8:6565–6576.
- [Wang et al., 2012] Wang, S. W., Zhang, Q., Streets, D. G., He, K., Martin, R. V., Lamsal, L. N., Chen, D., Lei, Y., and Lu, Z. (2012). Growth in NO_x emissions from power plants in China: bottom-up estimates and satellite observations. *Atmos. Chem. Phys.*, 12:4429–4447.
- [Wenig et al., 2003] Wenig, M., Spichtinger, N., Stohl, A., Held, G., Beirle, S., Wagner, T., Jähne, B., and Platt, U. (2003). Intercontinental transport of nitrogen oxide pollution plumes. *Atmos. Chem. Phys.*, 3:387–393.
- [Williams et al., 2017] Williams, J. E., Boersma, K. F., Le Sager, P., and Verstraeten, W. W. (2017). The high-resolution version of TM5-MP for optimized satellite retrievals: description and validation. *Geosci. Model Dev.*, 10:721–750.
- [World Health Organisation, 2003] World Health Organisation (2003). *Health Aspects of Air Pollution with Particulate Matter, Ozone and Nitrogen Dioxide*. World Health Organisation, Bonn.
- [Yang et al., 2014] Yang, K., Carn, S. A., Ge, C., Wang, J., and Dickerson, R. R. (2014). Advancing measurements of tropospheric NO₂ from space: New algorithm and first global results from OMPS. *Geophys. Res. Lett.*, 41:4777–4786.
- [Zara et al., 2018] Zara, M., Boersma, K. F., De Smedt, E., Richter, A., Peters, E., Van Geffen, J. H. G. M., Beirle, S., Wagner, T., Van Roozendaal, M., Marchenko, S., Lamsal, L. N., and Eskes, H. J. (2018). Improved slant column density retrieval of nitrogen dioxide and formaldehyde for OMI and GOME-2A from QA4ECV: intercomparison, uncertainty characterization, and trends. *Atmos. Meas. Tech.*, 11:4033–4058.
- [Zhou et al., 2009] Zhou, Y., Brunner, D., Boersma, K. F., Dirksen, R., and Wang, P. (2009). An improved tropospheric NO₂ retrieval for omi observations in the vicinity of mountainous terrain. *Atmos. Meas. Tech.*, 2:401–416.
- [Zoogman et al., 2017] Zoogman, P., Liu, X., Suleiman, R. M., Pennington, W. F., and Flittner, D. E., e. a. (2017). Tropospheric emissions: Monitoring of pollution (TEMPO). *J. Quant. Spectrosc. Radiat. Transf.*, 186:17–39.